

**Magnesium Transport In Mammalian
Erythrocytes And Its Effect On Platelet
Aggregation**

HAMAD SALEEM

A thesis submitted in fulfilment of the requirements for the degree of
(Master of Science by Research)

**Department of Applied Biology, University of Central Lancashire, Preston,
United Kingdom**

April - 1999

CONTENTS

Table of contents	I
Declaration	VI
Acknowledgements	VII
Abstract	VIII

Chapter One

General Introduction	1
1.1 Chemistry of Mg²⁺	2
1.2 Magnesium status and nutrition in the body	4
1.3 Relationship between magnesium and calcium signalling	5
1.4 Biological role of magnesium and its relationship with calcium signalling	8
1.5 Magnesium and cardiovascular dysfunctions	9
1.6 Magnesium affects vascular contractility	9
1.7 Magnesium deficiency, atherosclerosis and diabetes	11
1.8 Aetiology of clinical hypomagnesaemia	14
1.9 Magnesium transport in erythrocyte and models	15
1.10 Red blood corpuscles or erythrocytes	17
1.11 Role of Mg²⁺ in erythrocyte transport	17
1.12 Techniques for measuring magnesium in cells and its transport	18
1.12 (a) Fluorescence	18
1.12 (b) Ion selective microelectrodes	20
1.12 (c) Metallochromic dyes	20
1.12 (d) Radio labelled Mg²⁺	21

1.12 (e) Ionophores and AAS technique	22
1.13 Historical background on Atomic Absorbance Spectroscopy (AAS)	25
1.13 (a) What is Atomic Absorption Spectrometry (AAS)	26
1.13 (b) The Boltzmann Distribution	30
1.13 (c) The theory of Atomic Absorption Spectrometry	31
1.13 (c i) Absorption	31
1.13 (c ii) Emission	33
1.14 Nuclear Magnetic Resonance (NMR) and its application to study ion transport	34
1.14 (a) Intracellular Free Mg ²⁺ in living cells	35
1.14 (b) ³¹ P NMR Measurement of intracellular Free Mg ²⁺	36
1.14 (c) Application of the ³¹ P NMR for Free Mg ²⁺ determination	38
1.15 Role of Mg ²⁺ in Platelet Aggregation	38
1.15 (a) Platelet Aggregation	38
1.15 (a i) Platelets	38
1.15 (a ii) Aggregation	39
1.16 Role of Mg ²⁺ in Platelet Aggregation	40
1.17 Use of BioData Platelet Aggregation	40
1.18 Use of the BioData Platelet profiler (model PAP-3) in Aggregation	42
1.19 Percentage (%) Aggregation	43
1.20 Laboratory procedures	45
1.21 Preparation of plasma	46

1.22 Aims of this study	46
-------------------------	----

Chapter Two

Material and methods	48
2.1 Materials for Mg²⁺ transport	49
2.2 Materials for Platelet Aggregation	49
2.3 General procedure	49
2.4 Loading of pig and human erythrocytes with Mg²⁺	50
2.5 Measurement of Mg²⁺ using Atomic Absorbance Spectroscopy method (AAS)	51
2.6 Protein Assay: Assay of protein using BioRad method	51
2.7 Measurement of Cl⁻ using Cl⁻ titration	52
2.8 Measurements of Na⁺, K⁺ using flame photometry	53
2.9 Platelet Aggregation method	53
2.10 NMR method	54
2.11 Statistical Analysis	54

Chapter Three

Results	55
Results subdivided into four parts	
(a) Plasma ion level	
(b) Characterisation of Mg²⁺ transport	
(c) Platelet Aggregation	
(d) NMR study	56

3.1 Cations and Anion levels in pig and human plasma	57
3.2 Net Mg²⁺ efflux in Mg²⁺-loaded pig erythrocytes	57
3.3 Net Mg²⁺ and Ca²⁺ efflux in human erythrocytes	59
3.4 Mg²⁺ efflux in Pre- and Post-dialysis patients	60
3.5 Ca²⁺ efflux from Mg²⁺-loaded erythrocytes	61
3.6 Platelet Aggregation	61
3.7 NMR studies involving the measurement of intracellular Free Mg²⁺ and phosphate levels in human erythrocytes	63

Chapter Four

General Discussion	85
4.1 Cation and anion levels in pig and human plasma	87
4.2 Characterisation of Mg²⁺ transport	88
4.3 Platelet Aggregation	92
4.4 NMR experiment. Use of NMR	95
4.5 Conclusions	96
4.6 Scope for further studies	97

Chapter Five

References	98
-------------------	-----------

Chapter Six

Appendix	119
-----------------	------------

Appendix I	120
Appendix II	124
Appendix III	126
Appendix IV	137
Appendix V	139

Declaration

I declare that while registered as a candidate for the degree for which this submission is made I have not been a registered candidate for another award by any other awarding body. No material contained in this thesis has been used in any other submission for an academic award.

Hamad Saleem

Acknowledgements

I would like to express my appreciation and gratitude to my supervisor Professor Jaipaul Singh for his support, enthusiasm, motivation, patience and friendship throughout this investigation. I also thank Dr. Henning Wackerhage and Dr. Jack Waring for their advice and support. During my thesis I have acquired different techniques from both within University of Central Lancashire and Preston Royal Hospital. I express my gratitude to Dr. Sarfraz Khan from the Preston Royal Hospital, for initialising the co-operation between the two establishments. I am also grateful to Dr. Martin Myers, also from the Preston Royal Hospital, for his valuable time, his co-operation in securing the volunteers from the renal dialysis unit and the usage of the “HOT” analyzer in his department of pathology. I would like to thank all his staff for their hospitality and time to analyse my samples on the “HOT” analyser. I would like to thank the department of Haematology for the loan of the Platelet Aggregation Profiler. I would like to thank the hard working technicians in the University of Central Lancashire, Department of Physiology for all their help. Above all I give my deepest appreciation, love and Thank you from all my heart to my Father, Mother and twin brother, without whom I would never have completed this work.

Abstract

Renal failure is a decrease or cessation of Glomerular filtration. In acute renal failure (ARF) the kidneys abruptly stop working entirely or almost entirely. The main feature of ARF is suppression of urine flow, where the daily urine output is less than 250 ml or even less than 50 ml daily. Causes include low blood volume, decreased cardiac output and damaged renal tubules. Both the acute and chronic renal failure conditions show disturbances of ion transport systems in erythrocytes. In acute renal failure an elevation of intracellular free magnesium $[Mg^{2+}]_i$ has been reported.

The main aim of this study was to investigate and characterise magnesium (Mg^{2+}) transport in mammalian erythrocytes in the presence of various drugs. Healthy human controls and patients suffering from acute renal failure who are undergoing treatment via haemodialysis (Pre- and Post-dialysis) were employed for the study. The effects of varying extracellular Mg^{2+} on platelet aggregation was also investigated employing different concentrations of adenosine diphosphate (ADP) on the plasma from both pre- and post-dialysis patients. Healthy human controls were used as a comparison.

The Mg^{2+} level in plasma from both Pre- and post-dialysis patients was slightly lower than in human control. In the erythrocytes normal Mg^{2+} was lower in human control than in both the pre- and post-dialysis patients. Upon Mg^{2+} -loading, the human control Mg^{2+} was still lower than loaded erythrocytes from both pre - and post-dialysis patients. After a period of 50 min efflux, the human control Mg^{2+} level was higher than the efflux in both the pre- and post-dialysis patients, but both the pre- and post-dialysis patients had released smaller amounts of Mg^{2+} than human control, indicating acute renal failure is associated with large fluxes of Mg^{2+} . Amiloride (a sodium channel blocker) and *N*-methyl-D-glucamine (NMDG) a substitute for sodium were used to test the mechanism of Mg^{2+} transport.

Following Mg^{2+} -loading, in pre-dialysis patients the Mg^{2+} efflux in the presence of (10^{-3} M) amiloride was greatly elevated compared to untreated erythrocytes. When extracellular sodium chloride was replaced with NMDG there was a large and significant decrease in Mg^{2+} efflux compared to control. In post-dialysis patients a larger Mg^{2+} efflux was observed in the presence of amiloride (10^{-3} M), but in NMDG there was an initial reduction in Mg^{2+} efflux (lower than control) which increased and remained the same as control.

Mg^{2+} showed a time-dependent manner of uptake and release in erythrocytes, which suggested it would affect platelet aggregation. The plasma from healthy human controls as well as both pre- and post-dialysis patients was employed in the presence of ADP (10^{-3} - 10^{-7} M) and a varying range of extracellular Mg^{2+} (1-7 mM). In human control, ADP can aggregate platelets in a dose dependent manner. A perturbation of extracellular Mg^{2+} caused a decrease in the ADP induced platelet aggregation. However, during acute renal failure a perturbation of extracellular Mg^{2+} had no significant effect on platelet aggregation in plasma from acute renal failure patients compared to healthy human controls.

In conclusion, the results of this study employing blood (erythrocytes and plasma) from both pig and human (healthy control and acute renal failure patients) indicate that erythrocytes can take up Mg^{2+} and release it in a time-dependent manner. In some cases, the efflux was sensitive to either amiloride or extracellular sodium: In addition, ADP can induce a dose dependent increase in platelet aggregation, which was attenuated by a perturbation of extracellular Mg^{2+} . Further experiments are required to characterise precisely the transport of Mg^{2+} and its role in platelet aggregation during diseased states.

Chapter One

General Introduction

1.1 Chemistry of Mg²⁺

Magnesium is named after the Greek city, Magnesia, where large deposits of magnesium carbonate were found. Magnesium sulphate was isolated by Grew in 1195 from spring water from Epsom which is believed to have medicinal properties. In 1707 Valentine isolated magnesium carbonate while in 1755 Black isolated magnesium oxide. Subsequently in 1808, Sir Humphrey Davy became the first person to isolate the metal form of magnesium. The element magnesium occurs in nature in the forms of its various compounds which are known to be widely distributed in the earth's crust, the upper stratum, to a depth of 16 Km which has been estimated to contain an average of 3.45% of MgO₂ and it is the eighth element in order of abundance both terrestrially and cosmically (Emley, 1966). In nature, magnesium does not naturally occur in free state but in its principal of mineral forms as oxides, carbonates, chlorides, silicates, fluorides, sulphate and phosphate (Emley, 1966). In water, Mg²⁺ occurs as a chloride at a concentration of 5.0-5.5g Litre⁻¹.

Magnesium is extremely electropositive and readily loses two electrons to yield a divalent cation (Mg²⁺) in common with other alkaline earth metals. The alkaline earth metals decrease in electronegativity with increased atomic weight. Usually, the alkaline earth metals occur as salts of commonly found anions. For example, magnesium, calcium, strontium and barium occur in nature as sulphates and carbonates. Magnesium will form oxides on heating in air and its nitrates have very low thermostability. Many magnesium salts are insoluble in water while others are deliquescent. Isotopes of Mg²⁺ and their abundance are ²⁴Mg²⁺ (78.60%), ²⁵Mg²⁺ (10.11%) and ²⁶Mg²⁺ (11.29%) (Williams, 1993).

Magnesium ions (Mg^{2+}) have an ionic radius approximately two thirds that of calcium ions and sodium ions and half that of potassium ions. Therefore, due to its small size and relatively large charge, Mg^{2+} is the strongest metal ion in abundance in biological systems (Wacker, 1968, 1980; Williams, 1993). Cations usually form the most stable complexes with anions or ligands of similar hardness and hard ligands contain highly electronegative donor atoms. Therefore, Mg^{2+} can form stable complexes with phosphate or carboxylate ions and with nitrogen's lone pair of electrons. Mg^{2+} has a longer hydration energy than of Ca^{2+} due to Mg^{2+} 's greater polarising potential. This means that magnesium salts of large organic acids are more soluble than analogous calcium compounds (Wacker, 1968, 1980; Williams, 1993).

1.2 Magnesium status and nutrition in the body.

Magnesium is the second most abundant metal within cells, where its amount is exceeded only by potassium (Heaton, 1981). On average a human adult contains about 9 g of magnesium in the ionic form or free Mg^{2+} (Heaton, 1981). This is approximately one third of the total amount in the body (Heaton, 1981). In general the body contains about 27 g of magnesium in the free and bound forms.

Magnesium is present as a positively charged ion species (Mg^{2+}). Of the total body Mg^{2+} , one half is adsorbed to the surface of hydroxyapatite in bone, the other half is located intracellularly and only 1% is in the extracellular fluid.

Mg^{2+} is predominately located in cellular organelles in bone (approximately 52%), the remainder in muscle (28%), soft tissue (19%), serum (0.3%) and red blood corpuscles (0.5%) (Elin, 1987). About 30% of Mg^{2+} in the bone is believed to represent an exchangeable pool of Mg^{2+} . Mobilisation of Mg^{2+} from this pool is rapid in children compared to adults (Mudge and Weiner, 1992). Mg^{2+} in the human body is the second most abundant after the intracellular monovalent cation K^+ (Reinhardt, 1988). The concentration of plasma Mg^{2+} is approximately 0.75-1.1 mmol litre⁻¹ with two thirds of plasma Mg^{2+} being free Mg^{2+} and one third is bound to plasma proteins, albumin, thrombin, globulin, etc. (Mudge and Weiner, 1992). It is now the belief that Mg^{2+} in blood serum is in transit between the bone stores and actively metabolising tissues (Birch and Sadler, 1979; Phillips, 1989; Vormann and Gunther, 1993). In serum, 33% of Mg^{2+} is bound to proteins, 61% ionised and the remaining 6% complexed to ions including phosphate and citrate (Speich, Bousquet and Nicholas, 1981). Only the ionised Mg^{2+} is available to react in physiological and biochemical processes (Heaton, 1981). Thus, knowledge of intracellular free Mg^{2+} concentration $[Mg^{2+}]_i$ is essential in

understanding the physiological role of this important divalent cation in physiological and biological processes.

Normal magnesium intake is approximately 12-15 mmol per day. Foods rich in magnesium include nuts, green leafy vegetables, cereals and red meat (Heaton, 1981). Of the magnesium taken in orally, approximately one-third is absorbed by the small bowel. The kidneys maintain magnesium homeostasis by excreting the magnesium absorbed by the gut. Because approximately one third of serum magnesium is bound to albumin, the filtered load of magnesium is bound at the renal level. Of the filtered magnesium, approximately 25-30% is reabsorbed by the proximal tubules, 50-60% is reabsorbed by the ascending limb of Henle's loop, and 2-5% is reabsorbed distally (Quamme and Dirks, 1986).

1.3 Relationship between magnesium and calcium signalling.

Magnesium (Mg^{2+}) is the second most abundant divalent cation and is present in all living cells. Its physiological role is primarily intracellular and preservation of intracellular Mg^{2+} concentration ($[Mg^{2+}]_i$) is essential for normal functioning of the heart (Whang, Oei and Aikawa, 1994). Molecular evolution in mammals has resulted in the development of over 300 Mg^{2+} -dependant enzymes (Flatman, 1991; Wacker, 1968) and thus Mg^{2+} plays a regulatory role in many cellular functions including many of those involved in the glycolytic process, those catalysing the transfer of phosphate and most of those utilising ATP (Flatman, 1991). In essentially all reactions where ATP is a substrate, the true substrate is Mg^{2+} -ATP. The regulatory role of Mg^{2+} in many cellular processes is attributed to free $[Mg^{2+}]_i$ (Murphy, Freudenrich and Lieberman, 1991) and intracellular Mg^{2+} has been shown to modulate Ca^{2+} flux

through the L-type Ca^{2+} - channel in cardiomyocytes (Fry, Buri, Chen, Illner, Kickenweiz, McGuigan, Noble, Powell and Twist, 1993; Agus, Kelepouris, Dukes and Morad, 1989) and Ca^{2+} efflux in pancreatic acinar cells (Francis, Lennard and Singh, 1990; Singh and Wisdom, 1995) whilst extracellular Mg^{2+} concentration affects amplitude of contraction (Howarth, Waring, Singh and Hustler, 1994) and digestive enzyme secretion (Francis *et al*, 1990; Singh and Wisdom, 1995). Experiments using $^{28}\text{Mg}^{2+}$ have demonstrated that both intracellular and extracellular Mg^{2+} are exchangeable in the isolated working rat heart (Page and Polimeni, 1972) and that free and bound Mg^{2+} are exchangeable, depending on the cell type (Günther, 1990). These exchanges create a Mg^{2+} buffer which ensures that intracellular Mg^{2+} is maintained (Gunther, 1993). The regulation of intracellular Mg^{2+} involves the permeability of the plasma membrane, intracellular buffering by proteins and transport of Mg^{2+} in the plasma membrane and organelles (Flatman, 1991). Mechanisms therefore must exist whereby Mg^{2+} is transported through the cell membrane in both an inward and outward direction, so as to maintain a steady-state intracellular Mg^{2+} concentration. The electrochemical gradient across the cell membrane would tend to promote influx of Mg^{2+} , so some mechanism(s) must exist to extrude Mg^{2+} against this gradient.

It has been suggested that Mg^{2+} deficiency or reduced dietary Mg^{2+} intake may play an important role in the aetiology of many diseases including many of those involving the cardiovascular system, such as hypertension, cardiac arrhythmias, atherosclerosis and ischaemic heart disease (Page *et al*, 1972; Altura and Altura, 1995). Magnesium deficiency is common in patients who have suffered acute myocardial infarction and studies have shown that intravenous infusion of Mg^{2+} in the acute phase of myocardial infarction, significantly reduces arrhythmia's and mortality (Abbot and Rude, 1993;

Galloe, Rasmussen, Jorgensen, Aurup, Balslov, Cinton, Graudal and McNair, 1993; Woods, Roffe and Fletcher, 1994). Heart disease is one of the most common causes of death in the western world at the present time; it is therefore of some interest to understand factors and mechanisms which regulate Mg^{2+} homeostasis in the heart (Woods *et al*, 1994; Altura *et al*, 1995).

Although interest in divalent cations has tended to focus on changes in cytosolic free calcium ($[Ca^{2+}]_i$), there is considerable growth in the appreciation of the potential roles of Mg^{2+} both as a direct metabolic regulator and as a modulator of Ca^{2+} sensitivity (Altura and Altura, 1981; Flatman, 1984; Grubbs and Maguire, 1987). The activities of many ion transport mechanisms are regulated by Mg^{2+} in the physiological range of 0.1-1.0mM (Flatman, 1991). In secretory epithelia, fluid secretion is regulated by intracellular Ca^{2+} and intracellular Na^+ (Petersen and Gallacher, 1988). Mg^{2+} plays a key role in these processes as an essential cofactor for the activation of Ca^{2+} and Na^+ pumps (Fujise and Lauf, 1988). Squire and Petersen (1987) demonstrated that Mg^{2+} can evoke a physiological dose dependent activation of K^+ channels in mouse parotid acinar cells, while in red blood cells Mg^{2+} activates the $Na^+ - K^+ - Cl^-$ cotransporter (Flatman, 1988). These findings again suggest an important function of Mg^{2+} in fluid secretion, since in epithelial cells this transporter is the primary uptake mechanism for Cl^- ions, which are required to drive fluid and electrolyte secretion (Petersen and Gallacher, 1988; Petersen, 1992; Mooren and Singh, 1997). Thus, regulation of cytosolic free Mg^{2+} concentration is critical for many cellular functions, including fluid and electrolyte secretion, enzyme activity, cell growth and proliferation (Petersen and Gallacher, 1988; Flatman, 1991; Petersen, 1992; Mooren and Singh, 1997).

Magnesium is both a universal and essential biological element, which is found in abundant quantities in cells. It plays an important role in the regulation of cell function. Despite its wide range of important functions and distribution in the body its study has been neglected, compared to the second messenger, calcium. This was thought to be the fact that accurate biological techniques were not available to measure intracellular free magnesium concentration and in most cases calcium seems to interfere with the techniques (Hurley, Ryan and Brink, 1992). However, over the past 6-7 years persistence in magnesium biology research and moreover, alternative strategies have been found to study magnesium homeostasis in different cell types. Research in several laboratories (Singh and Wisdom, 1995; Mooren and Singh, 1997) over the past few years has concentrated with the characterisation of magnesium transport and its second messenger role in the exocrine pancreas.

1.4 Biological roles of magnesium and its relationship with calcium signalling.

Mg²⁺ exists as an abundant divalent cation and it is involved in several physiological and biochemical processes during cellular homeostasis. It is an important co-factor for over 300 enzymes (Wacker, 1968, 1980). Mg²⁺ is involved in the synthesis and replication of RNA and DNA (Henrotte, 1993) and with muscle contraction (Altura and Altura, 1995), and the secretion of enzymes (Francis *et al.*, 1990; Nielsen and Petersen, 1972; Wisdom, Geada and Singh, 1996) and hormones (Grodsk and Bennett, 1966; Curry, Joy, Holley and Bennett, 1977; Baker and Knight, 1978). Mg²⁺ also plays an important physiological role in transmembrane movements of ions (e.g. Na⁺: K⁺ - ATPase, Ca²⁺ - ATPase, K⁺: H⁺ - ATPase, K⁺: Na⁺: Cl⁻ and Na⁺: Cl⁻ transporter and Ca²⁺: Na⁺ and HCO₃⁻: Cl⁻ exchanges) and regulation of ion channel activities e.g. Na⁺, K⁺, Cl⁻ and Ca²⁺ (Flatman, 1984, 1990, 1993; Agus *et al.*, 1989; Gunther and

Vormann, 1990). Furthermore, Mg^{2+} is also involved with metabolic pathways, protein synthesis, bioenergetic and structural properties of cells, stabilisation of membrane and electrical potentials across cells (Birch, 1993).

1.5 Magnesium and cardiovascular dysfunctions.

Experimental, epidemiological and clinical studies published over the last decade point to the active involvement of magnesium ions in the maintenance of cardiovascular function as well as in the aetiology of cardiovascular disease when problems arise in magnesium intake and balance (Altura and Altura, 1995; Woods *et al*, 1994). Dietary magnesium deficiency as well as abnormalities in magnesium metabolism appears to influence a variety of cardiovascular disease states.

Hazard and Wurmser, in 1932 recognised that systemic administration of magnesium ions could induce rapid vasodilation and reduction in arterial blood pressure.

Little more than that was known about the cardiovascular actions of magnesium in 1961, when some researchers from the British Medical Association (B.M.A) were investigating the physiological responses of isolated blood vessels to vasopressors and vasodilators. Removal of all the magnesium from artificial physiological salt solution produced vasospasm, enhanced responses to vasopressors, and decreased responses to dilator agents (Altura and Altura, 1995). Their findings were the first to report such dramatic results of a magnesium free medium on vascular smooth muscle tone or reactivity.

1.6 Magnesium affects vascular contractility.

Blood normally contains magnesium ion in three states; bound to plasma proteins, complexed to small anion ligands such as bicarbonate or peptides, and free. It is well documented that most clinical laboratories measure total magnesium levels by

colorimetry or atomic absorption spectrophotometry. However, it is the free ionised form of magnesium [Mg^{2+}] that is physiologically active. Usual estimates of free Mg^{2+} concentration have relied upon total magnesium measurements in protein free ultrafiltrates, which of course exclude the protein, bound magnesium (Altura and Altura, 1995). Anion levels can be very significant in pathological states, and in view of the role played by magnesium in cellular homeostasis, it is desirable to directly measure free Mg^{2+} in blood and other body fluids. With this in mind, magnesium sensitive ion selective electrodes were designed to obtain these measurements in the presence of cationic interferences. In 1980, Altura and Altura demonstrated that diverse large and small mammalian coronary arteries subjected to reductions in extracellular Mg^{2+} concentrations underwent rapid spasm and potentiation of circulating vasoconstrictor hormones. Similar observations have been made in human coronary attacks. They therefore initiated ion sensitive electrode studies to determine whether patients with acute myocardial infarction or coronary heart disease exhibited significantly lowered levels of Mg^{2+} as a percentage of total magnesium was also significantly lowered. These types of studies provoked a number of cardiologists to examine the potential use of magnesium in the therapy of acute myocardial infarction and congestive heart failure (Woods *et al*, 1994; Altura and Altura, 1995).

Animal studies provided evidence for magnesium modulation of hypertensive events. With respect to both experimental and genetically induced hypertension, several reports support the idea that magnesium deficiency or derangement in magnesium metabolism results in high blood pressure (Altura and Altura, 1995).

Experiments by Altura and Altura (1995) indicated that in rats, dietary deficiency of magnesium resulted in elevation of arterial blood pressure, decreased arteriolar, venular, and precapillary lumen sizes, and decreased numbers of microvessels,

accompanying with decreased flow in the capillaries. An elevated ratio of Ca^{2+} to Mg^{2+} was also found in the vascular walls, which was expected to result in enhanced vascular tone, enhanced reactivity to endogenous vasoconstrictors, and diminished reactivity to endogenous vasodilators (Altura and Altura, 1995).

They also found that ultrafilterable Mg^{2+} is significantly attenuated and that there is an elevated Ca: Mg ratio in hypertensive rats. It was also reported that intracellular free Mg^{2+} is lowered in striated muscle and aortic smooth muscle of these rats (Altura and Altura, 1995). These findings support the hypothesis that the level of free ionised Mg^{2+} in the extracellular fluid and at the level of the vascular smooth muscle cell membrane plays an important role in controlling vascular tone, contractility of blood vessels, and eventual prevention of hypertensive vascular disease. Many independent clinic studies showed that patients with hypertension of diverse aetiologies exhibited hypomagnesemia in serum or in tissues, or both. On average, patients with long term hypertension had at least a 15% deficit in total magnesium. Reports from around the world clearly demonstrated inverse correlations between total magnesium in serum or tissue and arterial blood pressure (Altura and Altura, 1995).

In 1994 Nadler demonstrated that controlled short-term (four weeks) dietary deprivation of magnesium in humans significantly elevated arterial blood pressure. Other studies showed evidence that certain hypertensive patients exhibited reduced urinary excretion of magnesium, which is inversely correlated with diastolic blood pressure levels (Altura and Altura, 1995).

1.7 Magnesium deficiency, atherosclerosis and diabetes.

Hypercholesterolemia has been accepted as a factor for atherosclerosis. It is not clear how the lipoproteins and Ca^{2+} gain access to the normal impermeable arterial walls, but magnesium deficiency may be involved (Altura and Altura, 1995). Evidence from

both animal and human studies suggest that dietary and blood levels of Mg^{2+} may modulate serum levels of lipids and lipoproteins (Altura and Altura, 1995). In the hypertensive diabetic patient population, hyperinsulinemia, insulin resistance, and hypertensive vascular disease are often associated with decreased serum high density lipoprotein (HDL) cholesterol, increased low density lipoprotein (LDL) cholesterol, and elevated triglyceride levels. With respect to experimental diabetes and magnesium, a number of studies point to firm relationship between the diseased state and magnesium deficiency. There appears to be a strong association between clinical diabetes, hypertension, dyslipidemias, and abnormal glucose tolerance. Experimental studies have suggested that control of diabetes is inversely related to magnesium deficiency (Altura and Altura, 1995). Diabetic retinopathy is clearly associated with a state of magnesium deficiency. Both insulin- dependent and non-insulin-dependent diabetes are associated with reduced serum total magnesium and intracellular Mg^{2+} concentration as well as increased urinary loss of magnesium (Altura and Altura, 1995). Even though not all diabetic patients who had been studied exhibited a simultaneous reduction in serum total magnesium and intracellular free Mg^{2+} , oral treatment with magnesium salts improved control of both types of diabetes, in the few studies performed at the time (Altura and Altura, 1995).

Using ion-selective electrodes to measure free Mg^{2+} in fasting subjects with and without type II diabetes and ^{31}P -NMR spectroscopy to measure intracellular free Mg^{2+} in red blood cells, Altura *et al*, 1995 found that both Mg^{2+} levels were significantly reduced in diabetic compared to non-diabetic subjects. A close relationship was seen between serum free Mg^{2+} and intracellular free Mg^{2+} . They thus proposed that magnesium deficiency, both extracellular and intracellular, was a characteristic of

chronic, stable, mild non-insulin-dependent diabetes and it may predispose patients to the excess cardiovascular mortality of the diabetic state.

In collaboration with Gupta, Altura and Altura (1995) performed in vitro ^{31}P -NMR spectroscopy experiments on the intact perfused heart. The findings indicated that acute elevation of extracellular free Mg^{2+} concentrations increased phosphocreatine levels, intracellular pH, and intracellular free Mg^{2+} levels. Intracellular inorganic phosphate levels decreased, and the cytosolic phosphorylation potential and free energy of ATP hydrolysis increased accordingly. Acute reductions in extracellular free Mg^{2+} resulted in opposite effects on cardiac performance. These findings suggest that magnesium regulates cardiac performance, oxygenation, and substrate delivery in the myocardium (Altura and Altura, 1995).

Gender related differences in haemodynamic characteristics have had attention, because premenopausal women are known to be less susceptible than men to numerous cardiovascular disorders. In the early 1980's a diverse range of both endogenous and exogenous vasodilators were experimented with, these showed to exert their effects on endothelial cells. In 1980 Furchgott showed a substance called "endothelial-derived relaxing factor" (EDRF) and also known as Nitric Oxide to be released by the endothelial cells in response to vascular smooth muscle relaxants. Experiments by Altura and Altura (1995) on male and female isolated rat aortas demonstrated that in male isolated aortas, withdrawal of extracellular free Mg^{2+} and concomitant reduction in extracellular Na^{+} induced significantly increases of basal tone. Surprisingly, this did not occur in intact aortas removed from female rats, though it was observed in endothelium-denuded aortic preparations from both sexes. The observed gender-related differences were not dependent on animal strain or type of tissue preparation. No tension development was observed in aortas from castrated males treated with

estradiol. Aortic tissues of sexually immature male and female rats, however, exhibited marked tension development when exposed to zero extracellular free Mg^{2+} and low extracellular Na^{+} (Altura and Altura, 1995). These studies suggested that sex steroid hormones, probably 17β estradiol, could influence contractile responsiveness of vascular smooth muscle. A possible mechanism is mediating effects on endothelial cells, possibly via modification of magnesium-regulated internal sodium dependent calcium influx. This may help to explain why magnesium-deficient women, unlike men, are protected against ischemic heart disease, hypertensive vascular disease and cerebrovascular disease until menopause (Altura and Altura, 1995).

Magnesium intake has been linked to cardiovascular disease, and an epidemiological study by Schroder in the USA and Crawford in London suggested a link between water hardness and protection against cardiovascular disease. The hardness of water depends on the calcium and magnesium concentrations, and hard water does not always contain high magnesium (Altura and Altura, 1995). Following some studies in which the magnesium levels were ascertained very carefully, it is clear that there is an inverse relationship between magnesium intake and ischemic heart disease, sudden cardiac death, and hypertensive vascular disease.

1.8 Aetiology of clinical hypomagnesaemia.

The many causes of clinical hypomagnesaemia and magnesium depletion can be divided into four broad categories: renal, gastrointestinal, endocrine and miscellaneous (Whang, 1993). The renal causes include, administration of diuretics and antibiotics, which result in enhanced magnesiuria, hereditary renal magnesium wasting and alcoholism (Shah, Alvarado and Kirshenbaum, 1990). Magnesium depletion and hypomagnesaemia have been found in association with the following gastrointestinal

aetiologies: malnutrition, alcoholism, prolonged intravenous therapy without magnesium administration, malabsorption associated with non-tropical sprue, short bowel syndrome, intestinal surgery for morbid obesity and adenoma and nasogastric suction. Diabetic ketoacidosis, hyperaldosteronism, excessive losses of magnesium resulting from bulimarexia, laxative abuse, diarrhoea, villous hyperparathyroidism, and hyperthyroidism constitute endocrine causes of hypomagnesaemia and magnesium depletion. Exchange transfusions, acute intermittent porphyria, excessive lactation and theophylline toxicity constitute miscellaneous causes of magnesium deficiency (Whang, 1993).

1.9 Magnesium transport in Erythrocytes and models.

Magnesium's role in regulating membrane transport first became evident in studies performed in the 1950s. Rats were used in the experiments, they were made magnesium deficient, they showed electrolyte imbalances and, in particular, their skeletal potassium content was reduced (Flatman, 1993). Skou (1957) who showed that the sodium pump had an absolute requirement for magnesium provided a partial explanation of these effects. Continuing work has now shown that many transport systems are affected by the concentration of magnesium both inside and outside the cell. Much work has been done on red blood cells, as these provide a convenient model for transport studies (Flatman, 1984; 1993). However, the findings are relevant to transport in other situations. Some are particularly important in red cell behaviour. These provide explanations for physiological and pathophysiological phenomena, which may permit therapeutic exploitation.

The importance of magnesium in regulating ion transport was first recognised in experiments on the sodium pump. Activity of the pump's Na, K-ATPase was shown to have an absolute requirement for magnesium (Skou, 1957; Dunham and Glynn, 1961). Since then magnesium has been shown to play a vital role in many other partial reactions of the pump including, phosphorylation of the enzyme from ATP or P₁ (Post, Sen, and Rosenthal, 1965; Post, Toda and Rogers, 1975), ATP-ADP exchange (Robinson, 1976; Beauge and Glynn, 1979; Beauge and Campos, 1986), Na-ATPase (Beauge and Campos, 1986; Rossi and Garrahan, 1989), sodium-potassium exchange (De Weer, 1976; Flatman and Lew, 1981).

Sodium-sodium exchange (Flatman and Lew, 1981) potassium-potassium exchange (Karlsh and Stein, 1982 a, b; Sachs, 1988b). Calcium pumps are widely distributed in animal cell membranes. Magnesium plays an important role in the operation of these pumps probably affecting both the phosphorylation and dephosphorylation of the transporter. The pumps have all been studied using both animal and human models. Experiments using red blood cells have also been used ranging from red blood cells from squirrel (Marjanovic, Gregory, Ghosh, Willis and Dawson, 1993), chicken (Gunther, Vormann and Forster, 1984), sheep (Lauf, 1985), pig (Taylor, Singh, 1997). Human blood has also been used both for platelet aggregation (Ravn *et al*, 1995; 1996), NMR studies (Gupta, 1980). Clinical trials in hospitals have also been performed on patients suffering from a range of cardiovascular disorders, renal problems and diabetic problems (Resnick, Barbagallo, Gupta and Laragh, 1993). Rats have also been employed, their heart tissues have been used to measure how their magnesium levels varied in the presence of specific channel ion blockers e.g. amiloride (Gunther and Vormann, 1987).

1.10 Red Blood Corpuscles or erythrocytes.

Red blood corpuscles or erythrocytes have many advantages for use in studies of membrane transport. They have a simple shape and lack intracellular or extracellular compartments so the fluxes can be measured precisely and unambiguously. Changes to the cytoplasmic components can be performed by applying reversible haemolysis (“ghosting”) or ionophores, hence enabling the effects of intracellular factors on transport to be studied, (Reed and Lardy, 1972).

The erythrocytes have a simple metabolism mechanism, which allows a more direct assessment of the role of metabolism and metabolic intermediates in transport. Their membranes contain fewer transport systems and have low cation permeability. Over the course of evolution, different animal species have had various transport systems deleted from the erythrocytes without affecting their viability or competence in oxygen and carbon dioxide transport.

1.11 Role of Mg²⁺ in erythrocyte transport.

The effects of magnesium on cation transport have been studied extensively in erythrocytes. The magnesium dependence of the sodium pump (Flatman and Lew, 1981), Na, K, Cl, cotransporter (Flatman, 1988) and KCl transport (Lauf, 1985; Brugnana and Tosteson, 1987) have all been well established.

There is evidence from several species that in vitro erythrocytes, magnesium content falls as the cells get older. Berstein in 1959 experimented by separating the blood into its different fractions. The different fractions contained different magnesium levels; the younger cells contained approximately twice as much magnesium as did the older

denser fractions. Various other workers experimented on similar lines and the results presented similar findings. Dunn (1974) gave early evidence for net magnesium transport in human red cells in vitro. His findings showed that magnesium is lost from cells containing a high magnesium concentration when they are incubated in medium containing zero or 0.8 mM magnesium.

1.12 Techniques for measuring magnesium in cells and its transport.

There are numerous techniques which are available to measure total and ionized magnesium in cells. These include labelled isotopes, fluorescent bioprobes, magnesium sensitive electrodes, NMR and atomic absorbance spectroscopy.

1.12 (a) Fluorescence

Visible and ultraviolet (UV) radiation can be used to induce electronic transitions between the ground state and the higher energy excited states of a molecule, resulting in absorption or UV/visible spectra. The excitation energy is lost in the form of heat to the medium. However, fluorescence occurs if the excitation energy emitted when the molecule in a singlet excited state returns to the ground state. Both the ground state and singlet excited state have the electronic spins paired up, leading to intense transitions in the fluorescence spectrum. Fluorescence occurs at a lower frequency or longer wavelength than does absorption, because the energy of the emitted radiation is less than that of excitation energy by an amount corresponding to the vibrational energy lost to the medium. The fluorescence emission spectrum is the mirror image of the absorption spectrum. The fluorescence frequencies are different from the excitation frequencies; therefore no interference from the excitation source occurs. Fluorescence is a highly sensitive technique that can detect concentrations as low as 10^{-8} M, as opposed to 10^{-4} M for NMR spectroscopy (Freitas and Dorus, 1993). The dependence

of the fluorescence intensity on the wavelength of the emitted light is the emission spectrum. In contrast, the excitation spectrum represents the dependence of the fluorescence intensity on the wavelength of the exciting light. Synthetic fluorescence indicators are required for most biological applications (Freitas and Dorus, 1993). The work using fluorescence is performed by using the fluorescent indicator Fura-2 acetometyler (fura-2 (AM)), which contains a furan ring as a fluorophore (Tsien, 1983). This is a Ca^{2+} indicator. This indicator was then modified to give a Mg^{2+} indicator FURAPTRA (Raju, Murphy, Levy, Hall and London, 1989). Upon Mg^{2+} binding there is a shift in excitation maximum, hence the free intracellular Mg^{2+} concentration that is measured from the fluorescence excitation spectrum of FURAPTRA can be obtained from the ratio method according to (Raju *et al*, 1989):

$$[\text{Mg}^{2+}]_f = K_D \cdot S_{\min} (R - R_{\min}) / S_{\max} (R_{\max} - R)$$

where R is the fluorescence intensity ratio at wavelengths 335 and 370 nM observed for the biological sample, R_{\min} and R_{\max} are the fluorescence intensity ratios in the absence and presence of saturating amounts of Mg^{2+} , and S_{\min} and S_{\max} are the fluorescence intensities in the absence of Mg^{2+} and in the presence of saturating Mg^{2+} , respectively. The main advantage of the ratio method is that Mg^{2+} measurements are independent of the concentration of the fluorescence indicator used.

The use of the fluorescence indicator has been validated in isolated rat hepatocytes and cultured chicken heart cells (Murphy *et al*, 1989) and pancreatic acinar cells (Lennard and Singh, 1991; Mooren and Singh, 1997; Wisdom and Singh, 1996). The good match between the K_D value for the complex between Mg^{2+} and FURAPTRA and free intracellular Mg^{2+} concentrations and the rapid response of fluorescence make it a promising aid for the monitoring of Mg^{2+} fluxes in biological tissues. Due to the larger intracellular Mg^{2+} concentrations relative to those of Ca^{2+} , the possibility that the

FURAPTRA indicator will interfere and buffer the Mg^{2+} levels being measured is less likely than that for fluorescence of Ca^{2+} indicators (Raju *et al*, 1989). Mag-fura-2 is the commercial name of FURAPTRA.

1.12 (b) Ion selective microelectrodes

Early electrode work used neutral ionophore *N,N'* diheptyl-*N,N'*-dimethylsuccinamide (ETH-1117). Its Mg^{2+} selectivity was not high, and was interfered by Na^{+} and K^{+} hence preparations of calibrating solutions were required. The selectivity of Mg^{2+} selective microelectrodes for Mg^{2+} relative to Ca^{2+} is low. A new resin, ETH-5214, which is not interfered by K^{+} and Na^{+} ions was used for Mg^{2+} selective electrodes (Hu, Bruhrer, Muller, Rusterholz, Rouilly and Simon, 1989; Buri and McGuigan, 1990; 1991). The advantages of Mg^{2+} selective microelectrodes include: direct measurement of free intracellular Mg^{2+} levels as opposed to the indirect measurements based on ^{31}P and ^{19}F NMR and fluorescent dyes, low cost of equipment and fast response. The main disadvantages are the need for large cells and the invasive nature of the measurement (Freitas and Dorus, 1993).

1.12 (c) Metallochromic dyes

Metallochromic dyes are reagents that change their colour and, consequently, their optical spectrum, in the presence of different concentrations of free metal ions. The metallochromic dyes eriochrome blue SE, arsenazo III, and antipyrilazo III have been

used to determine free intracellular Mg^{2+} concentrations in biological samples (Scarpa, 1979). Optical measurements require a reagent that is pH insensitive and has a high degree of specificity for Mg^{2+} relative to other metal ions, in particular Ca^{2+} . By multi-wavelength spectrophotometry, it is possible to correct for pH effects and interference from other metal cations, provided that the optical spectrum of the Mg^{2+} - dye complex differs sufficiently from other interfering factors (Scarpa, 1979; Tsien, 1983). This method, requiring loading of the dye into the intracellular compartment via microinjection, is restricted to giant cells such as squid axons and muscle fibres. Unless the spectral properties of a metallochromic dye in a given medium are known, this method should be used with caution.

Since this project involves the use of AAS and NMR, emphasis is placed on these two powerful techniques to measure total Mg^{2+} .

1.12 (d) Radio labelled Mg^{2+}

Two radio isotopes of Mg^{2+} exist ^{27}Mg and ^{28}Mg , respectively which are employed for the investigation of cellular magnesium transport mechanisms (Gunther, Eds: Sigel, Sigel and Decker, 1990; Vormann and Gunther, Ed: Birch, 1993). Both the isotopes are difficult to manipulate and their use is limited due to their short half-lives 9.46 min and 20.9 hours for ^{27}Mg and ^{28}Mg , respectively (Flik, Velden and Kolar. Ed. Birch, 1993). The isotopes are not commercially available. ^{27}Mg is obtained from thermal neutron irradiation of ^{26}Mg of natural isotopic composition or magnesium enriched ^{26}Mg which is a expensive process. ^{28}Mg is obtained from reactor irradiated Li/Mg alloy (Kolar, Velden, Vollinga, Zandbaerger and Goejj, 1991). Gamma-spectrometry and liquid scintillation counting techniques are used to measure both isotopes (Flik, Van der Velden and Kolar, Ed. Birch, 1993).

Radio labelling is based on the observation that plasma membrane permeability for magnesium increases when the cells are incubated in a Ca^{2+} -free medium in the presence of the calcium ionophore A23187, which mediates the electroneutral exchange of 1 Mg^{2+} for 2 H^+ . Incubating media with varying concentrations of Mg^{2+} can be used from which $[\text{Mg}^{2+}]_i$ can be calculated from the pH gradient and from the extracellular Mg^{2+} concentration ($[\text{Mg}^{2+}]_o$) according to the following equation :-

$$[\text{Mg}^{2+}]_i = [\text{Mg}^{2+}]_o * [\text{H}^+]_i^2 / [\text{H}^+]_o^2.$$

since A23187 permeabilizes both plasma and organelle membranes (Tsien, 1983), other researchers (Corkey, Duszynski, Rich, Matschinsky and Williamson, 1986) have employed digitonin, which is selective for plasma membrane. The technique is mainly limited by its requirement for high-density cell suspensions.

1.12 (e) Ionophores and AAS technique.

The techniques for measuring magnesium transport has progressed from labelled isotopes to the more precise and accurate use of ionophores. The ionophores were first recognised through their effect of stimulating every linked transport in mitochondria (Moore, Pressman, 1964, Pressman, 1963,1965). This not only provided a valuable tool for studies on the linkage between metabolism and transport, but also prompted extensive studies to provide insight into the molecular basis of ionophore action. Ionophores are compounds of moderate molecular weight (200-2000), that form lipid soluble complexes with polar cations of which K^+ , Na^+ , Ca^{2+} , Mg^{2+} and biogenic amines are the most significant biologically (Flatman, 1991).

The ion selectivity of ionophore on artificial thick membranes, have provided the technological basis for a novel series of ion selective electrodes. Many ionophores are now available as physiological tools to study membrane transport. The one of most

interest to researchers derives from the ability of the carboxylic ionophores X-537A and A23187 to transport the key biological control ion Ca^{2+} across the membranes (Pressman, 1976; Reed *et al*, 1972; Pfeiffer, Reed and Lardy, 1974). These findings eventually led to the administration of ionophores to intact animals to evaluate their pharmacological potential.

Ionophores in general may be regarded as molecules with backbones on diverse structures that contain strategically spaced oxygen atoms. The backbone is capable of assuming critical conformations that focus these oxygens about a ring or cavity in space into which a complexible cation may fit more or less snugly.

The liganding oxygen systems (filled in black) or representatives ionophores are shown in black in Fig A (Pressman, 1976).

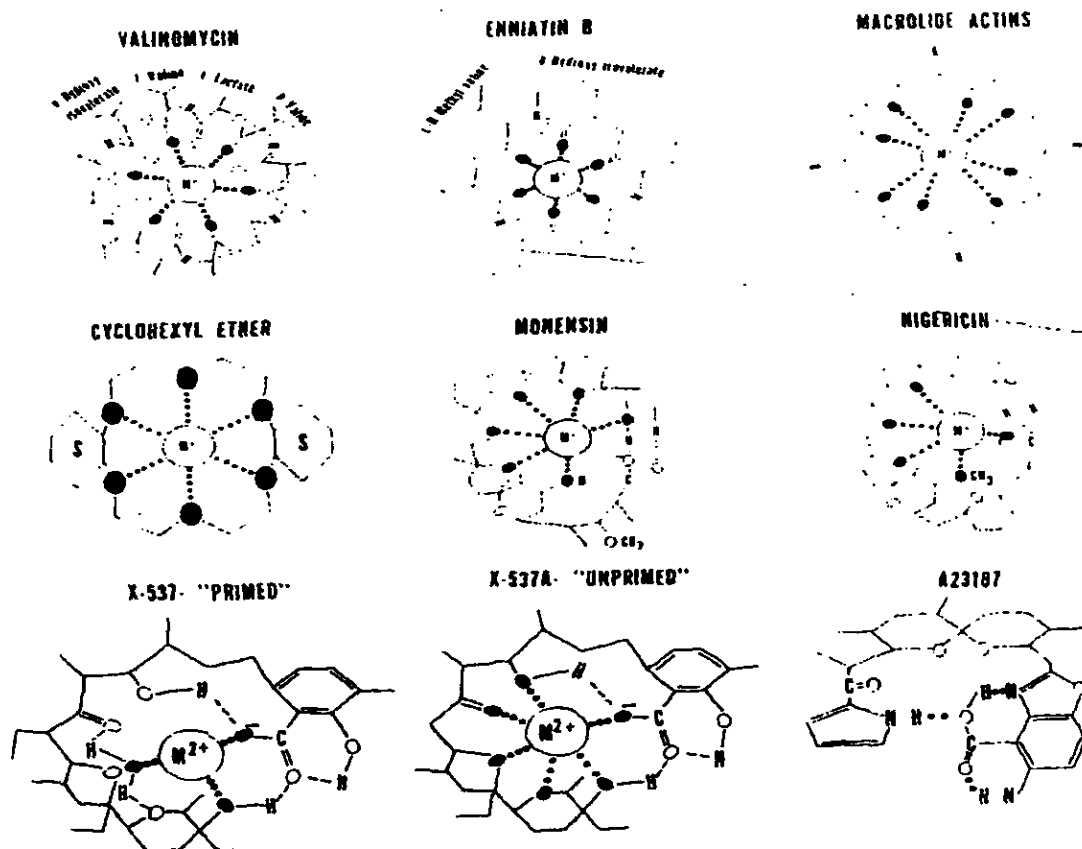


Figure A Structures of representative ionophores.

A23187 differs from X-537A in having a high selectivity for divalent over mono valent ions (Pfeiffer *et al*, 1974). If added to energised mitochondria, it causes the release of endogenous Mg^{2+} without corresponding depletion of Ca^{2+} or K^+ . A23187 also facilitates the entry of Ca^{2+} into erythrocytes (Reed *et al*, 1972).

A23187 releases energy linked accumulation of Ca^{2+} from vesicles derived from sarcoplasmic reticulum. This indicates that the Ca^{2+} is concentrated within the vesicles against a concentration gradient, rather than being bound at a low chemical activity by an energy linked mechanism (Caswell and Pressman, 1972; Entman, Gillette, Wallich, pressman and Schwartz, 1972; Scarpa, Balasserre and Inesi, 1972).

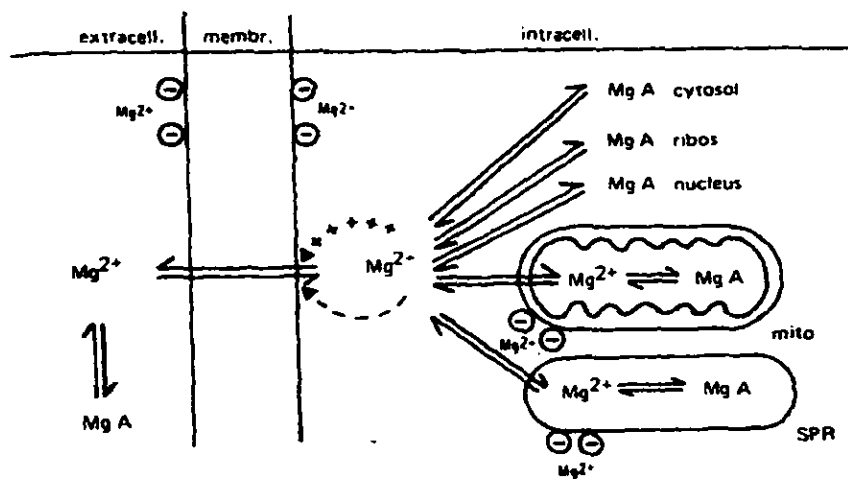


FIG. B Schematic representation of cellular Mg^{2+} metabolism. Part of the Mg^{2+} is bound (MgA), in the extracellular compartment mainly to albumin. Mg^{2+} can be transported into or out of the cell when the concentration of intracellular free Mg^{2+} is changed. +, Gating of net Mg^{2+} efflux when $[Mg^{2+}]_i$ is increased; -, feedback inhibition of net Mg^{2+} efflux when $[Mg^{2+}]_i$ reaches normal values. MgA cytosol, MgA ribos. and MgA nucleus, are Mg^{2+} bound in the cytosol, in ribosomes and the nucleus, respectively. Mito and SRP, mean that Mg^{2+} can be taken up and released from mitochondria or sarcoplasmic reticulum, respectively, and can be partly bound in these organelles. Moreover, Mg^{2+} is enriched at negatively charged groups (\ominus) of cellular membranes. (Reproduced with permission from Günther (1987).)

Fig B shows a general scheme of cellular compartmentation and metabolism of cellular Mg^{2+} .

1.13 Historical background on Atomic Absorbance Spectrometry (A.A.S)

The technique of Atomic Absorbance Spectroscopy (A.A.S) can be thought of having its origins in 1666 with Isaac Newton who used a prism to separate the colours of the solar spectrum. Wollaston in 1802 recorded his observation that dark lines in fact interrupted the spectrum of sunlight, which was at the time thought to be continuous. Later in 1814 Fraunhofer found a series of lines in the visible region of the solar spectrum and labelled the principal lines alphabetically without identifying their chemical origin.

In 1832, Brewster, who is associated with the invention of the kaleidoscope investigated the absorption of light by various vapours and suggested that Fraunhofer lines were due to certain vapours in the sun's atmosphere. Kirchhoff in 1860 deduced from Fraunhofer's results the presence of certain elements in the solar atmosphere and with Bunsen in 1861 laid the foundations of a new method of chemical analysis using flames. Fraunhofer and Kirchhoff had been observing atomic absorption and atomic emission, respectively.

In 1902 Wood illustrated the emission-absorption relationship by heating sodium in a partially evacuated glass bulb and irradiated the bulb with light from a sodium flame. He demonstrated an increase in absorption effect by heating the bulb more strongly. Wood named the lines emitted and absorbed by sodium atoms resonance lines and carried out experiments to show the possibility of using resonance effect to detect traces of mercury. This may have been the first analysis carried out by atomic absorption spectrometry.

In 1924 Angerer and Joos studied the atomic absorption spectra of metals in the iron group and Frayne and Smith in 1926 of indium, gallium, aluminium and thallium. Hughes and Thomas in 1927 studied the absorption and resonance effects of mercury. Lunegardh in 1928 demonstrated atomic emission spectroscopy (AES) in an air-acetylene flame using a pneumatic nebulizer. In 1930 Mueller and Pringsheim published an atomic absorption method of measuring mercury content of air thereby carrying on Woods original project of 1913 and 1919.

Walsh in 1955 and subsequently Alkemade in 1960 made the first real applications of atomic absorption spectroscopy to chemical analysis in the same year. They made significant contributions to the development of AAS as an analytical tool. They used the hollow cathode lamps as a line source, greatly reducing the resolution required for successful analysis. Their introduction of modulation into the system permitted the detector to distinguish between absorption and emission by atoms at the same wavelength. They also utilised the flame for atomisation.

1.13 (a) What is Atomic Absorption Spectrometry (AAS)?

Atomic absorption is a process involving the absorption by free atoms of an element of light at a wavelength specific to that element, or a more simplified it is a means by which the concentration of metals can be measured (Unicam, 1980).

In Atomic Spectrometry, emission and absorption, energy is put into the atom population by thermal, electromagnetic, chemical and electrical forms of energy and are converted to light energy by various atomic and electronic processes before

measurement. Atomic Absorption Spectrometry is useful not only for the identification but also the quantitative determination of many elements present in samples. The technique is specific, in that individual elements in each sample can be reliably identified and it is sensitive, enabling small amounts of an element to be detected down to around $1 \mu\text{g g}^{-1}$ (1ppm) i.e. one part in one million using simple flame procedures. Lower levels can be determined down to 0.001 ppm using procedures that are more sophisticated (Unicam, 1980).

When a sample or sample solution is burned in a flame or heated in a tube, the individual atoms of the sample are released to form a cloud inside the flame or tube. Each atom consists of a positively charged nucleus surrounded by a number of electrons in rapid motion around the nucleus. For each electron in each atom there is a discrete set of energy levels that the electron can occupy. The spacing of the energy levels is different for each electron in the atom, but for similar atoms corresponding electrons have identical spacing. The energy levels are usually labelled E_0 , the ground state, through E_1 , E_2 etc. to E_∞ . Fig C shows the general energy level states.

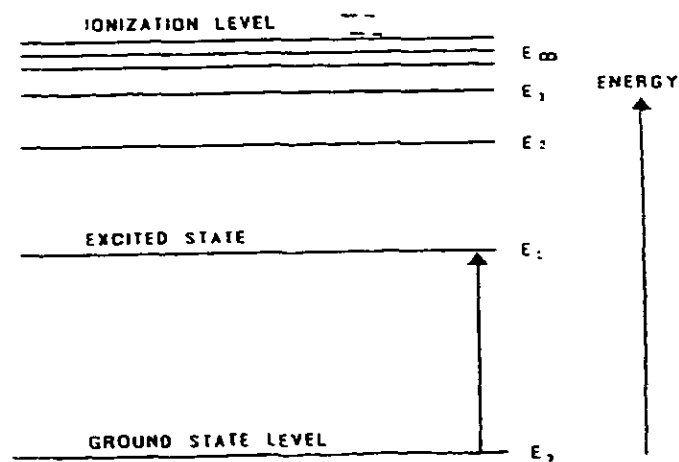


Figure C Energy level diagram

For an unexcited atom, each electron is in the ground state. To excite the atom, one or more electrons can be raised to the first or higher energy levels by the absorption of energy by the atom. This energy can be supplied by photons or by collisions due to heat. Those electrons furthest away from the nucleus require least energy to go from the ground state E_0 to the first energy level E_1 . The energy E corresponds to the energy gap between the ground state and the first energy level.

$$E = E_1 - E_0$$

The energy required for this transition can be supplied by a photon of light with energy given by:

$$E = h \nu$$

Where h = Planck's constant and ν the frequency.

This corresponds to a wavelength (λ) of:

$$\lambda = hc/E$$

where c is the speed of light in vacuum.

However, for all non-conducting elements (insulators) and for most of the electrons in the atoms of conducting elements, the energy gap $E_1 - E_0$, is very large and thus a very energetic photon, either in the vacuum, UV or x-ray region would be required to excite the atom. Metallic and metalloid elements contain so called valence electrons, which

are relatively loosely bound to the nucleus, and which can be excited by photons of wavelengths in the optical range 190-900 nm. For each atom of a metal or metalloid the energy gap E_1-E_0 for a particular valence electron is nearly identical. Furthermore the energy gap is not found in any other element. If light of sufficient narrow wavelength range, centred on

$$hc / (E_1-E_0)$$

is sent through a cloud of various atoms, only atoms of one particular element will absorb photons. Hence the selectivity of atomic absorption technique.

Atoms in the cloud move at high speed and collide with each other, and absorb over a very narrow range of wavelengths. The width of a typical absorption line is about 0.001nm. For atomic absorption purposes, an emission source with an emission line of the same frequency and a width of about 0.001nm is normally used. This requirement is usually satisfied by an emission spectrum of the element of interest, generated by a hollow cathode lamp (HCL).

Another requirement to obtain a high absorption signal is that atoms should be in the ground state and a large number of electrons should be able to be excited to the first state when a photon of correct frequency is absorbed. The general statement of the Maxwell-Boltzmann law gives the number of atoms in the ground state and the first excited state.

1.13 (b) The Boltzmann Distribution.

The electron in an excited atom involved in transitions to a higher energy level is that electron with the least energy. In chemical terms it is the valence electron. An electron can be promoted from the ground state to an upper excited state by heating a population of atoms. If a whole population of atoms is heated, the actual number of electrons in any particular orbit can be calculated by the Maxwell-Boltzmann equation. This states that if there are N_1 atoms in an excited state and N_0 atoms in the ground state, then

$$N_1/N_0 = (g_1/g_0) e^{-\Delta E/kT}$$

Where:

E = energy difference between the ground state and excited state.

T = the temperature of the atom population ° k.

K = Boltzmann constant

g_1/g_0 = statistical weights in energy states 0 and 1.

The law assumes that the population of atoms has a constant uniform temperature. It also assumes that the energy levels are single energy levels.

1.13 (c) The theory of Atomic Absorption Spectrometry.

This will be discussed using the wavelength region from 190-900 nm i.e. the ultra violet and visible regions.

1.13 (c i) Absorption.

The absorption of energy by atoms follows well-known physical laws, which provide us with a basis for quantitative analytical chemistry. The radiant energy or photons, absorbed by atoms are generally in the form of very narrow lines of characteristic wavelength originating from the visible or ultraviolet spectrum. During the absorption process the outer valence electrons of the atoms are promoted to a higher orbital and the atom is electronically excited. There is a relationship and equilibrium between the populations of excited and unexcited atoms involving photons, and between atomic absorption and atomic emission spectroscopy (Unicam, 1980).

A photon behaves in a similar manner to an alternating electric field and interacts with the negatively charged electrons in an atom. Under certain conditions, an atom can absorb a photon. The energy levels in an atom are quantized; i.e. they have certain well-defined energies. As a consequence of this, the photon energy, $h\nu$, must be exactly equal to the energy gap between a filled energy level E_0 the ground state, and an unoccupied energy level E_1 the first energy state, as represented below Fig D:

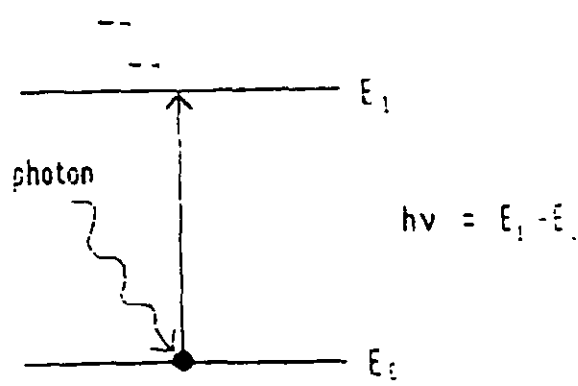


Figure D Absorption process

The wavy arrow in fig D represents a photon colliding with and being absorbed by a ground state atom E_0 . The vertical arrow represents the simultaneous excitation of the atom from ground state E_0 to the excited state E_1 . This process involves an electron being promoted from a filled atomic orbital to a more energetic orbital, normally unoccupied. An over simplified Bohr Orbit diagram can describe the absorption process (fig E).

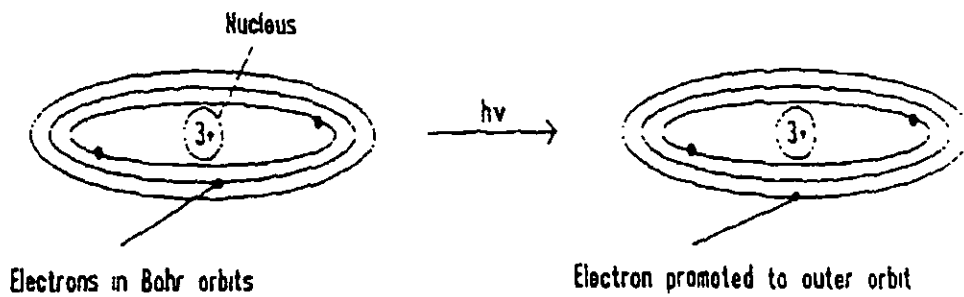


Figure E Bohr orbit representation of light absorption by a lithium atom

This is a simple representation of absorption, as transitions between orbitals within the same electronic shell can be induced, as well as transitions between different electronic shells. An example of the former, is the promotion of an electron in a 4s orbital in a potassium atom to the orbital by light of wavelength 766.5nm.

1.13 (c ii) Emission.

The process of emission is the reversal of absorption. The atom in an excited energy level can revert to the ground state by emitting as a photon (fig F).

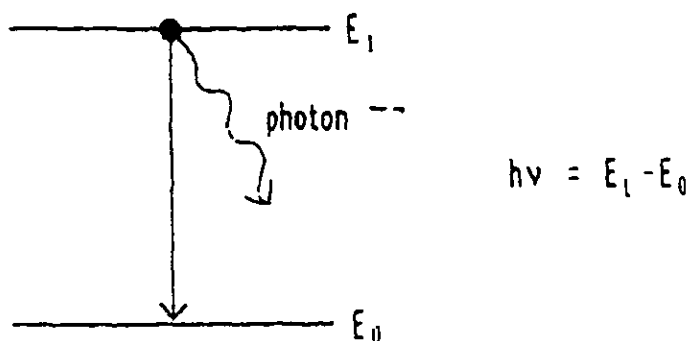


Figure F Emission process

The photon of energy $h\nu$ is equal to the energy gap ($E_1 - E_0$). The emission of a photon when the electron moves to the unexcited state from the excited state forms the basis

of emission spectroscopy. In this technique the light generated in the emission process is measured at a specific wavelength. In any atom there are a numerous permitted energy levels and numerous transitions permitted between different excited energy levels and the ground state. The existence of numerous upper excited states means that the equilibrium between ground state atoms and excited atoms is not as simple as the diagram shows (Fig F).

1.14 Nuclear Magnetic Resonance (NMR) and its application to study ion transport.

Nuclear magnetic resonance (NMR), a spectroscopic technique that measures magnetic nuclei and their environment, has gained considerable success and popularity in studying the dynamic state of inorganic ions and organic metabolites in whole and isolated living cells, tissues, and organs (Balschi, Cirrillo and Springer, 1982, Civan, Degani Margalit and Shporer, 1983). The main advantage of NMR is that it is non-invasive, so that ionic and metabolic changes in the cellular environment can be observed as they take place within an essentially unperturbed living system. With the introduction of sophisticated and continuously improving high field superconducting spectrometers, the NMR technique is approaching the status of a common, non-invasive analytical tool for cellular studies and research (Gupta and Gupta, 1984).

The work of Moon and Richards in 1973 on human red blood cells appears to be the first published account of a high resolution NMR spectrum of a cell system. There have been notable advances during the last few years, the most outstanding have been the applications of NMR to the study of intracellular pH, free Mg^{2+} , free Ca^{2+} , free Na^+

and K^+ ions, and the application of NMR to the study of ^{31}P metabolites in human (Balschi *et al*, 1982, Gadian, 1983).

Intracellular metal ions (Na^+ , K^+ , Mg^{2+} , Ca^{2+} ,) and pH appear to modulate a variety of cellular and tissue functions (Boynton, McKeehan and Whitfield, 1982; Nuccitelli and Deamer, 1982). Exploration of possible regulatory roles of these ions in cellular proliferation, differentiation, volume regulation, and hormonal control of various cellular processes as well as understanding how the concentrations of intracellular ions are managed by various membrane transport processes is important. It may aid in the understanding of how such regulation goes astray in disorders such as cancer (Cameron, Smith, Pool and Sparks, 1980; Gupta and Gupta, 1982), hypertension (Blaustein, 1977, and Hamlyn, Ringel, Schaeffer, Levinson, Hamilton, Kowarski and Blaustein, 1982), and sickle cell disease (Tosteston, 1955). NMR spectroscopy has provided a unique non-invasive tool for such studies.

The information available from NMR often complements that available from other techniques. Unlike the atomic absorbance spectroscopy, NMR may in suitable cases provide information on free ions. Absorption and flame emission techniques that yield the total amounts of various ions in a cell.

1.14 (a) Intracellular Free Mg^{2+} in living cells.

Since Mg^{2+} ion plays an important role in the diverse biochemical reactions occurring within a cell, knowledge of cellular free Mg^{2+} level is essential for an accurate understanding of a functioning intact cell. It is relatively easy to measure total Mg^{2+} content of a cell by atomic absorption techniques; such is not the case for the

measurement of free Mg^{2+} . A non-invasive ^{31}P NMR technique for determining free Mg^{2+} in intact cells has been used.

1.14 (b) ^{31}P NMR Measurement of intracellular Free Mg^{2+} .

The ^{31}P NMR technique for measuring free Mg^{2+} is based on an accurate measurement of the frequency difference between the αP and βP resonances in the ^{31}P NMR spectrum of intracellular ATP. Because the positions of the ^{31}P resonances of frequencies of phosphorus groups of ATP in an NMR spectrum depend on its state of complexation with Mg^{2+} (the predominant divalent cation component of the cell), the NMR spectrum allows a determination of the fraction of total ATP that exists as the Mg^{2+} complex as well as total Mg^{2+} . An accurate knowledge of the dissociation constant of $MgATP$ (K_D^{MgATP}) under simulated intracellular ionic conditions then yields free Mg^{2+} directly from the NMR spectral data (Gupta, 1980; Gupta, Benovic and Rose, 1978).

For a comparison of the measured Mg -dependent separation between the αP and βP resonances of intracellular ATP ($\delta_{\alpha\beta}^{ATP}$) and $MgATP$ ($\delta_{\alpha\beta}^{MgATP}$) controls under simulated intracellular ionic conditions and pH, by calculating a value of ϕ , which is defined as the fraction of total ATP not complexed to Mg^{2+} according to the following equation:

$$\phi = ([ATP]_f) / ([ATP]_T) = (\delta_{\alpha\beta}^{cell} - \delta_{\alpha\beta}^{MgATP}) / (\delta_{\alpha\beta}^{ATP} - \delta_{\alpha\beta}^{MgATP}).$$

As long as only a single set of resonances is observed, consistent with fast exchange averaging of the resonances of ATP and $MgATP$, the frequencies of phosphorus resonances reflect the state of Mg^{2+} complexation of ATP. Misawa, Lee and Ogawa

(1982), noted that at higher ^{31}P NMR frequencies (≥ 145 MHz) and lower temperatures ($\leq 10^\circ\text{C}$), the assumption of rapid exchange of ATP and MgATP may not entirely be valid.

The following equation is then used to derive a value for free Mg^{2+} in the intact cell directly from the spectral data:

$$[\text{Mg}]_f = K_D^{\text{MgATP}} \{(1/\phi)-1\}.$$

An important assumption which is implicit in the application of this technique to intact cellular systems is that the chemical shifts of the ^{31}P resonances of intracellular ATP respond to the presence of Mg^{2+} in a manner similar to that observed for total ATP. Many cell systems have been examined, in which much of the total cellular ATP is complexed to Mg^{2+} , the critical part of the assumption states that, upon saturating cells with Mg^{2+} , the separation $\delta_{\alpha\beta}^{\text{cell}}$ will decrease to that observed in isolated MgATP. Gupta in 1980 tested this assumption by saturating oxygenated erythrocytes with a high level of internal Mg^{2+} (~ 10 $\mu\text{mol/ml}$ cells). The observed separation between the αP and βP resonances changed from its value of 353 ± 1 Hz at 40.5 MHz and 37°C in unperturbed oxygenated erythrocytes to a value of 338 ± 1 Hz, indistinguishable from that observed in extracellular MgATP control 337 ± 1 Hz under simulated intracellular ionic conditions. Similar shifts for the intracellular MgATP in human erythrocytes and extracellular MgATP control have been observed which indicate, that the shifts of the ^{31}P resonances of the red cell ATP are determined primarily by the normal interactions of Mg^{2+} and ATP. The validity of the ^{31}P NMR method for determining free Mg^{2+} in the red cells suggests that it is likely to be valid in other cell types as well.

1.14 (c) Application of the ^{31}P NMR method for free Mg^{2+} determination.

Intracellular free Mg^{2+} has been measured by the NMR procedure in human normal and sickle red blood cells (Gupta *et al*, 1978), frog skeletal muscle (Gupta *et al*, 1980), Ehrlich ascites tumour cells (Gupta *et al*, 1980), murine lymphoma cells (Erdos and Maguire, 1983), human lymphocytes (Rink, Tsien and Pozzan, 1982), dog erythrocytes (Wyrwicz, Schofield and Burt, 1982), perfused and ischemic heart muscle (Gupta, Gupta, Yushok and Rose, 1983), rabbit urinary bladder and uterus smooth muscles (Dillon, Meyer and Kushmerick 1983), and in amphibian oocytes (Morrill, Kostellow, Weinstien and Gupta, 1983).

Gupta *et al*, 1984 concluded that low availability of Mg^{2+} would limit the rates of cellular reactions in which the substrate is the Mg^{2+} complex of ADP or another compound that binds Mg^{2+} weakly. Low cellular free Mg^{2+} levels support an important role for Mg^{2+} in the regulation of metabolic processes in agreement with the Mg^{2+} - co-ordinated control of metabolism and growth proposed by Rubin and co-workers (Rubin, 1975; Rubin, Terasakai and Sanui, 1979).

1.15 Role of Mg^{2+} in Platelet Aggregation.

1.15 (a) Platelet Aggregation

1.15 (a i) Platelets

Platelets or thrombocytes, though non-nucleated and, thus, strictly speaking, not entitled to be classified as cells, are capable of a complex variety of reactions, which are essential for haemostasis and important for the healing of damaged blood vessels.

Platelets are small, non-nucleated disc-shaped bodies derived from megakaryocytes in

the bone marrow and present in the blood at a concentration of 150,000 to 400,000 per μl . They are about 0.8 microns in depth and 2.3 microns in diameter, and they contain mitochondria, a complex system of tubules and three sorts of granules- dense granules, alpha granules and lysosomes. The plasma membrane has an external coat consisting of protein and glycosaminoglycans (mucopolysaccharides); it contains two glycoproteins - IIb and IIIa - which are important in platelet aggregation.

1.15 (a ii) Aggregation

Platelets and their interaction with the vessel wall are important for the initiation and development of arterial thrombosis (Fuster, Steele and Chesebro, 1985) and several pharmacological treatments have been introduced to obtain an efficient platelet inhibition. Rupture of an arteriosclerotic plaque may trigger thrombus formation (Falk, 1992). When the surface of a plaque ruptures, platelets adhere and become activated to release proaggregatory and vasoconstricting substances (Kristensen, Martin, 1991). The primary thrombus formed in the artery consisting of platelets, but activation of the coagulation system leads to the formation of a platelet fibrin clot. A predisposing factor in the development of arterial thrombosis is now platelet hyperreactivity (Fuster, Steele and Chesebro, 1985; Nadler, Malayan, Luong, Shaw, Natarajan and Rude, 1992). Moreover that Mg^{2+} has shown beneficial effects in the treatment of patients with acute myocardial infarction (MI) (Teo, Yusuf, Collins, Held and Peto, 1991; Woods, Fletcher, Roffe and Haider, 1992; Shechter, Hod, Chouraqui, Kaplinsky and Rabinowitz, 1995) and preeclampsia (Watson, Moldow, Ogburn and Jacob, 1986), which are conditions associated with increased platelet activity, indicates a possible anti-platelet effect of magnesium.

1.16 Role of Mg²⁺ in Platelet Aggregation

Mg²⁺ is known to inhibit experimental arterial thrombus formation (Acland, 1972; Adams and Mitchell, 1979; Gertz, Rebecka, Wajnberg and Uretzky, 1987). This could be caused by decreased platelet accumulation, but may also result from increased thrombus dispersion due to enhanced fibrinolytic activity. In vitro studies have demonstrated that Mg²⁺ is able to inhibit platelet aggregation in a dose dependent manner (Watson *et al*, 1986; Hwang, Yen and Nadler, 1992; Gawaz, Ott, Reininger and Neumann, 1994; Ravn, Vissinger, Kristensen and Husted, 1996). It has recently also been demonstrated that the platelet inhibitory effect of Mg²⁺ in vitro is present at low, clinically applicable concentrations (Ravn *et al*, 1996) and this encouraged Ravn *et al*, (1996) to look for a possible effect of Mg²⁺ on platelet activity following intravenous administration.

1.17 Use of BIODATA Platelet Aggregation.

Platelet aggregation is measured routinely in clinical laboratories using a BIODATA Platelet aggregation profiler (Figs Ga and Gb).

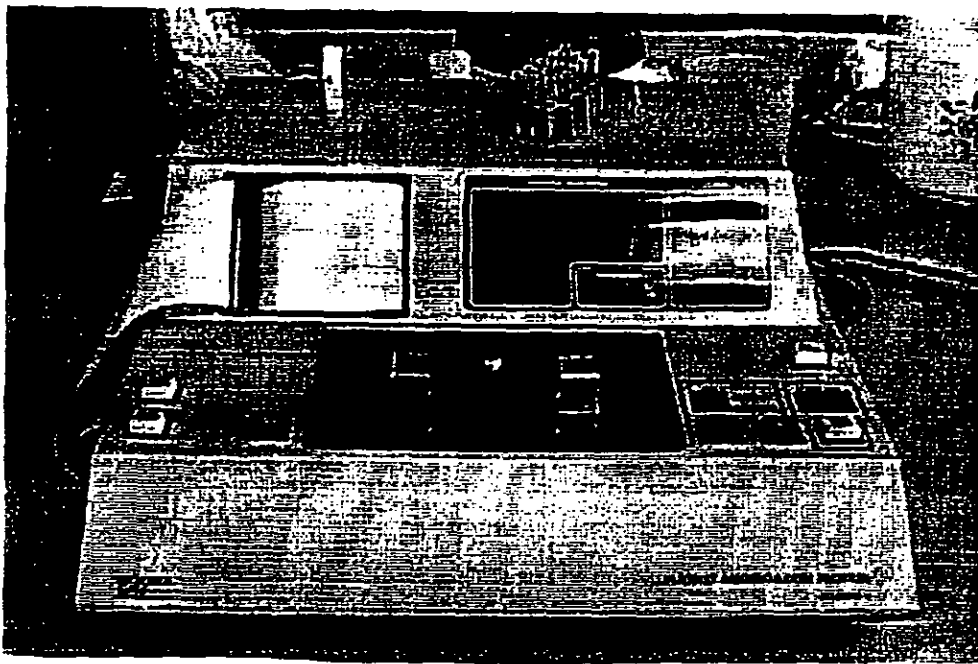


Fig Ga Photo of BIO/DATA PLATELET AGGREGATION PROFILER MODEL PAP-3.

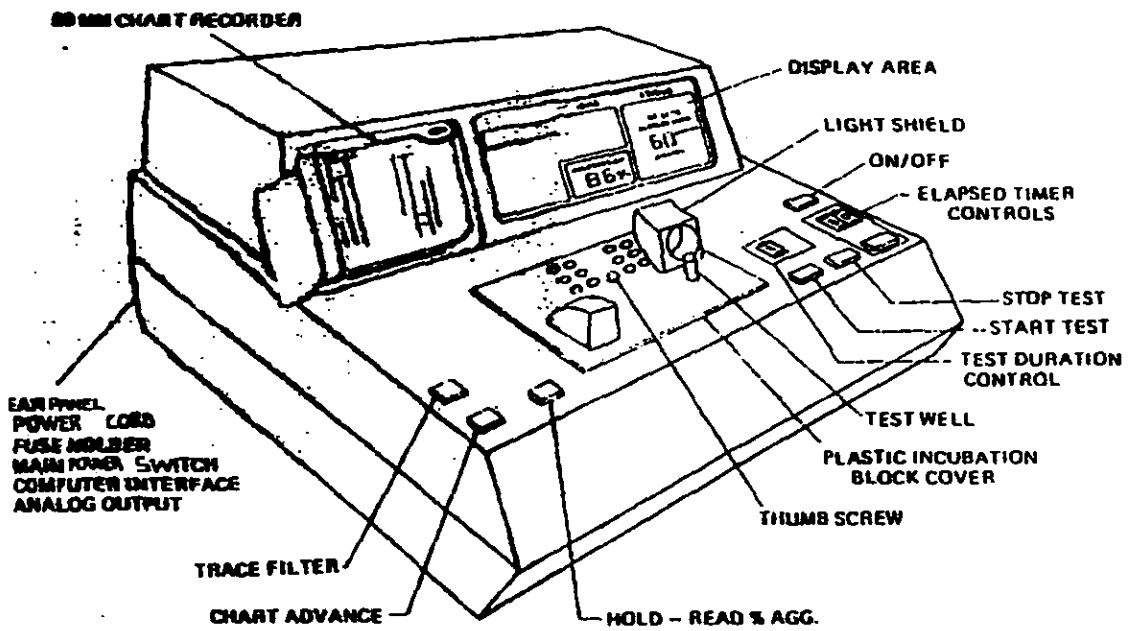


Fig Gb BIO/DATA PLATELET AGGREGATION PROFILER®
MODEL PAP-3

1.18 Use of the BIO DATA Platelet profiler (model PAP-3) in Aggregation.

BIO/DATA Platelet Aggregation Profiler, model PAP-3, operates via a photo-optical scanning system, a continuous differential amplifier system and an automatic recorder calibration and standardisation system.

The operation involves two samples of the plasma. One sample is platelet -rich plasma (PRP), and the other platelet poor plasma (PPP). These are inserted into the labelled optical test wells. The PAP-3 utilises the difference in optical density between the PRP and PPP and determines whether the platelet count is correct for proper testing. If the platelet count is too high or too low, the appropriate warning indicators are activated alerting the operator to the problem and the correct action to be used.

Following the insertion of the plasma samples, light received through the test specimens by the photo detectors are transformed into electrical signals, which are continuously and differentially compared and then amplified. The final amplified signal is split into two components, with the first component fed into the galvanometer-actuated recorder from which the aggregation curve is generated. The patented control and standardisation circuitry automatically adjusts the recorder for the full-scale deflection based upon the initial optical density levels of the test samples. This removes the need to establish or re-establish the chart baseline.

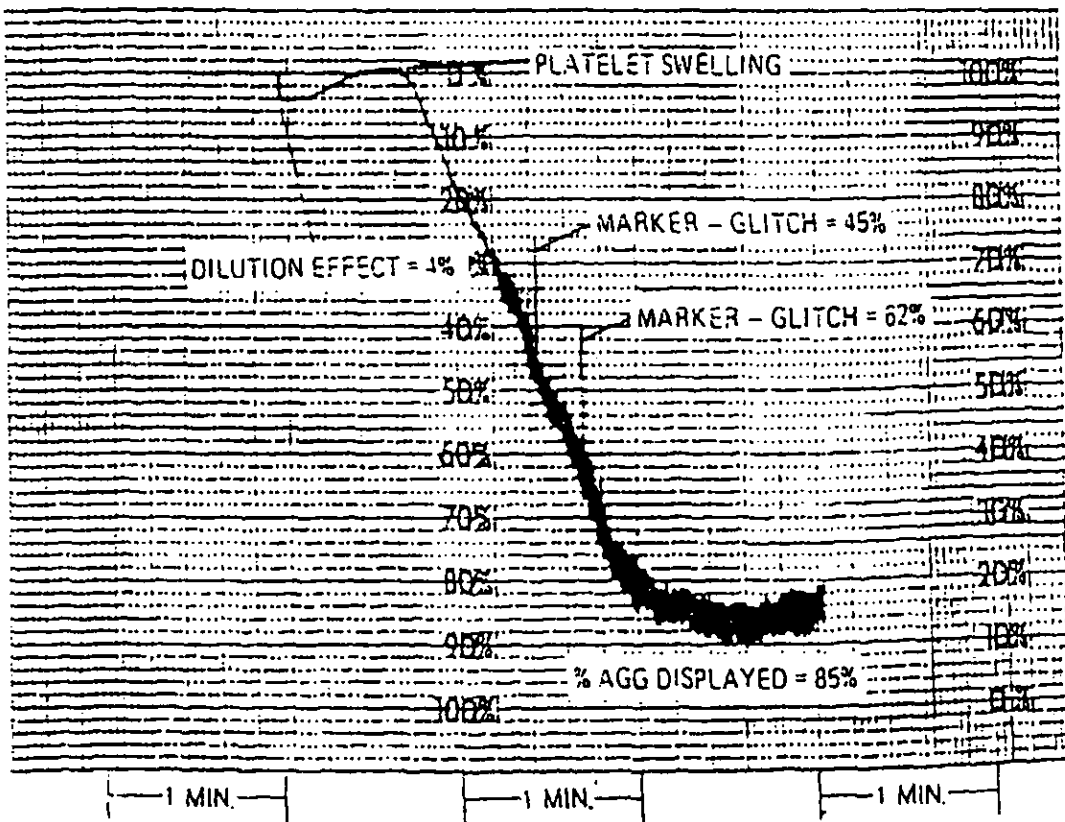
The second part is fed simultaneously into a micro processor where it is electronically measured, converted to numerical values and then displayed on a continuous basis, as the aggregation curve is generated. At the end of a defined test, the final total aggregation is displayed until the next test is initiated.

The chart paper is moved at a constant rate of 25 mm min^{-1} and is made of a heat sensitive material. This then removes the requirement of an ink system (Fig H). The actual aggregation pattern may be displayed as either a filtered or unfiltered trace. In the unfiltered trace, the curve trace contains oscillations, which are related to aggregate size and shape, while in the filtered trace the curve trace is free of the oscillations and the resultant line is then based upon the arithmetic average of the oscillations.

The PAP-3 works at a constant fixed temperature of 37°C ; this is monitored and controlled automatically. The machine cannot operate until this temperature is reached. The PAP-3 has a digital display, which presents a step by step method of operation.

1.19 Percentage (%) Aggregation.

All aggregation patterns that are produced by the PAP-3 are automatically and continuously analysed for the percentage (%) aggregation beginning when the START TEST button is depressed and continuing until the PRP scan is stopped either manually or automatically. (A typical trace is shown in fig H), (Bio/Data corporation, 1974).



EXAMPLE

Base Line = 0%.

Dilution Effect = 4%.

Total Aggregation = 85%.

Absolute % Aggregation = Total Aggregation - Dilution Effect.

Absolute % Aggregation = 85% - 4% or 81%.

Fig H shows an original chart recording of platelet aggregation in a sample of blood.

Caution has to be employed to maintain a standard set of experimental conditions and protocol. The PAP-3 cannot be standardised if any of the following exist in either a combination or as a single condition: -A stir bar is not inserted into the platelet rich specimen before testing. The instrument cannot be standardised due to insufficient difference in the optical density of platelet-rich versus platelet-poor samples as a result of low initial platelet count or improper centrifugation.

Platelet aggregation is the most useful in-vitro test of platelet function presently available (Day and Holmsen, 1972). Platelet aggregation is clinically significant in the detection and diagnosis of acquired or congenital qualitative platelet defects. The platelet's ability to respond to particular aggregating agents is the basis for differentiating platelet dysfunctions. (Marcus and Zucker, 1965).

1.21 Preparation of Plasma.

The collection, handling and preparation of the plasma sample particularly the plasma-rich plasma is extremely important and must therefore be performed with precision. Failure to follow proper procedures result in poor or erroneous test results. All blood samples must be collected and handled in plastic containers. It is important that under no circumstances glass syringes or other glass containers be used, as the platelets will adhere to them.

1.22 Aims of this study.

This study was designed mainly to characterise Mg^{2+} transport in Mg^{2+} -loaded erythrocytes and to investigate the role of Mg^{2+} in platelet aggregation.

The specific aims are: -

- (a) To measure plasma and erythrocyte Mg^{2+} and other cation concentrations using atomic absorption spectroscopy method. Initial experiments involved the use of blood from pig in order to establish the technique and a good working hypothesis. Subsequent experiments involved the use of human blood both in control and in patients who have acute renal failure.

- (b) To characterise Mg^{2+} transport on erythrocytes taken from both pig and human using a number of transport inhibitors.
- (c) To investigate the role of Mg^{2+} in platelet aggregation in blood taken from both pig and human. Blood from the pig was employed mainly to establish the technique.
- (d) To measure Mg^{2+} concentration in erythrocytes in whole blood using NMR technique.

2.1 Materials for Mg²⁺ transport

Mg²⁺ standards (0, 0.625, 1.25, 2.5, 5 and 10 mM). Samples of plasma and erythrocytes. An atomic absorption spectrophotometer (model Unicam 929) set at 285.2 nm. Solutions such as (Mg²⁺-loading solution, Mg²⁺-free solution, washing solution, calcium ionophore A23187 at concentration (10⁻⁶ M), 10 % TCA/0.175 % LaCl₃) (see appendix III for recipes and contents of each solution including physiological salt solutions). In addition, the Sherwood flame photometer (model 410) and Cl⁻ titrator (model Jenway) were also employed in this study. Reagents for these techniques include Na⁺ (100 mmol), K⁺ (5 mM), Cl⁻ (100 mmol), distilled water, Gilson pipette (p 20).

2.2 Materials for platelet aggregation

Plasma of type Platelet rich plasma (PRP) and platelet poor plasma (PPP), a magnetic stirrer bar and a BIO DATA platelet aggregation profiler of type PAP-3.

Drugs used in this study: Adenosine diphosphate (ADP), amiloride and *N*-methyl-D-glucamine (NMDG).

2.3 General procedure. Fresh Pig and human blood samples were obtained routinely from the local abattoir and from Royal Preston Hospital, respectively. The pig blood was collected in plastic bottles containing 0.4% sodium citrate (anticoagulant), whereas the human blood from the hospital was collected in 10 ml heparinised tubes. The blood was centrifuged at 2750 rpm at room temperature for 7 min to separate the plasma from the red blood cells. The plasma was employed to measure the concentration of such ions Na⁺, K⁺, Ca²⁺, Mg²⁺, Cl⁻ whereas the erythrocytes or red blood cells were used to measure Mg²⁺ transport. In some experiments, Ca²⁺

transport was also measured for comparison. In the experiments involving platelet aggregation, the blood was centrifuged to obtain platelet rich plasma (PRP) and platelet poor plasma (PPP) and the hospital method was used to measure aggregation.

2.4 Loading of pig and human erythrocytes with Mg²⁺

Either human or pig blood was centrifuged at 2750 rpm for 7 min. The plasma portion was obtained for the assay of ions. The remaining plasma and buffy coat was discarded and a sample of unloaded erythrocytes was retained for Mg²⁺ measurement and protein assay. A 10% cell suspension sample of remaining erythrocytes were loaded with Mg²⁺ (12 mM MgCl₂) in the presence of 10⁻⁶ M calcium ionophore (A23187), incubated for 30 min at 37°C in a shaking water bath. After the loading process the cells were centrifuged for 7 min at 2750 rpm, and the supernatant discarded. The residue pellet was then resuspended in medium (composing of 140 mM KCl, 50 mM sucrose, 5 mM glucose, 30 mM Hepes / Tris pH7.4, 12 mM MgCl₂ and 1% bovine serum albumin (B.S.A)) and centrifuged at 2000g for 5 min to remove the calcium ionophore. This process was performed 3 times. Loaded erythrocytes were retained for Mg²⁺ measurement and protein assay. The Mg²⁺ efflux was measured by reincubating a 10% cell suspension of loaded erythrocytes at 37°C in a control Mg²⁺ free NaCl (140 mM) medium (composing of 140 mM Na⁺, 50 mM sucrose, 5 mM glucose and 30 mM Hepes / tris pH 7.4) at 5, 10, 20 30, 40, 50 min intervals. Following the efflux duration samples of the cell suspension were centrifuged at 2750 rpm for 7 min. The supernatant of each aliquot was retained for Mg²⁺ measurement and the pellet for protein assay. At the end of the 50 min efflux period the erythrocytes were also assayed for Mg²⁺ to determine the remaining cellular Mg²⁺. In some experiments the same procedure was repeated by substituting the NaCl in Mg²⁺ free medium with either NMDG or 10⁻³ M amiloride.

2.5 Measurement of Mg²⁺ using Atomic absorbance spectroscopy method (AAS)

Mg²⁺ in either plasma or erythrocyte efflux samples were measured using atomic absorbance spectrophotometry (AAP).

The AAP was set up for Mg²⁺ measurement (lamp 4 and wavelength 285.2 nm). It was standardised with distilled water and then the Mg²⁺ standards were aspirated for 3 sec beginning with the most dilute i.e 0.625 mM up to 10 mM. The readings were used to convert the absorbance into units of Mg²⁺. The sample was collected by centrifugation of the whole blood at 2750 rpm for 7 min. the plasma was then treated with solid 5% tetrachloroacetic acid (TCA), it was centrifuged at 2500 rpm for 5 min and the supernatant kept and residue discarded. A 1:100 dilution using 10% TCA and 0.175% lanthium chloride solution was performed to the supernatent and then tested via AAS. For the erythrocytes 100 µl of erythrocytes were used to which 2 ml of 10% TCA solution was added and centrifuged as for the plasma. The same was then done to the supernatant and tested with the AAS. All values were expressed as net Mg²⁺ flux (µM /100 mg cell protein)⁻¹).

2.6 Protein Assay: Assay of protein using BioRad method

Protein standards of the range 0 mg ml⁻¹ - 25 mg ml⁻¹ were made using bovine serum albumin (BSA) and diluting with 1% triton X-100. Using a Gilson pipette, 100 µl of each standard was transferred into a 5 ml test tube. Reagent A (alkaline copper tartrate solution) was added at a volume of 500 µl to each standard and each tube was

immediately vortexed (mixed) for 5 sec. Using a pipette, 4 ml of reagent B (dilute Folin Caicaltean Reagent) was added to each standard and the mixture was vortexed for a further 5 sec. The standard mixtures were allowed to stand for 15 min prior to testing using a spectrophotometer (Parmacia LKB, Novaspec II) set at absorbance of 750 nm. The samples were used to produce a calibration curve. A sample of 1 % Triton X-100 was used to blank the machine. The samples were also treated in the same way and the calibration curve was used to determine their protein content.

2.7 Measurement of Cl⁻ using Cl⁻ titration

A Jenway PCLM 3 model Cl⁻ titrator was used for the measurement of Cl⁻ in the samples. Using a pipette 15 ml acid buffer was added to a titration pot. To this 10 drops of gelatin solution were added and the mixture stirred. Using a Gilsons pipette, 20 µl of 100 mmol Cl⁻ was added to the mixture and the titrator conditioned for 2 sec by pressing "Condition". The display increased above 100. Another 20 µl of 100 mmol Cl⁻ was added and the titrator conditioned again for another 2 sec. The display reading was ~100, hence the titrator was calibrated. Sample of volume 20 µl was added and this time "Titrate" was pressed to engage titration. The theory of Cl⁻ titration is based upon the principle that a constant current is passed between the two silver electrodes which then liberate silver ions at a constant ratio into the solution. These silver ions combine with the chloride ions in the solution and are precipitated as insoluble silver chloride. When all the chloride has combined with the generated silver, free silver ions become available in the solution and their presence was detected by two further silver electrodes. All values were expressed in mM values.

2.8 Measurement of Na⁺, K⁺ and using flame photometry

The Sherwood flame photometer (model 410) was standardised using distilled water which was aspirated into the flame for 20 min. The correct filter was selected and Na⁺ and K⁺ standards of 100 mmol and 5 mM were then used, respectively to standardise the flame photometer. The samples were then diluted 10 times and then tested. All values were obtained in mM values.

2.9 Platelet Aggregation Method

The precise operational method is shown in appendix I. Our modifications to the Corporation protocol were to collect 10 ml of blood in a plastic syringe and dispense into a 10 ml lithium heparin polypropylene tube (LiP equipment Ltd, Catalog No: 71038 LH10 PP/WSC). The tube was capped with the screw cap and gently inverted to mix the solution. The platelet rich plasma (PRP) was prepared by centrifugation at 800 RPM AT 25°C, for 5 min. The centrifuge was allowed to stop gradually by removing the braking system, the plasma was checked for the absence of erythrocytes. If any erythrocytes were present the sample was re-centrifuged for 5 min. A Gilson and a plastic tip were used to transfer the PRP into a plastic Elkay graduated 10 ml pro mailing tube. The tube was sealed with the polyethylene screw cap and allowed to stand for 60 min at room temperature. The platelet poor plasma (PPP) was prepared by re-centrifugation of the sample at 2750 R.P.M for 20 min. The tube was removed from the centrifuge and the PPP was transferred using a Gilson pipette into another mailing tube and capped. The plasma samples were then tested within 2 hours of collection. The % of aggregation was displayed on a chart recorder which was built into the aggregator. The original chart recordings were used to calculate the mean

±standard error of the mean (SEM) % of platelet aggregation. In some experiments the original chart recordings were in the result section.

2.10 NMR method

Whole blood was carefully transported on ice (4°C), and placed in a NMR tube containing Heparin. Deuteriated water (D₂O) was added for the magnet to lock onto. It was then exposed to NMR via a magnet. A fully automated computer program was used to perform the experiment. (see appendix IV for details).

2.11 Statistical Analysis

All results are presented as mean ± standard error of the mean (SEM). Values were compared using the Student's t - test and only values with P < 0.05 were taken as significant. In this study 96 samples of pig blood, 10 samples of human control and 12 samples of patients with acute renal failure were employed. In some experiments involving platelet aggregation samples of original chart recordings were also given.

Chapter Three

Results

The results are subdivided into four parts

(a) Plasma ion level

(b) Characterisation of Mg²⁺ transport

(c) Platelet Aggregation

(d) NMR study

3.1 Cations and Anion concentrations in plasma

Tables 1 and 2 show the concentration of the cations Na^+ , K^+ , Mg^{2+} and Ca^{2+} and the anion, Cl^- in plasma of either pig (Table 1) and healthy human controls and pre- and post-dialysis patients (Table 2). The results show that Na^+ concentration was lower in pig compared to healthy human. In contrast, in pre-and post-dialysis patients, Na^+ concentration was almost treble. The results also show that K^+ was lower in pig compared to healthy human. However, in pre-and post-dialysis patients K^+ concentration was 20 times higher compared to pig, but similar when compared to human controls. The results show that Ca^{2+} was 45 times lower in pig compared to healthy human. In pre-and post-dialysis patients, Ca^{2+} was also similar compared to healthy human. The result show Mg^{2+} was 17 times lower in pig compared to healthy human. In contrast, in pre-and post-dialysis patients, Mg^{2+} was slightly lower than in healthy human. It is particularly noteworthy that plasma samples for pig were analysed in our laboratories using the techniques of AAS, flame photometry and Cl^- titration, whereas plasma samples for human control and pre- and post-dialysed patients were analysed using a colorimetric method on equipment housed in the clinical laboratory at Royal Preston Hospital.

3.2 Net Mg^{2+} efflux in Mg^{2+} loaded pig erythrocytes

Figure 1 shows the mean \pm SEM concentration of Mg^{2+} in pig erythrocytes before loading (a), following loading with 12 mM MgCl_2 in the presence of 10^{-6} M A23187 (b) and following efflux of Mg^{2+} for 50 min (c). The results show that unloaded erythrocytes contain a basal Mg^{2+} level of $0.01 \pm 0.001 \mu\text{M}$ (100 mg cell protein) $^{-1}$ n= 96. Following loading for 30 min, Mg^{2+} level was elevated in erythrocytes to $0.06 \pm 0.01 \mu\text{M}$ (100 mg cell protein) $^{-1}$, n=96. After 50 min of incubation of Mg^{2+} -loaded erythrocytes, Mg^{2+} levels decreased to $0.042 \pm 0.01 \mu\text{M}$

(100 mg cell protein)⁻¹, n=96. The study has demonstrated that erythrocytes can take up Mg²⁺ during loading and they can lose the Mg²⁺ during incubation in a Mg²⁺ free medium. The results show a significant (P < 0.05) decrease in Mg²⁺ during incubation for 50 min, however, Mg²⁺ still remained high within the erythrocytes even after 50 min of efflux.

Figure 2 shows the time course of net Mg²⁺ (solid diamonds) and Ca²⁺ (solid squares) effluxes for Mg²⁺-loaded pig erythrocytes. The results show that there was a rapid and large increase in Mg²⁺ efflux over the first 5 min and this level remained the same after 50 min. In contrast, Ca²⁺ efflux occurred gradually reaching around 0.006 ± 0.0002 μM (100 mg cell protein)⁻¹, n = 96 after 50 min. The level of Ca²⁺ in unloaded erythrocytes was 0.01 ± 0.001 μM (100 mg cell protein)⁻¹, n=96.

Figure 3 shows the time course of net Ca²⁺ efflux for Mg²⁺ loaded erythrocytes in control (normal Mg²⁺ free solution, solid diamonds) and in Mg²⁺ free solution containing either NMDG (solid square) or 10⁻³ M amiloride (solid triangle). The results show that erythrocytes can release Ca²⁺ in a time dependent manner. However, in the presence of either amiloride or NMDG Ca²⁺ efflux was much higher compared to control. The efflux in amiloride was twice the values compared to the presence of NMDG.

The time course of net Mg²⁺ efflux from Mg²⁺-loaded pig erythrocytes in the absence (solid diamonds) and presence of either 10⁻³ M amiloride (solid triangles) or NMDG (solid squares) is shown in Figure 4. The results show that there was a rapid increase in Mg²⁺ in the presence of a Mg²⁺ free physiological salt solution. In the presence of either NMDG or amiloride, the net Mg²⁺ efflux was decreased indicating that efflux is dependent upon extracellular Na⁺.

3.3 Net Mg²⁺ and Ca²⁺ efflux in human erythrocytes

In addition to pig erythrocytes it was also possible to employ human erythrocytes taken from healthy people and patients who had acute renal failure. Figure 5 shows the concentration of Mg²⁺ in human erythrocytes of normal (A) and pre (B) and postdialysis (C) patients before Mg²⁺ loading (c, column), following Mg²⁺ loading with 12 mM MgCl₂ and (10⁻⁶ M A23187) for 30 min (Ld, column) and after 50 min of Mg²⁺ efflux from loaded erythrocytes (Eff, column). The results show that normal healthy human erythrocytes contain a very small amount of Mg²⁺. It was also difficult to load the cells with Mg²⁺ and as a result there was little Mg²⁺ efflux. In contrast, erythrocytes taken from pre- and post-dialysis patients contain more Mg²⁺ compared to human control. In addition, the erythrocytes take up a large amount of Mg²⁺ during the loaded period and most of the Mg²⁺ is released during the 50 min efflux period. The results indicate that acute renal failure is associated with large fluxes of Mg²⁺.

Figure 6 shows the time course of Mg²⁺ efflux from normal Mg²⁺ loaded (12 mM MgCl₂ + A23187) human erythrocytes in the absence (solid diamonds) and the presence of either 10⁻³ M amiloride (solid squares) or NMDG (solid triangles). The results show that normal Mg²⁺-loaded human erythrocytes can release Mg²⁺ rapidly reaching a maximum after 5 min of incubation. This level remained high throughout the time course response. Pre-treatment of the erythrocytes with 10⁻³ M amiloride resulted in a significant (p < 0.05) decrease in Mg²⁺ efflux compared to human control. In contrast, NMDG had no effect on Mg²⁺ efflux compared to human control. Only at 30 and 40 min there seemed to be a significant inhibition in Mg²⁺ efflux.

3.4 Mg²⁺ efflux in pre- and post-dialysis patients

The time course of Mg²⁺ efflux from erythrocytes of pre-dialysis patients is shown in Figure 7. The result shows that the erythrocytes can take up similar levels of Mg²⁺ during loading as human control (see Figure 5 for comparison) and release the Mg²⁺ with maximal efflux occurring at 5 min following incubation (solid diamonds). There after, Mg²⁺ efflux decreased slightly and remained at that level throughout the time course response. Pre-treatment of the erythrocytes with 10⁻³ M amiloride (solid squares) resulted in a significant (p< 0.05) elevation in Mg²⁺ efflux compared to untreated erythrocytes. In contrast, when NaCl was replaced with NMDG (solid triangles), there was a large and significant (P< 0.05) decrease in Mg²⁺ efflux compared to control. The results of this study employing NMDG suggest that the Mg²⁺ efflux of pre-dialysis erythrocytes is partially dependent upon extracellular sodium since the efflux was reduced but not abolished completely. In contrast, the results obtained with amiloride indicate an enhancement of Mg²⁺ efflux. It is possible that in the pre dialysis patient amiloride acts to enhance the efflux since the opposite is observed in human control (see Figure 6 for comparison).

The time-course of Mg²⁺ from Mg²⁺-loaded erythrocytes taken from human post-dialysis patients is shown in figure 8. The results shows that there was an initial rapid increase in Mg²⁺ efflux in the control (Mg²⁺ free Krebs) followed by a decrease in the level which remained throughout the time course response. Pre-treatment of the erythrocytes with 10⁻³ M amiloride resulted in a much larger efflux of Mg²⁺ compared to control. In contrast, when NaCl was replaced with NMDG, there was a significant (p< 0.05) reduction of Mg²⁺ efflux at 5 min compared to the control. There after the Mg²⁺ efflux remained at the same level as the control. In some aspect

these results are similar to human control except for the results of NMDG after 5 min of incubation.

3.5 Ca²⁺ efflux from Mg²⁺-loaded erythrocytes

Figure 9 shows the time course of Ca²⁺ efflux for Mg²⁺ loaded erythrocytes taken from healthy human controls. The results show that erythrocytes can release large amounts of Ca²⁺ within 5 min of incubation (solid diamonds). This net Ca²⁺ efflux remained at the same level throughout the time course response. Both 10⁻³ M amiloride (solid squares) and NMDG (solid triangles) had no significant effect on Ca²⁺ efflux compared to the response obtained in the absence of these substances.

3.6 Platelet aggregation

Since erythrocytes can take up Mg²⁺ and release it in a time-dependent manner it was also relevant to find out whether a perturbation of extracellular Mg²⁺ can affect platelet aggregation. Figure 10 shows samples of original chart recordings of the effect of different concentration (10⁻⁷ - 10⁻⁴ M) of ADP on human platelet aggregation. The results show that ADP can aggregate human platelets in a dose-dependent manner with maximal effect occurring at 10⁻⁴ M. These experiments were performed several times and the mean ± SEM data are shown in Figure 11. The concentration of Mg²⁺ in normal human plasma was 0.91 ± 0.05 mM, n=12.

Since ADP at 10⁻⁴ M can induce maximal effect on platelet aggregation it was decided to employ this concentration to study the effect of perturbation of extracellular Mg²⁺ on platelet aggregation. Figure 12 shows the effects of 7 mM extracellular MgCl₂ on the ADP induced platelet aggregation. Original chart recordings are shown in Figure 12 A and the mean ± SEM results are shown in Figure 12 B. The results show that perturbation of Mg²⁺ from 0.91 mM (normal) to 7 mM resulted in a significant (P < 0.05) inhibition of ADP-evoked platelet aggregation

especially at high concentration (e.g. 10^{-4} M) of ADP. Typically, the ADP (at 10^{-4} M) induced aggregation in normal plasma was 45 ± 2.5 % (n=10) compared to 5 ± 1.2 % (n=12) in 7 mM Mg^{2+} . Since 7 mM extracellular Mg^{2+} can reduce the ADP-elicited platelet aggregation, it was relevant to ascertain whether other concentrations can do the same employing 10^{-4} M ADP. Figure 13 shows the effect of different concentrations (1-7 mM) of Mg^{2+} on ADP (10^{-4} M) induced human platelet aggregation. Original chart recordings of the responses are shown in Figure 13 A and the mean \pm SEM data are shown in Figure 13 B. These results show that Mg^{2+} can elicit a concentration dependent inhibition of human platelet aggregation with maximal effect occurring at 7 mM Mg^{2+} .

Since a perturbation of extracellular Mg^{2+} can decrease the ADP-induced human platelet aggregation it was decided to determine the effect of different concentrations of extracellular Ca^{2+} on the ADP-evoked platelet aggregation. Original chart recordings of the ADP (10^{-4} M)-elicited responses from 1 mM to 7mM $CaCl_2$ are shown in figure 14. The mean \pm SEM data are shown in figure 15. The effect of ADP in normal plasma Ca^{2+} concentration (control) is also shown for comparison. Normal plasma Ca^{2+} concentration was 2.39 mM (100 mg cell protein)⁻¹). The results show that a perturbation of extracellular $CaCl_2$ elicited a gradual decrease in the ADP-evoked platelet aggregation with maximal inhibition occurring at 3 mM. Further increase in extracellular Ca^{2+} resulted in an increase in ADP-induced human platelet aggregation.

The effects of ADP alone and during perturbation of extracellular $MgCl_2$ were investigated in blood taken from patients who experienced acute renal failure. Both

pre- and post-dialysis blood samples were employed for comparison. Figure 16 shows samples of original chart recordings of ADP (10^{-4} M) induced human platelet aggregation in plasma from normal healthy control and pre- and post-dialysis patients in the absence and presence of 7 mM extracellular $MgCl_2$. The mean \pm SEM data are shown in Figure 17. The results show that a perturbation of extracellular Mg^{2+} had no significant effect on platelet aggregation in acute renal failure patients compared to healthy human control.

3.7 Nuclear magnetic resonance

Figure 18 shows an original chart recording of the one and only successful NMR experiment. Several attempts were made to perform this part of the experiment, but due to a number of factors only one set of results were obtained, for human control blood. No experiments were performed on human patient blood as a result.

The result shows a series on left between (10 and 0) this is a series of 4 spikes, two large and two small. Then between (0 and -20) there are 3 more spaced out smaller peaks.

Table 1. Concentration of Na⁺, K⁺, Ca²⁺, Mg²⁺ and Cl⁻ in pig plasma. All values are mean ± SEM, n=96.

Concentration (mM) of ions in pig plasma			
Ions	Mean	SEM	n
Na ⁺	79	1.1	96
K ⁺	0.2	0.01	96
Ca ²⁺	0.052	0.027	96
Mg ²⁺	0.051	0.026	96
Cl ⁻	113	6.6	96

Table 2. Concentrations of Na⁺, K⁺, Ca²⁺, Mg²⁺, and Cl⁻ in human plasma in normal healthy people and pre- and post-dialysis patients. All values are mean ± SEM (n= 12).

Concentration (mM) of ions in human plasma									
ions	Human Control			Pre-dialysis patients			Post-dialysis patients		
	mean	SEM	n	mean	SEM	n	mean	SEM	n
Na	136.83	0.98	6	138	3.63	12	135	3.1	12
K	4.38	0.42	6	4.2	0.75	12	3.8	0.31	12
Ca	2.39	0.06	6	2.2	0.36	12	2.57	0.14	12
Mg	0.91	0.05	6	0.77	0.08	12	0.71	0.06	12
Cl	102.83	2.32	6	96	10.34	12	99	3.2	12

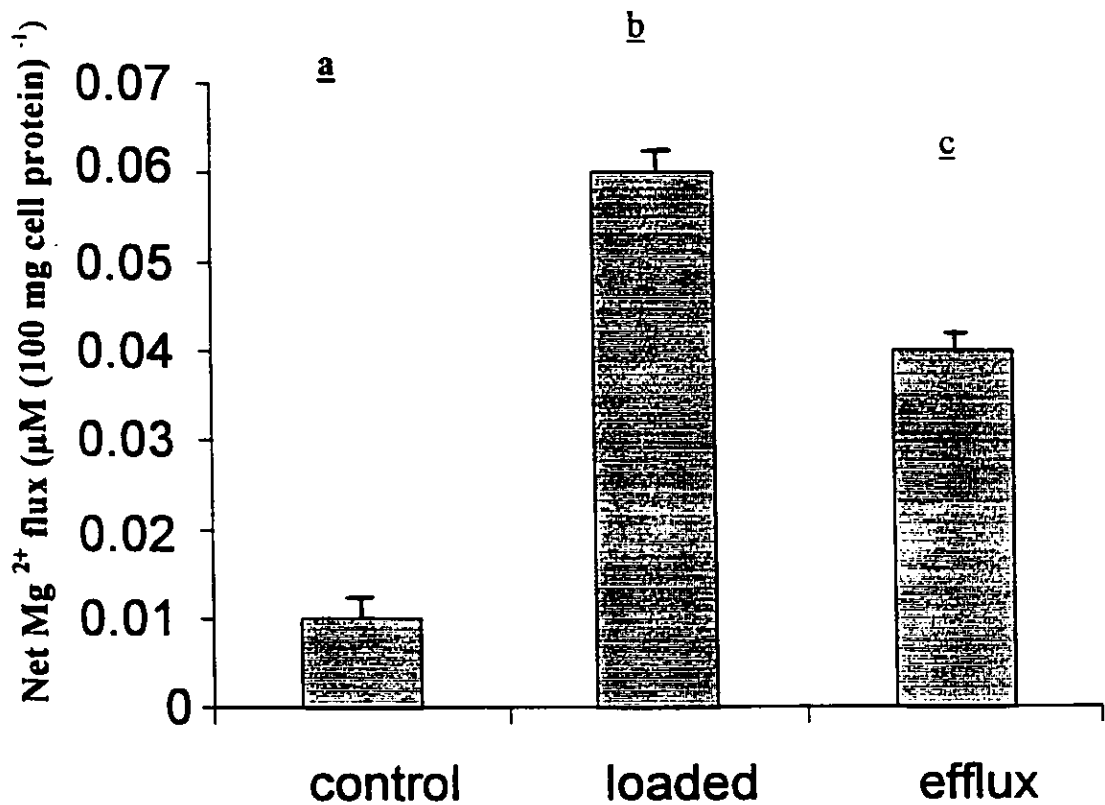


Figure 1. Concentration of Mg²⁺ (uM (100 mg cell protein)⁻¹) in pig erythrocytes before (control) loading (a), following loading (b), and 50 min following Mg²⁺ efflux (c). Each point is mean ± SEM (n=6). Erythrocytes were loaded for 30 min in the presence of 10⁻⁶ M A23187 at 37 °C.

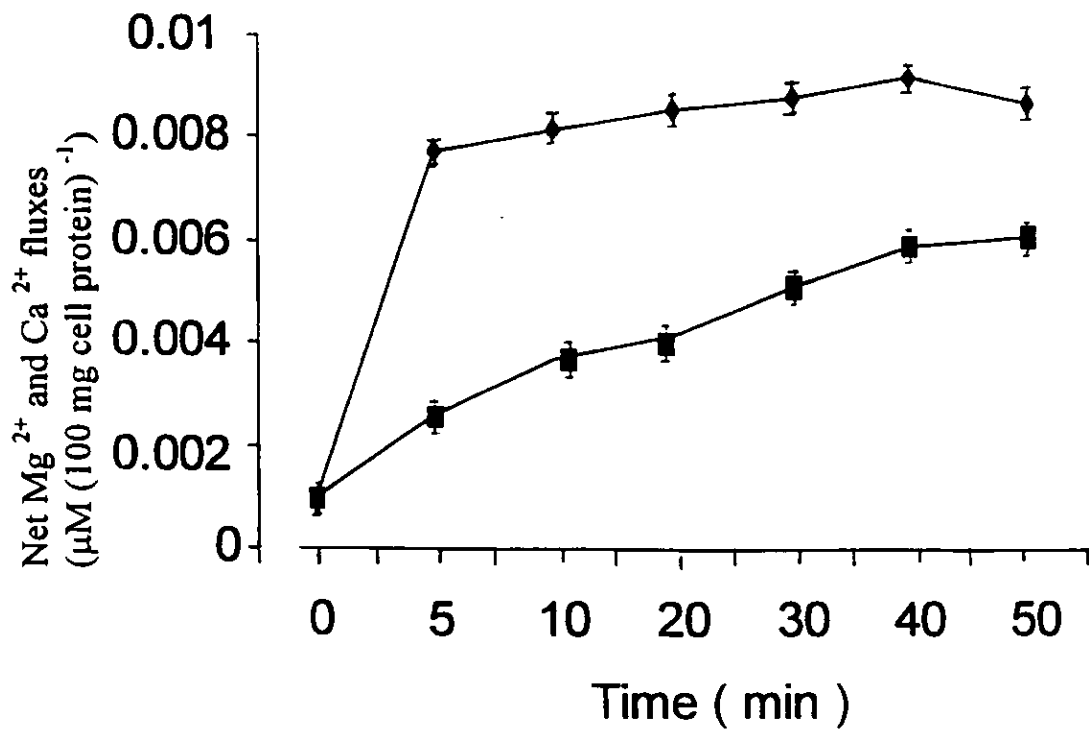


Figure 2. Time course of net Mg²⁺ (solid diamonds) and Ca²⁺ (solid squares) efflux from Mg²⁺-loaded erythrocytes. Each point is mean ± SEM (n=96).

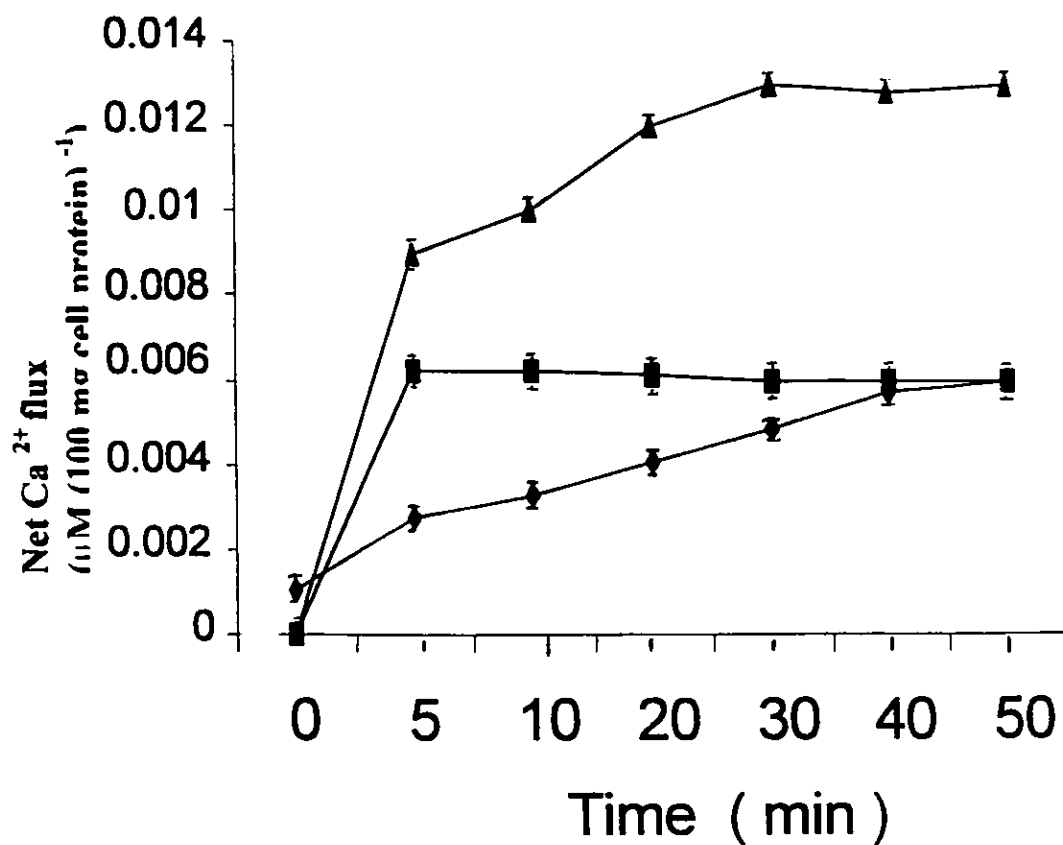


Figure 3. Time course of net Ca²⁺ efflux from Mg²⁺ loaded erythrocytes in the absence (solid diamonds) and presence of either NMDG (solid squares) or 10⁻³ M amiloride (solid triangles). Each point is mean ± SEM, n=96. Note that all the Na⁺ in the physiological salt solution was replaced by NMDG.

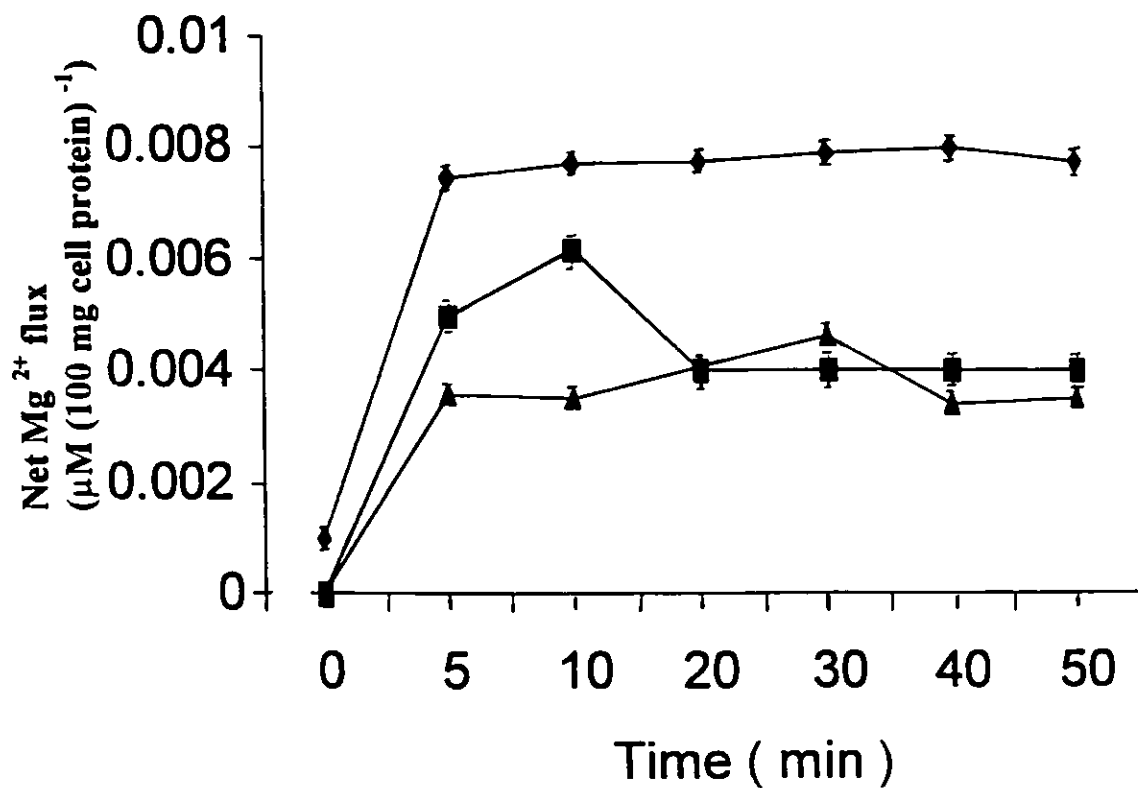


Figure 4. Time course of net Mg²⁺ efflux from Mg²⁺ loaded pig erythrocytes in the absence (solid diamonds) and presence of either 10⁻³ M amiloride (solid triangles) or NMDG (solid squares).

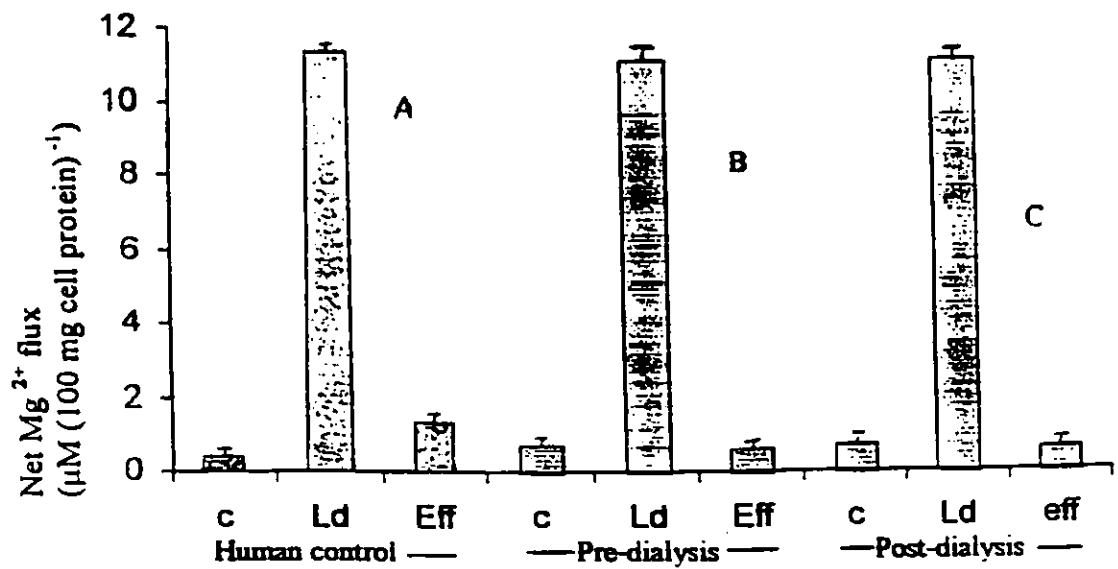


Figure 5. Concentration of Mg²⁺ (c; before loading), Mg²⁺ loaded (Ld) and following 50 min efflux (eff) in erythrocytes taken from human control (A) and pre (B) and post dialysis (C) patients. Each point is mean \pm SEM, n=10.

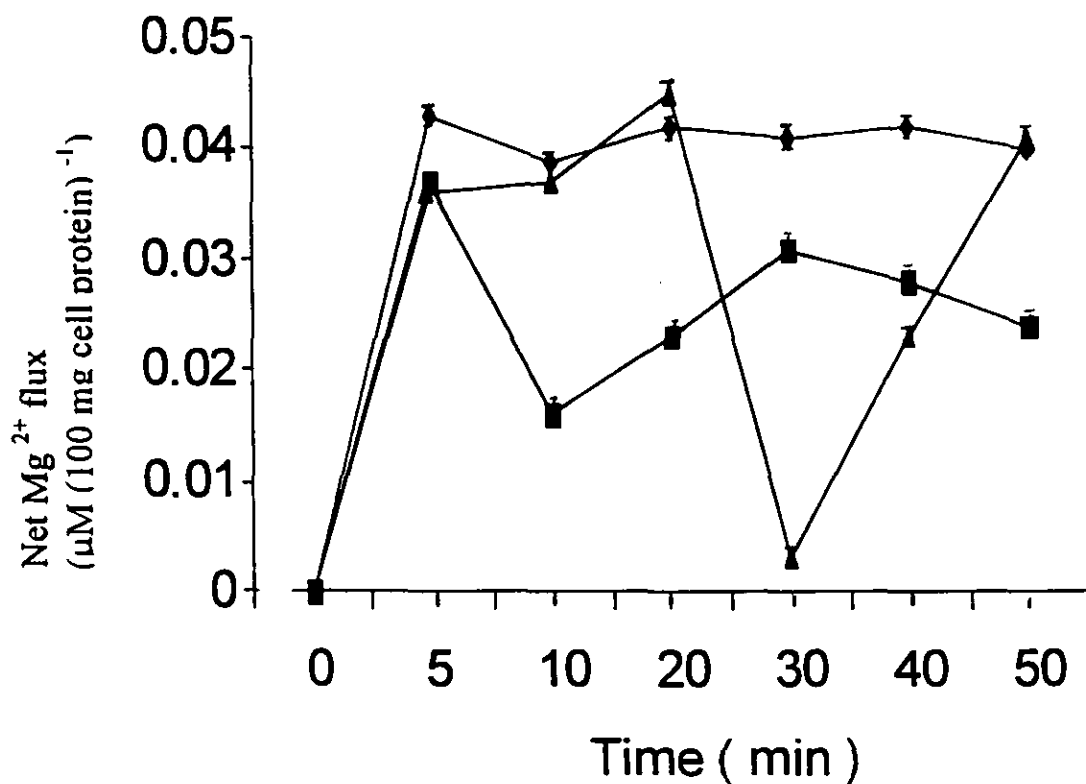


Figure 6. Time course of net Mg^{2+} efflux for Mg^{2+} loaded erythrocytes taken from healthy people in Mg^{2+} free physiological salt solution (solid diamonds), and in the presence of either 10^{-3} M amiloride (solid squares) or NMDG (solid triangles). Each point is mean \pm SEM, $n=10$. Note that all the NaCl was replaced with NMDG.

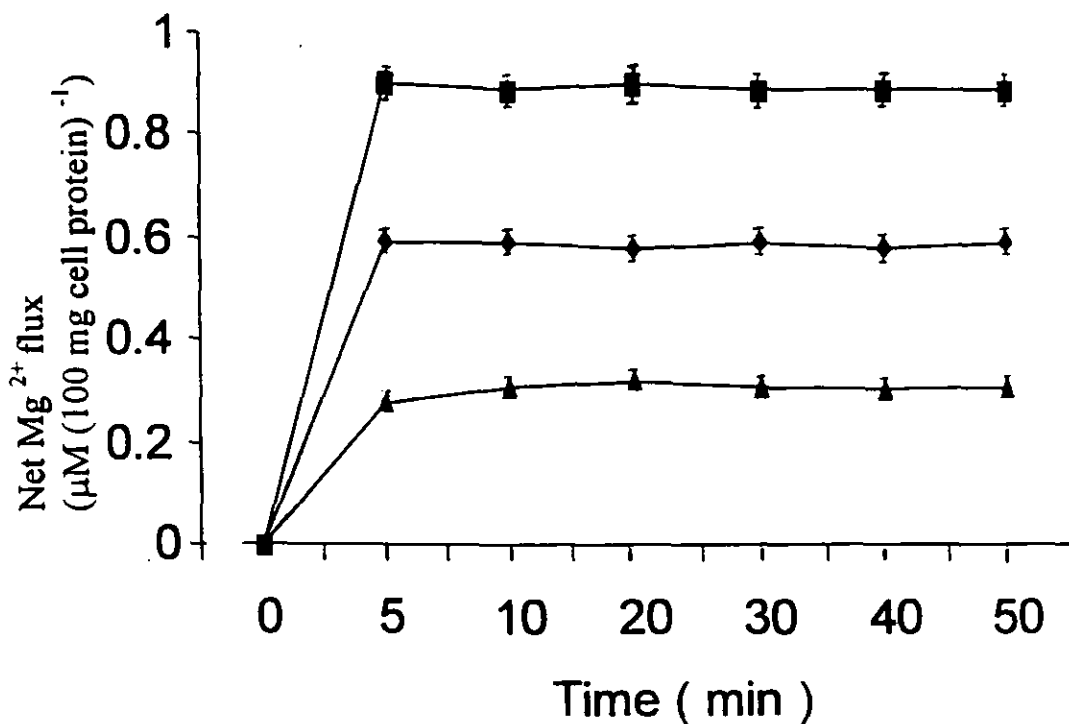


Figure 7. Time course of Mg²⁺ efflux for Mg²⁺ loaded (12 mM MgCl₂ + 10⁻⁶ M A23187) human pre-dialysis erythrocytes in the absence (solid diamonds) and presence of either 10⁻³ M amiloride (solid triangles) or NMDG (solid squares). Each point is mean ± SEM, n= 12. Note that all the NaCl was replaced with NMDG.

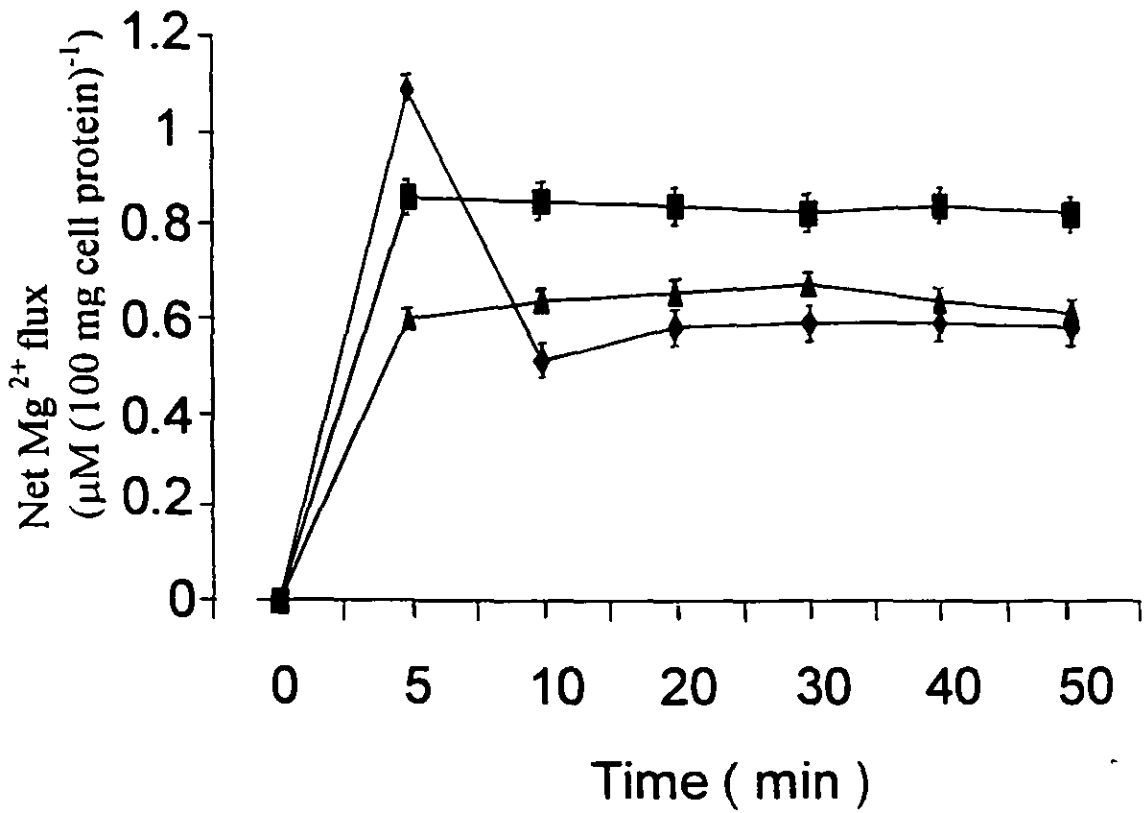


Figure 8. Time course of Mg²⁺ efflux for Mg²⁺ loaded (12 mM MgCl₂ + 10⁻⁶ M A23187 for 30 min) erythrocytes taken from postdialysis human patients in the absence (solid diamonds, control) and presence of either 10⁻³ M amiloride (solid squares) or NMDG (solid triangles). Each point is mean ± SEM, n= 12.

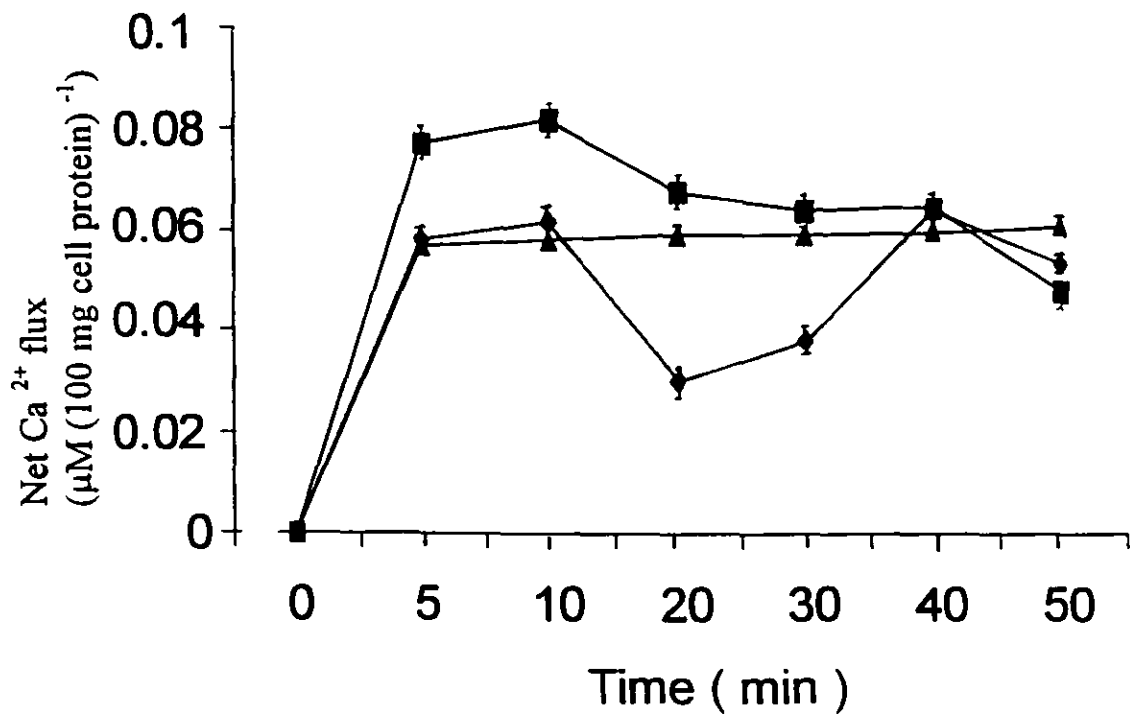


Figure 9. Time course of Ca²⁺ efflux for Mg²⁺ loaded human erythrocytes in control (solid diamonds) and following pre-treatment with 10⁻³ M amiloride (solid squares) or replacement of extracellular sodium with NMDG (solid triangles). Each point is mean ± SEM, n=10.

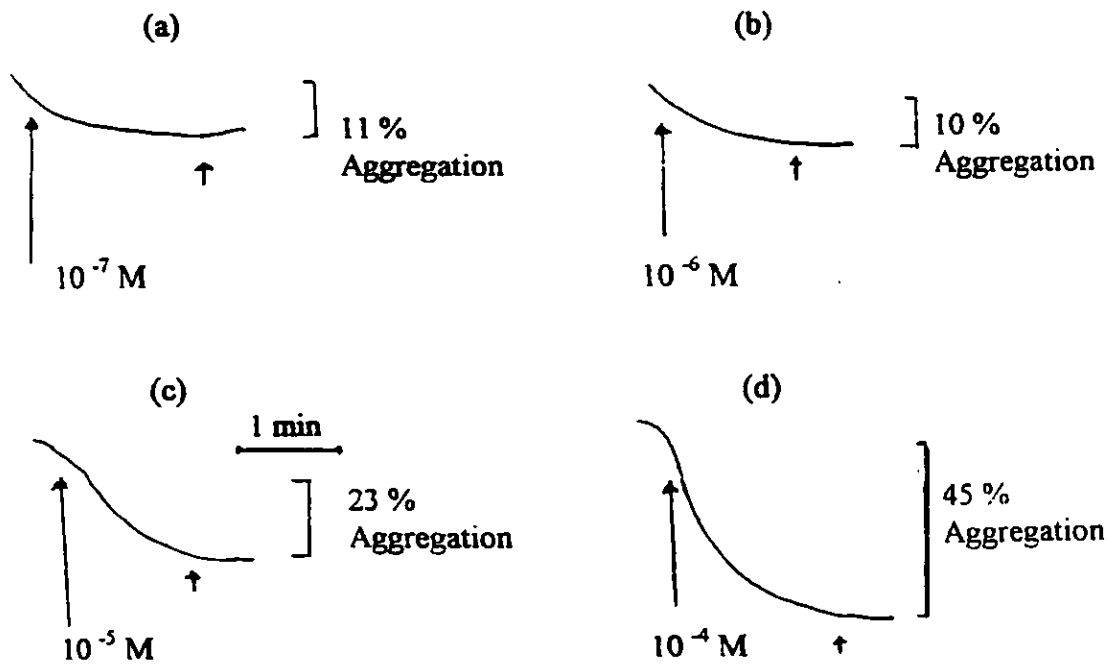


Figure 10 Original chart recordings of the effect of different concentrations (10^{-7} - 10^{-4} M) ADP on platelet aggregation. These traces are typical of 10 such experiments. The first arrow indicates the point of addition of ADP and the second arrow indicates the steady state time when the measurements were made.

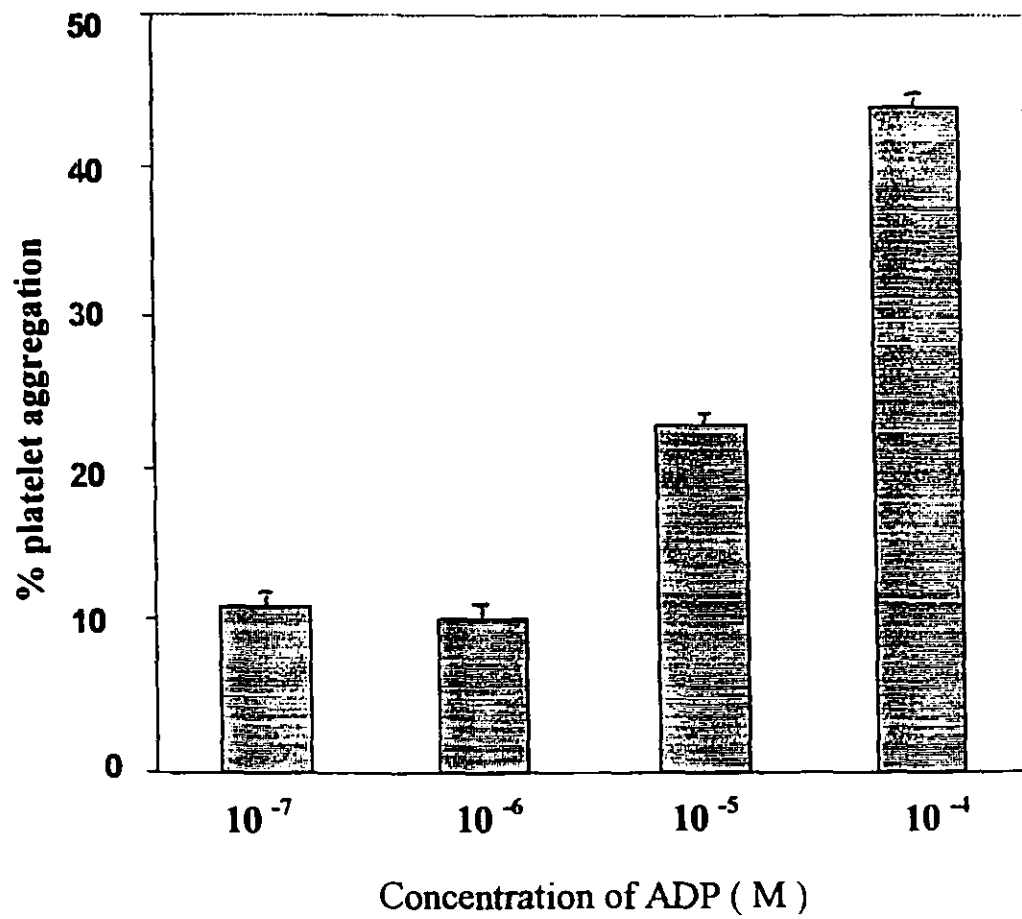


Figure 11: Bar charts showing the effect of different concentrations (10^{-7} - 10^{-4} M) of ADP on human platelet aggregation. Each point is mean \pm SEM, n= 10.

(A)

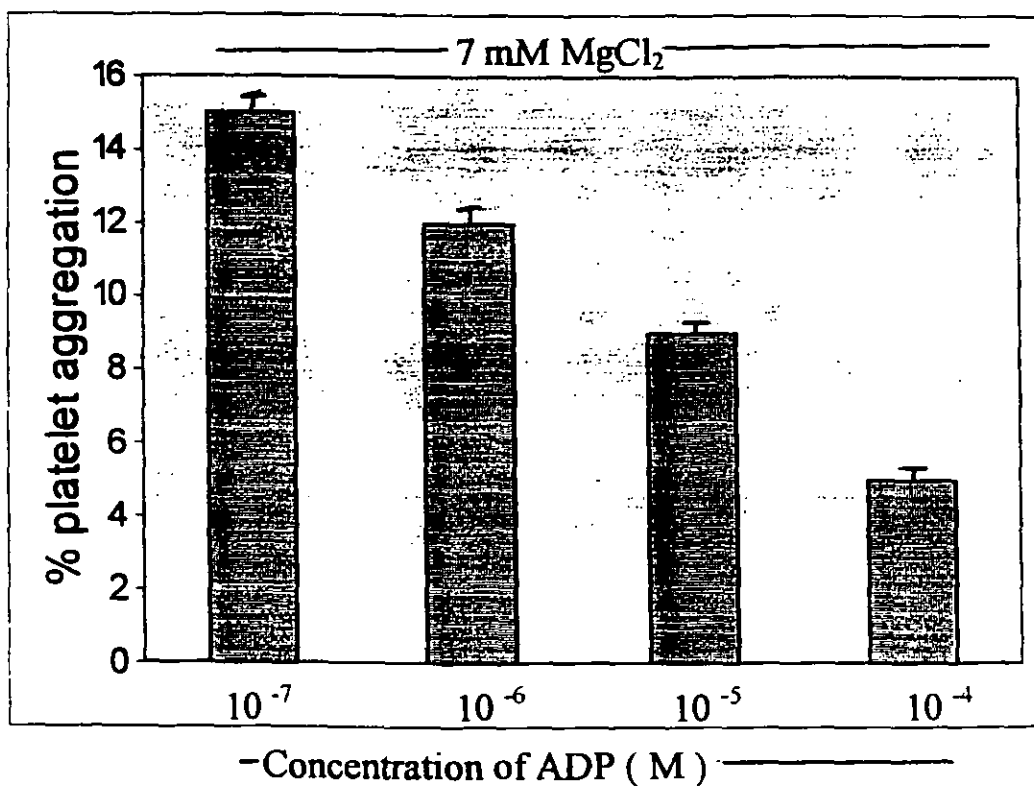
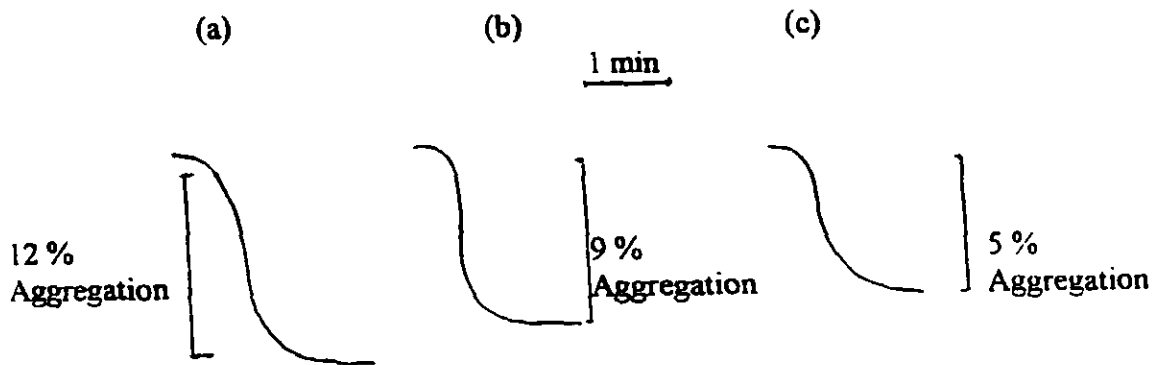


Figure 12A. Original chart recordings showing the effect of different concentrations ((a) 10^{-6} M, (b) 10^{-5} M and (c) 10^{-4} M) of ADP on human platelet aggregation in the presence of 7 mM MgCl₂. Each point is mean \pm SEM, n=10. Traces are typical of 10 experiments.

B Histograms showing the effect of 10^{-7} - 10^{-4} M on human platelet aggregation in 7 mM extracellular MgCl₂. Each point is mean \pm SEM, n=10.

(A)

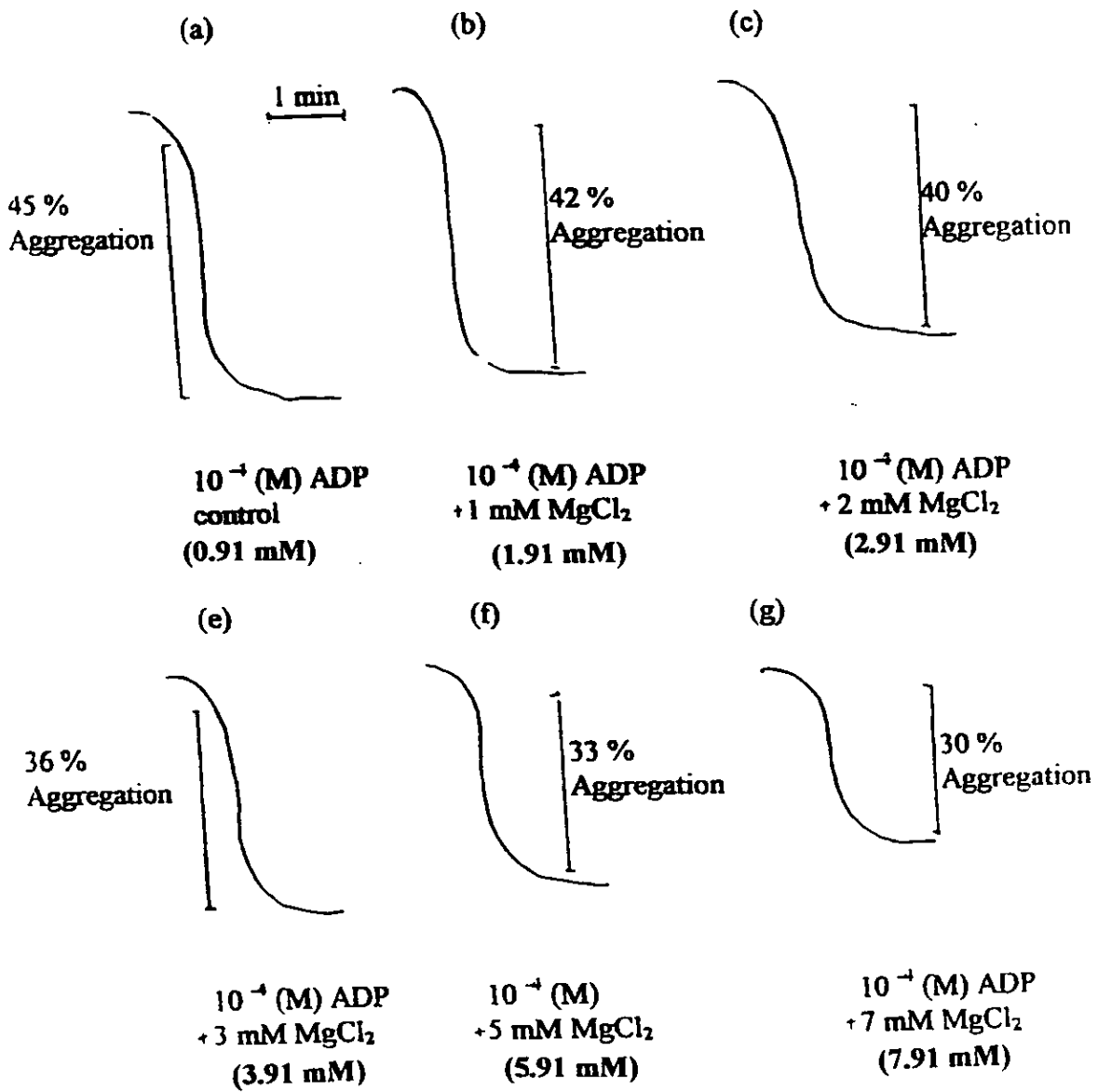


Figure 13 (A). Original chart recordings showing the effect of different concentrations (1-7 mM) of MgCl_2 on ADP (10^{-4} M)-induced human platelet aggregation. The control response (a) is shown for comparison. Traces are typical of 6 such experiments. Note that the concentration of Mg^{2+} in plasma is 0.91 mM.

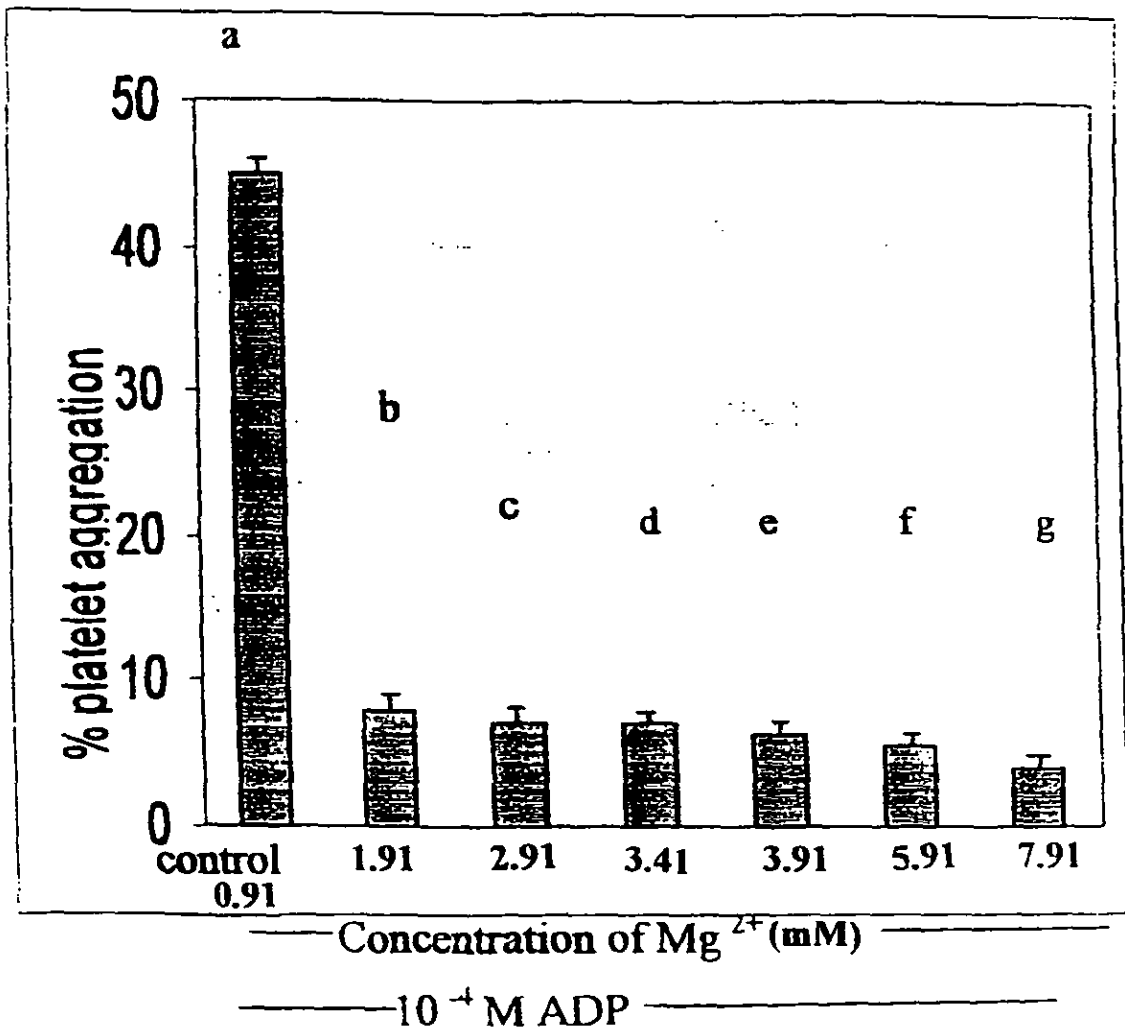


Figure 13 B Histograms showing the mean \pm SEM platelet aggregation in response to 10^{-4} M ADP in normal (a) and during perturbation of extracellular $MgCl_2$, (1-7 mM or b - g), $n=10$.

Note that the concentration of Mg^{2+} in plasma is 0.91 mM.

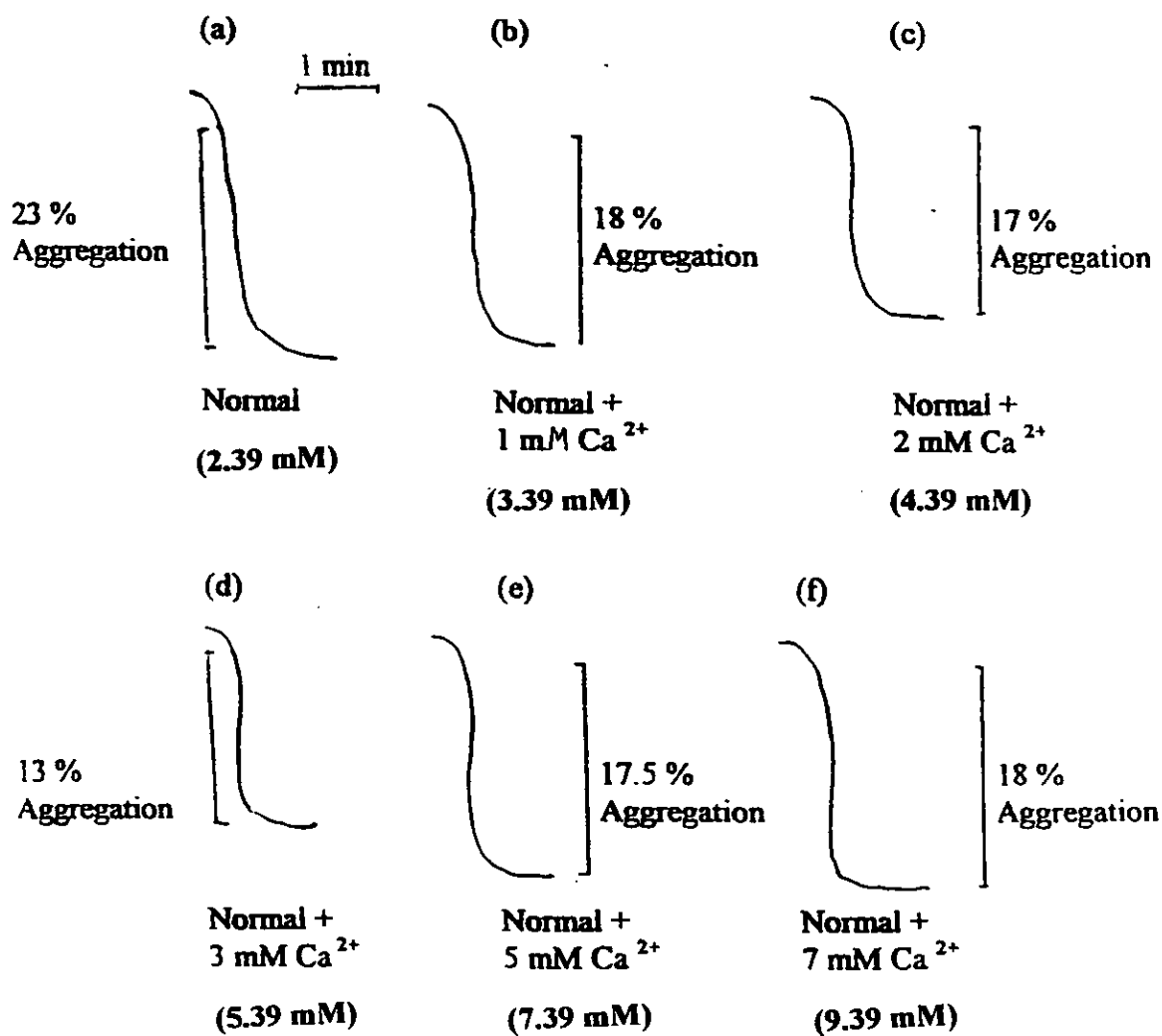


Figure 14 . Original chart recordings of the effect of 10^{-4} M ADP on platelet aggregation during perturbation (1 - 7 mM) of extracellular Ca^{2+} . Traces are typical of 10 such experiments.

Note that the concentration of Ca^{2+} in plasma is 2.39 mM.

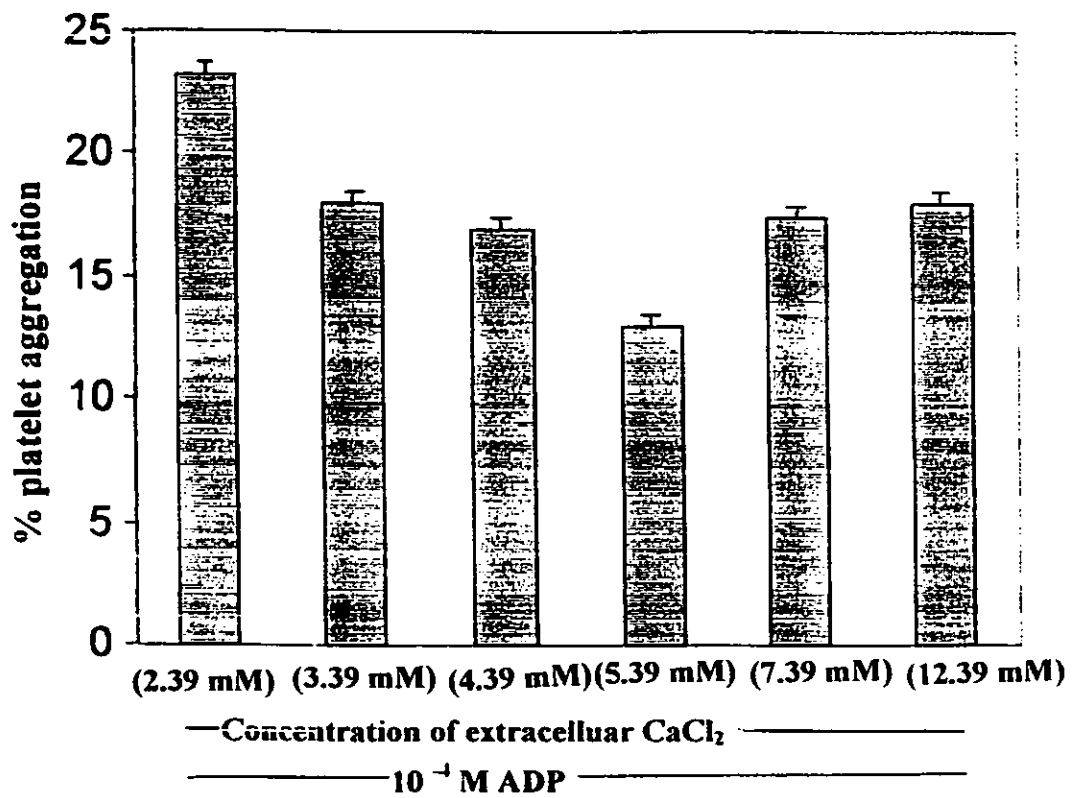


Figure 15. Histograms showing the mean \pm SEM human platelet aggregation induced by 10^{-4} M ADP during perturbation of the extracellular Ca^{2+} , $n=10$.

Note that the concentration of Ca^{2+} in plasma is 2.39 mM.

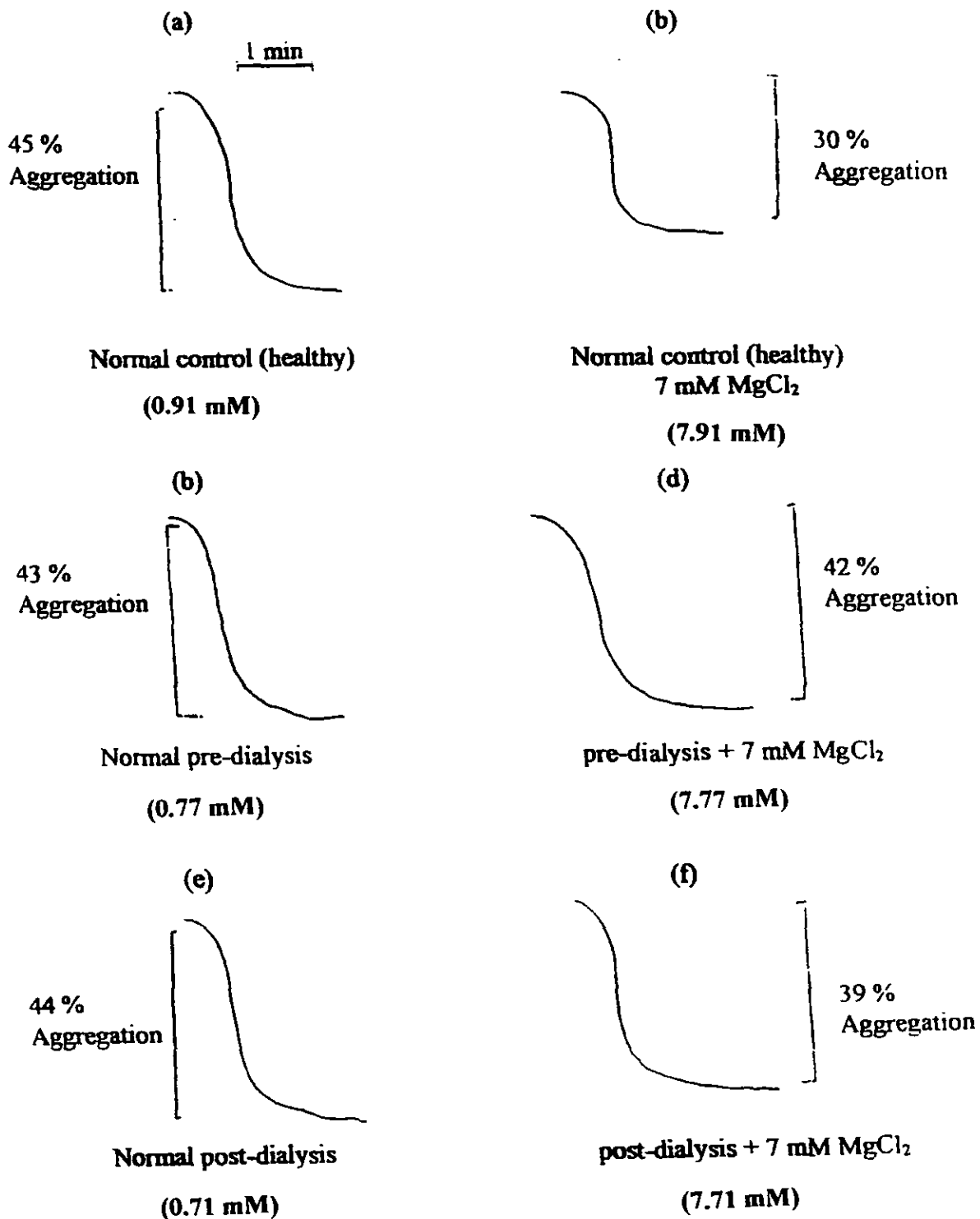


Figure 16. Original chart recordings of the effect of 10^{-4} M ADP in the absence (a-c) and presence (d-e) of 7 mM extracellular MgCl₂ in plasma taken from human control (a and d), predialysis patients (b and e) and postdialysis patients (c and f). These traces are typical of 10 such experiments.

Note that the concentration of Mg²⁺ in healthy control and both pre- and post-dialysis is 0.91, 0.77 and 0.71 mM.

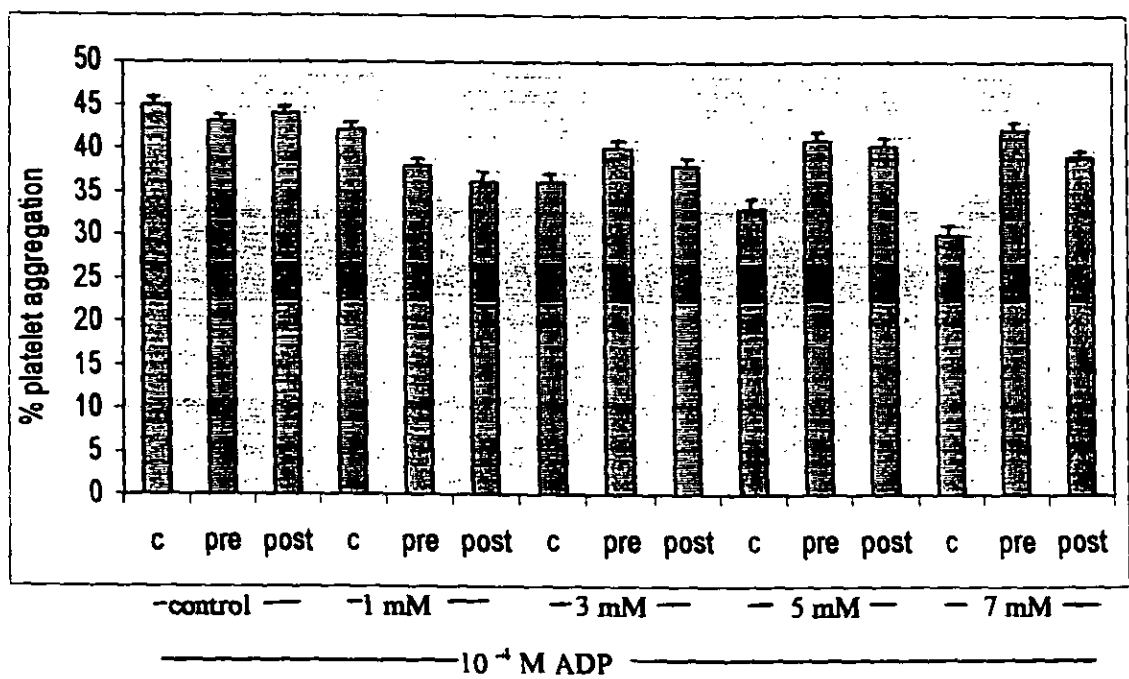


Figure 17. Bar chart showing ADP (10^{-4} M) induced platelet aggregation in plasma taken from normal healthy people and pre and postdialysis patients in the absence and presence of different concentrations of extracellular $MgCl_2$. Each point is mean \pm SEM, n=10.

Chapter Four
General Discussion.

The study employs blood from pig, human control and human patients to measure the levels of Mg^{2+} , Ca^{2+} , Na^+ , K^+ and Cl^- in plasma and to characterise Mg^{2+} transport in erythrocytes. In addition, the study also investigated the role of Mg^{2+} in platelet aggregation. The results have demonstrated marked changes in the levels of the ions in the plasma and Mg^{2+} concentration for loaded erythrocytes. Moreover, Mg^{2+} seems to play an important physiological role in platelet aggregation. For the sake of clarity, the discussion is divided into four major sections. The first part is concentrated on the level of ions in the plasma. In the second section the characterisation of Mg^{2+} transport is discussed. In the third section, emphasis is placed on the role of Mg^{2+} during platelet aggregation and finally section four is concerned with the NMR study.

4.1 Cation and anion levels in pig and human plasma.

Levels of Na^+ , K^+ , Ca^{2+} , Mg^{2+} and Cl^- were measured in both pig and human controls as well as human patients in pre- and post-dialysis states (tables 1 and 2, respectively). Plasma samples for pig were analysed in our laboratory using the flame photometer, the atomic absorbance spectrophotometer and Cl^- titration, whereas samples for human controls and both pre- and post-dialysis patients were measured at the clinical laboratory at Royal Preston Hospital employing a colorimetric technique. The results obtained in our laboratory using the AAS equipment was found to be very unreliable in producing viable and consistent measurements of the ions. Factors which may influence lower readings on the AAS include: contaminated nebulizer tube, a dirty flame head, a dirty lamp, dilution factors and low flame fuel level. In plasma taken from pig the level of Na^+ was almost half the level as the Na^+ found in human control and both pre- and post-dialysis patients. The level of K^+ in pig was more significantly ($p < 0.05$) lower than in both human control and human patients in both pre- and post-dialysis conditions. The levels were 20 times lower in pig. Ca^{2+} was lower in pig compared to human control by a measured factor of 460. This measured pig Ca^{2+} value was obtained by AAS and it is apparently incorrect. In contrast, Ca^{2+} was similar in both pre- and post-dialysis patients compared to healthy human. Mg^{2+} was greatly lower in pig compared to human control. This again was measured by AAS and is incorrect. However, in both pre- and post-dialysis patients the Mg^{2+} levels were between 10 and 12 times greater than in pig and but lower than in human control. These findings are consistent with work performed by previous studies (Taylor and Singh, 1997). The Cl^- in pig was again lower than in human control but higher than in both pre and post dialysis patients. The human control level of Cl^- was also higher than the levels found in human pre and postdialysis patients.

4.2 Characterisation of Mg²⁺ transport.

The findings of this study have demonstrated significant changes on the magnesium transport mechanism in erythrocytes taken from both the pig and human in both the normal and diseased states. The findings in the pig were similar to the results found in the pig and cow (Taylor and Singh, 1997). The findings for the human controls were also similar to results found by others (Taylor and Singh, 1996; Abraham and Rosenmann *et al*, 1987). The aim of the experiment was to characterise magnesium transport. It was shown to occur via Na⁺-dependant Mg²⁺. The initial step was to load the cells with magnesium. The results in both the pig and human control and acute renal failure patients showed an increase in intracellular Mg²⁺ (Figures 1 and 5). On incubation in a solution containing bovine serum albumin to bind and hence remove the ionophore, and following 50 min incubation in the Mg²⁺ free control solution, the intracellular Mg²⁺ content of erythrocytes of pig was decreased below that of the loaded cells (Figure 1). However, in the human erythrocytes, the intracellular Mg²⁺ content had increased above that of the loaded cells (Figure 5). In stark contrast, in human patient erythrocytes both in pre and postdialysis the highest Mg²⁺ efflux was seen as the intracellular Mg²⁺ content had decreased more greatly than the loaded erythrocytes and this was almost the same as the unloaded intracellular Mg²⁺ content (Figure 5).

Incubation of erythrocytes in the Mg²⁺ free control solution illustrated that loaded cells for the two species released Mg²⁺ in a time dependent manner, as expected (Figures 4, 6 and 7). However, with the exception of the pig erythrocytes (Figure 4), the maximum efflux did not appear to have been attained within the 50 minutes

permitted, suggesting that the cells from the human controls should be incubated for a longer period to assess the maximum efflux time and value. Previous studies employing pancreatic acinar cells have shown that loaded cells can release Mg^{2+} in a time dependant manner with maximal efflux occurring after 50 min (Wisdom *et al*, 1996).

The Mg^{2+} efflux was decreased in the presence of amiloride for loaded erythrocytes in pig and human patients both pre and post dialysis, as anticipated, due to its action in inhibiting sodium transport (Smith and Benos, 1991; Wisdom *et al*, 1996; see Figures 4 and 7, respectively). However, for the human control the same decrease of Mg^{2+} efflux was observed except for the 10 min incubation period which showed an increase (Figure 6). Furthermore, replacing the extracellular Na^+ with NMDG in the Mg^{2+} free solution also resulted in a decrease in the Mg^{2+} efflux for both the pig and human control, supporting the evidence for a Na^+ -dependent transport system for Mg^{2+} (Vormann and Gunther, 1993). However, in the human patients the Mg^{2+} efflux was increased in the presence of NMDG (Figure 7). Hence for the set of conditions in human patient erythrocytes, this does not support evidence for Na^+ -dependent transport for Mg^{2+} . As some Mg^{2+} efflux did occur in the presence of amiloride, or by replacing Na^+ with NMDG would suggest that either another transport mechanism is involved with Mg^{2+} transport, such as Na^+ -independent Mg^{2+} efflux (Feraý and Garay, 1986), or that some ionophore remained in the cell membrane and thus allowing some diffusion of Mg^{2+} to occur.

The results obtained for human patient erythrocytes both pre and postdialysis did not follow the same trend (Figures 7 and 8, respectively). Incubation of loaded-erythrocytes in the presence of amiloride or by replacing Na^+ with NMDG did not decrease the Mg^{2+} efflux compared to controls. Moreover, the efflux in the presence

of either amiloride or NMDG was greater than that obtained in the control. This may be due to another transport mechanism as the Mg^{2+} efflux in the human patient erythrocytes both in pre and postdialysis were significantly ($P < 0.05$) higher than in human control Mg^{2+} free solution (Figures 7 and 8, respectively). Evidence and support for Na^+ -independent Mg^{2+} efflux in human erythrocytes was obtained by Vormann and Gunther in 1989. In renal patients were treated via haemodialysis, the Mg^{2+} is higher compared to normal. This erythrocyte Mg^{2+} content is caused by increased plasma Mg^{2+} . This has been observed in this study (see table 2 and Figure 5) and during increased Mg^{2+} uptake following haematopoiesis in other study (Vormann and Gunther, 1996). The relatively lower erythrocyte Mg^{2+} in haemodialysis is produced by a higher rate of Na^+ - Mg^{2+} antiport (Vormann and Gunther, 1996). Early evidence for net magnesium transport in humans *in vitro* was given by Dunn (1974). He showed that magnesium is lost from cells containing a high magnesium concentration (5 - 8.7 mM) when they are incubated in media containing zero or 0.8 mM magnesium. Efflux is prevented by raising the external magnesium concentration above the total cell magnesium content (Flatman, 1988).

Feray and Garay (1986) loaded cells with Mg^{2+} using parachloromercuribenzenesulphonate (PCMBS) whilst, Ludi and Scharzmann (1987) loaded cells with the calcium ionophore A23187. Magnesium efflux from magnesium-loaded cells are subdivided into two components: a sodium independent "leak" flux and a sodium dependent flux (Feray and Garay, 1986). Feray and Garay (1986) estimated the leak permeability in their work as seven times greater than the ground permeability of red cell membranes to sodium or potassium (Flatmann, 1988). This observation suggested that this was not simple diffusion through the membrane lipid but by mediated

transport perhaps including residual effects of PCMBs. The same can be said in terms of A23187 residue observed in the work of Ludi and Schatzmann (1987). Feray and Garay (1986) explained their data by assuming that magnesium was binding to a single activating transport site. Ludi and Schatzmann (1987), however, suggested that at least two magnesium ions must bind to activate transport. Usage of various inhibitors showed that transport does not occur through the sodium pump, calcium pump, Na^+ , K^+ , Cl^- cotransporter, K^+ , Cl^- cotransporter or anion exchange system (Flatman, 1988; Wisdom *et al.*, 1996). Human red cells thus appear to have a specialised sodium -dependent magnesium transporter which also depends on the metabolic integrity of the cell (Flatman, 1988).

Ludi and Schatzmann (1987) suggested that sodium -dependent magnesium transport was not simple sodium-magnesium antiport where the energy for magnesium transport is obtained directly from the sodium gradient. Ludi and Schatzmann (1987) proposed the following models to explain transport. Sodium binds to an external site on the transport protein causing a conformational change. The sodium site then has access to the cytoplasm and sodium ion may be released here. Internal magnesium now has access to its binding sites either (model a) directly or (model b) after metabolic input of energy. The protein undergoes another conformational change and the magnesium sites now gain access to the external medium either (model a) after input of metabolic energy or (model b) directly (see Appendix V for diagram). Magnesium efflux therefore requires input of metabolic energy.

4.3 Platelet aggregation

The aim of this experiment was to observe changes to the aggregation of platelets between healthy human controls and humans suffering from acute renal failure. A series of experiments were performed to obtain a concentration of ADP that gave the best percentage of aggregation. Blood from pig was used initially to develop the correct protocol for the study. The initial step was to obtain the plasma. After centrifugation of the total blood into its components the platelet rich plasma (PRP) and platelet poor plasma (PPP), the optimum ADP concentration which gave the most aggregation was to be determined. The suggested range of ADP was (10^{-7} M - 10^{-2} M) (Royal Preston Hospital Haematology Dept.). The next step was to observe any differences in the aggregation in ADP concentrations (10^{-7} M - 10^{-4} M) during perturbation of extracellular magnesium. The normal magnesium value of both the pig and human plasma was already established in experiments to measure magnesium in plasma (tables 1 and 2, respectively), hence a range of (1 mM - 7 mM MgCl_2) was used. The initial experiment was to simply test a range of ADP concentrations on healthy human platelets. The results of this study showed that as the concentration of ADP was increased (from i.e. 10^{-7} M to 10^{-4} M) the % aggregation of platelets increased (Figures 10 and 11). It was decided to employ 10^{-4} M ADP for the rest of the experiments as this concentration gave maximal response. The next series of experiments was performed using extracellular MgCl_2 at concentration of 7 mM in the presence of varying ADP concentrations (10^{-7} M - 10^{-4} M). It was observed that as ADP increased in concentration in the presence of 7 mM MgCl_2 the platelet aggregation was inhibited via a dose dependent manner (Figure 12). The next sets of experiments were performed using varying Mg^{2+} concentrations (1.9 mM - 7.9 mM).

The results showed Mg^{2+} can evoke a dose dependent inhibition of platelet aggregation during the application of 10^{-4} M ADP (Figure 13). These findings are in agreement with previous studies (Ravn, Kristensen and Husted, 1996).

ADP concentration was then kept constant at (10^{-4} M), and the Ca^{2+} levels were then varied to observe if perturbation of Ca^{2+} would affect platelet aggregation. The range of Ca^{2+} used was (1- 7 mM). The results show that, at normal Ca^{2+} concentration in healthy human controls the aggregation was around 23 %. As the Ca^{2+} levels were increased from the levels found in the erythrocytes, 1 mM up to 3 mM the aggregation was also reduced to 19%, 18% and 14% respectively. At 5 mM Ca^{2+} the aggregation began to increase slightly to 17% and at 10 mM the aggregation was 18%. The results have demonstrated that Ca^{2+} exhibited a dose dependent inhibition of aggregation up to 3 mM concentration, hence, this was the best concentration to obtain inhibition of aggregation (Figure 14). Further discussion on this experiment is not possible as no literature has been found regarding Ca^{2+} on aggregation.

Lastly, experiments using ADP at (10^{-4} M) were performed on human controls and both pre- and post-dialysis patients in the presence of varying Mg^{2+} concentrations (1 mM - 7 mM) (Figure 15). The results showed that an elevation in extracellular Mg^{2+} was associated with marked inhibition in platelet aggregation for human controls. These results were again consistent with findings from other studies (Ravn, Vissinger, Kristensen and Husted, 1996; Ravn, Vissinger, Kristensen, Wennmalm, Thyngesen and Husted, 1996). Again the Mg^{2+} showed a dose dependent inhibition of human platelet aggregation.

The next stage of the study was to observe differences in aggregation in human patients who were diagnosed as renal failure patients. They were treated by haemodialysis and their plasma was then experimented on both in the pre and

postdialysis states. The ADP concentration was kept constant at (10^{-4} M) as this concentration elicited maximal aggregation and the Mg^{2+} concentrations were varied from (1 - 7 mM) as in previous experiments. The results showed that in normal (0.05 mM) Mg^{2+} level both pre- and post-dialysis gave the same degree aggregation (Figures 16 and 17, respectively). However, in plasma taken from pre-dialysis patients, a perturbation of extracellular Mg^{2+} elicited a biphasic effect. When Mg^{2+} was increased from 0.91 mM to 1 mM ADP evoked a small degree in platelet aggregation (i.e. from 45 % to 37 %). As extracellular Mg^{2+} was increased further to 3 mM, ADP induced a small increase in platelet aggregation (i.e. from 37 % to 40 %). This result showed that increasing extracellular Mg^{2+} concentration did not cause any further inhibition of aggregation but instead a slight promotion of aggregation was observed. In the doses 3, 5 and 7 mM the % aggregation did not change significantly and remained around 38%. However, in the presence of 10 mM Mg^{2+} the % aggregation increased to 45%. For the post dialysis patients a similar pattern to those seen in predialysis state was observed except an inhibition at 3 mM Mg^{2+} was seen (Figures 16 and 17, respectively).

4.4 NMR EXPERIMENT

Use of NMR.

The NMR experiment was not successful after a series of trial runs. The result obtained was not as expected (Figure 18). The blood sample was taken as whole blood and placed in a NMR tube containing heparin. An internal standard of deuterated water (D₂O) was added so that the magnet had some thing to lock onto. The sample was placed in to the magnet which was set up for proton (H⁺), and the parameters set. The samples were shimmed and the data collected. Four clear distinct peaks were obtained when human control blood was used, two of the peaks were close together and were large in size and were located around 5 ppm, three smaller peaks were also seen but these were more widely distributed.

Calculation of Mg²⁺ from the data obtained was performed using the equation below (Rude, Stephen and Nadler, 1991; 1992).

The chemical shift of the α and β phosphoryl groups of ATP is dependent of Mg²⁺. A comparison of δ_{αβ} for the cell with that of ATP and MgATP allows for calculation of theta (Rude *et al*, 1991; 1992):

$$\theta = (\delta_{\alpha\beta} \text{ cell} - \delta_{\alpha\beta} \text{ MgATP} / \delta_{\alpha\beta} \text{ ATP} - \delta_{\alpha\beta} \text{ MgATP})$$

and subsequent calculation of Mg²⁺:

$$\text{Mg}^{2+} = \text{Kd}^{(\text{MgATP}^{-1})} (\theta - 1)$$

With Kd^{Mg ATP} = 3.8 × 10⁻⁵ M at 37 °C and pH 7.2.

Experiments on human blood cell intracellular free magnesium has been performed by Rude *et al*, 1991; 1992. Their conclusions and findings, using Mg^{2+} depleted blood in human control and also patients compared to people with diabetes mellitus, showed that RBC reflected Mg^{2+} depletion as the RBC Mg^{2+} was reduced in all subjects tested under Mg^{2+} deprivation conditions. This was further supported by the fact that the mean RBC Mg^{2+} concentration was also significantly lower in hypomagnesemia patients.

From the experiments carried out in our laboratories, there was not sufficient experimental data to comment on the findings. The problem was to establish a reliable and reproducible set of methods to operate and utilise the NMR method. Great difficulty was experienced in achieving this one result which was not repeatable due to time constraints.

4.5 Conclusions

In conclusion, magnesium transport occurs by a number of different mechanisms, either via the Na^+ independent pump, or via the Na^+ dependent pump. Magnesium levels both extra and intracellularly affect the aggregation process, an increase of magnesium up to a certain level seems to inhibit aggregation in the presence of ADP in human controls, but in the presence of human blood from acute renal disorders this process is affected. These findings can be attributed to the lower levels of intracellular magnesium found in this type of blood. The NMR method is a great non-invasive tool for measuring Mg^{2+} and gives an accurate account of Mg^{2+} levels. More work on this experimental protocol is required to fully discuss the findings. The results of this study have provided a wide insight into the role and mechanism of magnesium transport in pig and human erythrocytes in normal and diseased states.

4.6 Scope for further studies.

- 1). Repeat experiments and account for the Na^+ and K^+ levels in both normal and diseased states of human blood.
- 2). For magnesium efflux experiments use channel blockers and inhibitors such as verapamil and ouabain. Also use PCMBs to gain knowledge of energy changes during efflux to establish mode of transport.
- 3). Use aspirin in aggregation experiments to see how this affects aggregation as it is not recommended for use whilst testing. It is also necessary to use thrombin and collagen to provide a clearer picture of the differences magnesium causes on rate of aggregation. This may help in the treatment and give clues to benefits of Mg^{2+} supplements.
- 4). Complete NMR experiments to provide an idea of how magnesium is transported.
- 5). Measure Mg^{2+} in erythrocytes using the fluorescent bioprobe Magfura 2.
- 6). Measure Mg^{2+} efflux using the tetra potassium salt of Magfura 2 employing a fluorimetric method.
- 7). Investigate the effect of different transport inhibitors on Mg^{2+} transport.

Chapter five

References

References

1. Abbot L.G. and Rude R.K. (1993). Clinical manifestations of magnesium deficiency. *Miner. Electrolyte Metab.* **19**: 314-322.
2. Abraham S.A , Rosemann D, Kramer M, Balkin J, Zion M.M, Farbstein H. and Eylath U. (1987). Magnesium in the prevention of lethal Arrhythmias in acute myocardial infarction. *Arch. Int. Med.* **147**, 735-755.
3. Acland R. (1972). Prevention of thrombosis in microvascular surgery by use of magnesium sulphate. *Br. J. plastic Surgery.* **25**: 292-299.
4. Adams J.H and Mitchell J.R.A. (1979). The effects of agents which modify platelet behaviour and of magnesium ions on thrombus formation in vivo. *Thromb. Haemost.* **42**: 603-610.
5. Agus Z.S, Kelepouris E, Dukes I and Morad M. (1989). Cytosolic magnesium modulates calcium channel activity in mammalian ventricular cells. *Am. J. Physiol.*, **256**, C452-C455.
6. Agus Z.S and Morad M. (1991). Modulation of cardiac ion channels by magnesium. *Ann. Rev. Physiol.* **53**, 299-307.
7. Altura B.M and Altura B.T. (1981). Magnesium ions and contraction of vascular smooth muscle: relationship to some vascular diseases. *Federation Proceedings.* **40**, 1672-1679.

8. Altura B.M and Altura B.T. (1995). Magnesium in cardiovascular biology. *Scientific American (May-June Ed)*. 28-37.
9. Baker P.F and Knight D.E. (1978). Calcium dependent exocytosis in bovine adrenal medullary cells with leaky plasma membrane. *Nature*. **276**, 620-622.
10. Balschi J.A, Cirrillo V.P and Springer C.S. Jr (1982). *Biophys. J.* **38**: 323-26. (quoted from Gupta R.K and Gupta P. (1984). NMR studies of intracellular metal ions in intact cells and tissues. *Ann. Rev. Biophys. Bioeng.* **13**: 221-41).
11. Beauge L.A and Glynn I.M. (1979). Sodium ions acting at high-affinity extracellular sites, inhibit sodium-ATPase activity of the sodium pump by slowing dephosphorylation. *J. Physiol.* **289**, 17-31.
12. Beauge L and Campos M.A. (1986). Effects of mono and divalent cations on total and partial reactions catalysed by pig kidney Na, K-ATPase. *J. Physiol.* **375**, 1-25.
13. Bio/Data Corporation (1977). Platelet Aggregation Profiler Model PAP-3. Operating Instructions and Methods Manual. Horsham PA 19044 U.S.A.
14. Birch N.J. (1993). In: *Magnesium and the Cell*. Pub. Academic press, London.
15. Birch N.J and Sadler P.J. (1979). Inorganic elements in Biology and Medicine. In: *Specialist periodical Report on Inorganic Biochemistry. Vol I* (Ed: Hill HAO, Pub: Chemical Society, London). Pp 365-420.
16. Blaustein M.P. (1977). Sodium ions, calcium ions, blood pressure regulation, and hypertension: a reassessment and a hypothesis. *Am. J. Physiol.* **232**: C165-C173.
17. Boynton A.L, McKeehan W.L and Whitfield J.F. (1982). Ions, cell proliferation and cancer. New York: Academic **551pp**.

18. Brugnana C and Tosteson D.C. (1987). Cell volume, K transport and cell density in human erythrocytes. *Am. J. Physiol* **252**, C269-C276.
19. Buri A and McGuigan J.A.S. (1990). Intracellular free magnesium and its regulation, studied in isolated ferret ventricular muscle with ion selective micro electrodes. *Exp. Physiol.* **75**, 751-761.
20. Buri A and McGuigan J.A.S. (1991). Intracellular free magnesium concentration in ferret heart muscle: its measurement and its regulation. In "Magnesium - A relevant Ion". (Ed B. Lasserre and J. Durlach), pp 201-214. John Libby, London.
21. Cameron I.L., Smith N.K.R, Pool T.B and Sparks R.L. (1980). *Cancer research* **40**: 1493-1503.
22. Caswell A.H and Pressman B.C. (1972). *Biophys. Biochem. Res. Commun.* **49**: 292.
23. Civan M.M, Degani H, Margalit Y and Shporer M. (1983). *Am. J. Physiol.* **245**: C213-19.
24. Corkey B.E, Duszynski J, Rich T.I, Matchinsky B and Williamson J.R. (1986). Regulation of free and bound magnesium in rat hepatocytes and isolated mitochondria. *J. Biochem.* **261**, 2567-2574.
25. Curry D.C, Joy R.M, Holley D.C and Bennett L. (1977). Magnesium modulation of glucose induced insulin secretion by the perfused rat pancreas. *Endocrinology.* **101** (1), 203-208.
26. Davey M.G and Lusher E.F (1968). Release reactions of human platelet induced by thrombin and other agents. *Biochem. Biophys. Acta* **165**: 490.
27. Day H and Holesen H. (1972). Laboratory tests of platelet function. *Annals of clinical laboratory science* Vol 2. No.1. pp63.

28. De Weer P. (1976). Axoplasmic free magnesium levels and magnesium extrusion from squid giant axons. *J. Gen. Physiol.* **68**, 159-178.
29. Dillon P.F, Meyer R.A, Kushmerick M.J. (1983). *Biophysics J.* 41: **252a** (Abstract).
30. Dunham E.T and Glynn I.M. (1961). Adenosine triphosphatase activity and the active movements of alkali metal ions. *J. Physiol.* **156**, 274-293.
31. Dunn M.J. (1974). Red blood cell calcium and magnesium: effects upon sodium and potassium transport and cellular morphology. *Biochem. Biophys. Acta* **352**, 97-116.
32. Elin R.J (1983). Assessment of magnesium stasis in cells, tissues and body. In: *magnesium in cellular processes and medicine* (Eds. Altura B, Durlach J and Seeling M). Pub: Karger press. Basel, pp67-76.
33. Emley E.F (1966). In; *Principles of magnesium technology*, Pub: Peramon press, London.
34. Entmann M.L, Gillette P.C, Wallick E.T, Pressman B.C and Scjwartz A (1972). *Biochem. Biophys. Res. Commun.* **48**: 847.
35. Erdos J.J and Maguire M.E. (1983). Hormone sensitive magnesium transport in murine S49 lymphoma cells: Characterisation and specificity for magnesium. *J. Physiol.* **337**: 351-371.
36. Falk E. (1992). Why do platelets rupture? *Circulation.* **86**:11130-42.
37. Feray J.C and Garay R. (1986). A Na⁺ stimulated Mg²⁺ transport system in human red blood cells. *Biochimica et Biophysica. Acta* **856**, 76-84.

38. Flatman P.W. (1984). Magnesium transport across cell membranes. *Journal of membrane Biology*. **80**, 1-14.
39. Flatman P.W. (1988). The effects of magnesium on potassium transport in ferret red cells. *Journal of Physiology*. **397**, 471-487.
40. Flatman P.W. (1991) mechanism of magnesium transport. *Ann. Rev. Physiol.* **53**, 259-71.
41. Flatman P.W. (1993). The role of magnesium in regulating ion transport. In; *Magnesium and the cell* (ed: N.J.Birch), Academic Press, pp197-216.
42. Flatman P.W and Lew V.L. (1981). The magnesium dependence of sodium-pump-mediated sodium-potassium and sodium -sodium exchange in intact human red cells. *Journal of physiology*. **315**, 421-446.
43. Flik G, Van der Velden J.A and Kolar Z.I. (1993). Radiotracer probes in cellular magnesium transport studies. In: *Magnesium and Cell*. (Ed. N.J. Birch), Academic Press, London.
44. Francis L.P, Lennard R and Singh J. (1990). Mechanism of action of magnesium on acteylcholine-evoked secretory responses in isolated rat pancreas. *Experimental Physiology*. **75**, 669-680.

45. Freitas D.M.D and Dorus E. (1993). Techniques for measuring Magnesium in tissues from hypertensive, psychiatric and neurological patients. In: magnesium and Cell (Ed: N.J.Birch), Academic press, pp50-79.
46. Fujise H and Lauf P.K. (1988). Na⁺-K⁺ pump activities of high-and low-potassium sheep red cells with internal magnesium and calcium altered by A23187. *Journal of Physiology*. **405**, 605-614.
47. Fuster V, Steele P.M and Chesebro J.H. (1985). Role of platelets and thrombosis in coronary atherosclerotic disease and sudden death. *J. Ann. Coll. Cardiol*. **5**: 175B-184B.
48. Fry C.H, Buri A, Chen S, Illner H, Kickenweiz E, McGuigan J.A.S, Noble D, Powell T and Twist V.W. (1993). The regulation of intracellular Mg²⁺ in guinea-pig heart studied with Mg²⁺-selective microelectrodes and fluorochromes. *Exp. Physiol*. **78**, 221-233.
49. Gadian D.G. (1983). *Ann. Rev. Biophys Bioeng*. **12**: 69-89. (quoted from Gupta R.K., and Gupta P. (1984). NMR studies of intracellular metal ions in intact cells and tissues. *Ann. Rev. Biophys. Bioeng*. **13**: 221-41).
50. Galloe A.M., Rassmussen H.S, Jorgensen L.N, Aurup P, Balslov, Cintin C, Graudal N and McNair P. (1993). Influence of oral magnesium supplementation on cardiac events among survivors of acute myocardial infarction. *Br. Med J*. **3087**: 585-587.

51. Gawaz M, Ott I, Reininger A.J and Neumann F.J. (1994). Effects of magnesium on platelet aggregation and adhesion. Magnesium modulates surface expression of glyco-proteins on platelets in vito and in vivo. *Thromb. Haemost.* **72**, 912-918.
52. Gertz S.D, Rebecka, Wajnberg A.K and Uretzky G. (1987). Effect of magnesium sulphate on thrombus formation following partial arterial constriction: implications for coronary vasospasms. *Magnesium.* **6**; 225-35.
53. Grodsky G.M and Bennett L.L. (1966). Cation requirements for insulin secretion in the isolated perfused rat pancreas. *Diabetes.* **15, 12**: 910-913.
54. Grubbs R.D and Maguire M.E. (1987). Magnesium as a regulatory cation: Criteria and evaluation. *Magnesium.* **6**, 113-127.
55. Gunther T. (1990). Functional compartmentation of intracellular magnesium. In: metal ions in biological systems compendium on magnesium and its role in biology. *Nutrition and Physiology.* Siegel and A. Siegel. **26**: 193-213. New York , Marcell dekker.
56. Gunther T. (1993). Mechanism and regulation of Mg²⁺ efflux and Mg²⁺ influx. *Miner. Electrolyte Metab.* **19**, 259-265.

57. Gunther T and Vormann J. (1987). Characterization of $\text{Na}^+ / \text{Mg}^{2+}$ antiport by stimulataneous $^{28}\text{Mg}^{2+}$ influx. *Biochem. Biophys. Res. Commun.* **148**: 1069-74.
58. Gunther T, Vormann J and Hollreigl V. (1990). Characterization of Na^+ -dependent Mg^{2+} efflux from magnesium loaded erythrocytes. *Biochem. Biophys. Acta* **1055**, 82-86.
59. Gunther T, Vormann J and forster R. (1984). Regulation of intracellular magnesium by Mg^{2+} efflux. *Biochemical and Biophysical research communications.* **119: No.1.** 124-131.
60. Gupta R.K. (1980). On the state of the magnesium ion in intact cells as observed by noninvasive ^{31}P NMR spectroscopy. *International Journal of Quantum Chemistry: Quantum Biology Symposium* **7**, 67-73.
61. Gupta R.K, Benovic J.L, Rose Z.B (1978). The determination of the free magnesium level in the red blood cell by ^{31}P NMR. *J. Biol. Chem.* **253**: 6165-71.
62. Gupta R.K, Gupta P. (1982). *J. Magn. Reson.* **47**: 344-50. Direct observation of resolved resonances from intra- and extracellular Sodium- 23 ions in NMR studies of intact cells and tissues using Dysprosium (III) tripolyphosphate as paramagnetic shift reagent. *J. Magnetic Resonance.* **47**, 344-350.

63. Gupta R.K and Gupta P. (1984). NMR studies of intracellular metal ions in intact cells and tissues. *Ann. Rev. Biophys. Bioeng.* **13**: 221-46.
64. Gupta R.K, Gupta P, Yushok W.D and Rose Z.B. (1983). *Biochem. Biophys. Res. Commun.* **117**: 210-16. (quoted from Gupta R.K. and Gupta P. (1984). NMR studies of intracellular metal ions in intact cells and tissues. *Ann. Rev. Biophys. Bioeng.* **13**: 221-41).
65. Gupta R.K and Moore R.D. (1980). ^{31}P NMR studies of intracellular free Mg^{2+} in intact frog skeletal muscle. *J. Biol. Chem.* **255**: 3987-93.
66. HAMLYN J.M, Ringel R., Schaeffer J, Levinson P.D, Hamilton B.P, Kowarski A.A and Blaustein M.P. (1982). A circulatory inhibitor of $(\text{Na}^{+} + \text{K}^{+})\text{ATPase}$ associated with essential hypertension. *Nature.* **300**: 650-53.
67. Heaton F.W. (1981). Distribution and function of magnesium within the cell. In: *magnesium and the cell.* (Ed. N.J.Birch). Academic Press pp121-135.
68. Herotte J.G. (1993). Genetic regulation of cellular magnesium content. In: *magnesium and the cell.* (Ed N.J.Birch). Academic press pp177-216.
69. Howarth F.C, Waring J, Singh J and Hustler B.I. (1994). Effects of extracellular magnesium and beta adrenergic stimulation on contractile force and magnesium mobilization in the isolated rat heart. *Magnes. Res.* **7**, 187-97.

70. Hu Z, Buhret T, Muller M, Rusterholz B, Rouilly M and Simon W. (1989). Intracellular magnesium ion-selective microelectrodes based on a neutral carrier. *Anal. Chem.* **61**, 574-576.
71. Hurley T.W, Ryan M.P and Brinck R.W. (1992). Changes of cytosolic Ca^{2+} interfere with measurements of cytosolic Mg^{2+} using magfura-2. *Am. J. Physiol.* **263**, C300-C307.
72. Hwang D.L, Yen C.F and Nadler J.L. (1992). Effect of extracellular magnesium on platelet activation and intracellular calcium mobilization. *Am. J. Hypertens.* **5**: 700-706.
73. Karlsh S.J.D and Stein W.D. (1982 a). Passive rubidium fluxes mediated by Na-K-ATPase reconstituted into phospholipid vesicles when ATP- and phosphate free. *J. Physiol.* **328**, 295-316.
74. Karlsh S.J.D and Stein W.D. (1982 b). Effects of ATP or phosphate on passive rubidium fluxes mediated by Na-K-ATPase reconstituted into phospholipid vesicles. *J. Physiol.* **328**, 317-331.
75. Kolar Z.I, Van der Velden J.A, Vollingen R.C, Zandberger P and Goejj J.J.M. (1991). Separation of ^{28}Mg from reactor-neutron irradiated Mg-Li alloy and redetermination of its half-life. *RadioChim. Acta.* **54**, 167-170.

76. Kristen S.D and Martin J.F. (1991). Platelet heterogeneity and coronary thrombosis. *Platelets*. **2**; 11-17.
77. Lauf P.K. (1985): passive K^+ - Cl^- fluxes in low K^+ sheep erythrocytes: - modulation by A23187 and bivalent cations. *Am. J. Physiol.* **249**, C271-C278.
78. Lennard R and Singh J. (1991). Secretagogue-evoked changes in intracellular free magnesium concentrations in rat pancreatic acinar cells. *Journal of physiology*. **435**, 483-492.
79. Ludi H and Schatzmann H.J. (1987). Some properties of a system for sodium-dependent outward movement of magnesium from metabolizing human red blood cells. **390**; 367-382.
80. Luscher E.F. (1971). Biochemical basis of platelet function. In Brinkhouse K (Ed). *The platelet. International academy of pathology monograph*, Williams and Wilkins company , Baltimore Md.
81. Marcus A.J and Zucker M.B. (1965). *Physiology of blood platelets*. Grune and stratton. New York.
82. Marjanovic M, Gregory C, Ghosh P, Willis J.S and Dawson M.J. (1993). A comparison of effect of temperature on phosphorous metabolites, pH and Mg^{2+} in human and ground squirrel red cells. *Journal of physiology*. **470**: 559-574.

83. Misawa K, Lee T.M and Ogawa S. (1982). A study on the exchange rate of magnesium with ADP. *Biochimica et Biophysica Acta* **718**, 227-229.
84. Moore C and Pressman B.C. (1964). Mechanism of action of valinomycin on mitochondria. *Biochem. Biophys. Res. Commun.* **15**: 562-567.
85. Mooren F.Ch and Singh J. (1997). Magnesium homeostasis and its role in exocrine pancreas in health and disease. *Magnesium bulletin* **19**, **2**: 46-56.
86. Morrill G.A, Kostellow A.B, Weinstein S.P and Gupta R.K. (1983). *Fed. Proc.* **42**: 1791 (Abstract). (quoted from Gupta R.K. and Gupta P. (1984). NMR studies of intracellular metal ions in intact cells and tissues. *Ann. Rev. Biophys. Bioeng.* **13**: 221-46).
87. Mudge G.M and Weiner I.M. (1992). Agents affecting volume and composition of body fluids. In: *Pharmacological basis of therapeutics. Vol I.* (eds. Goodman A, Gilman, Rall T.W, Nies A.S and Taylor P). Pub McGraw and Hill, New York 8th edition pp704-706.
88. Murphy E, Freudenrich C.C and Lieberman M (1991). Cellular magnesium and Na /Mg exchange in heart cells. *Ann. Rev. Physiol.* **53**: 273-287.
89. Murphy E, Steenbergen C, Levy L.A, Hall R.D and London R.E. (1989). Cytosolic free magnesium levels in ischemic rat heart. *J. Biol. Chem.* **264**, 5622-5627.

90. Nadler J.L, Malayan S, Luong H, Shaw S, Natarajan R.D and Rude R.K. (1992). *Diabetes Care*. **15**, No.7 835-841.
91. Nielsen S.P and Petersen O.H. (1972). Transport of calcium in the perfused submandibular gland of the cat. *J.Physiol. (Lond)*. **223**, 685-697.
92. Nuccitelli R, Deamer D.W. Eds. (1982). *Intracellular pH. Its measurements, regulation and utilization in cellular functions*. New York: Liss. 594pp.
93. Page E and Polimeni P.I. (1972). Magnesium exchange in rat ventricle. *J. Physiol*. **224**: 121-139.
94. Petersen O.H. (1992). Stimulus secretion coupling:- cytoplasmic calcium signals and control of ion channels in exocrine acinar cells. *American Journal of Physiology*. **256**, C540-C548.
95. Petersen O.H and Gallacher D.V. (1988). Electrophysiology of pancreatic and salivary acinar cells. *Annual review of physiology*. **50**, 68-80.
96. Pfeiffer D.R, Reed P.W and Lardy H.A. (1974). Ultraviolet and fluorescent spectral properties of the divalent cation ionophore A23187 and its metal ion complexes. *Biochemistry*. **13**, **19**: 4007-4015.

97. Phillips J.D. (1989). The transport and inorganic biochemistry of lithium and magnesium. (PhD thesis). University of Wolverhampton.
98. Post R.L, Sen A.K and Rosenthal A.S. (1965). A phosphorylated intermediate in adenosine triphosphate-dependent sodium plus potassium transport across kidney membrane. *J. Biol. Chem.* **240**, 1437-1445.
99. Post R.L, Toda G and Rodgers F.N. (1975). Phosphorylation by inorganic phosphate of sodium plus potassium ion transport adenosine triphosphate. *J. Biol. Chem.* **250**, 691-701.
100. Pressman B.C. (1963). In energy-linked functions of mitochondria, Ed. B. Chance p181. NY. Academ.
101. Pressman B.C (1965). *Fed. Proc.* **24**: 425. (quoted from Pressman B.C. (1976). Biological applications of ionophores. *Ann. Rev. Biochem.* **45**: 501-30).
102. Pressman B.C. (1965). *Pro.Natl. Acad. Sci. U.S.A.* **53**: 1076. (quoted from Pressman B.C. (1976). Biological applications of ionophores. *Ann. Rev. Biochem.* **45**: 501-30).

103. Pressman B.C. (1976). Biological applications of ionophores. *Ann. Rev. Biochem.* **45**: 501-530.
104. Quamme G.A and Dirks J.H. (1986). The physiology of renal magnesium handling. *Renal physiology.* **9**, 257-269.
105. Raju B, Murphy E, Levy L.A, Hall R.D and London R.E. (1989). A fluorescent indicator for measuring cytosolic free magnesium. *American Journal of physiology* **256**, C540-548.
106. Ravn H.B, Vissenger H, Kristensen S.D and Husted S.E. (1996). Magnesium inhibits platelet activity- An invitro study. *Thrombosis and Haemostasis.* **76 (1)** 88-93.
107. Ravn H.B, Vissenger H, Kristensen S.D, Wennmalm A, Thygesen K and Husted S.E. (1996). Magnesium inhibits platelet activity- and infusion study in healthy volunteers. *Thrombosis and Haemostasis.* **75 (6)** 939-44.
108. Reed P.W and Lardy H (1972). A23187: A divalent cation ionophore. *J. Biol Chem* **247**: 6970-6977.

109. Reinhardt R.A. (1988). Magnesium metabolism- a review with special reference to the relationship between intracellular content and serum levels. *Archive Int. Medicine* **148**, 2415-2420.
110. Resnick L.M, Barbagallo M., Gupta R.K and Laragh J.H. (1993). Ionic basis of hypertension in Diabetes Mellitus. Role of hyperglycemia. *Am. J. Hypertension*. **6**: 413-417.
111. Rink T.J, Tsien R.Y and Pozzan T. (1982). Cytoplasmic pH and free Mg^{2+} in lymphocytes *J. Cell Biol.* **95**:189-96.
112. Robinson J.D. (1976). The $(Na^{+}-K^{+})$ -dependent ATPase. Mode of inhibition of ADP/ATP exchange activity by $MgCl_2$. *Biochim. Biophys. Acta* **440**, 711-722.
113. Rodnam N.F. (1971). The morphological bases of platelet function: In Brinkhouse, K (Ed). *The platelet international academy of pathology monograph*. Williams and Wilkins company.
114. Rossi R.C and Garrahan P.J. (1989). Steady-State kinetic analysis of the Na^{+}/K^{+} -ATPase. The inhibition by potassium and magnesium. *Biochim. Biophys. Acta* **981**, 105-114.

115. Rubin H. (1975). Central role for magnesium in coordinate control of metabolism and growth in animal cells. *Proc. Natl. Acad. Sci USA* **72**: 3551-55.
116. Rubin H, Terasaki M and Sanui H. (1979). *Proc. Natl. Acad. Sci USA* **76**: 3917-21. (quoted from Gupta R.K. and Gupta P. (1984). NMR studies of intracellular metal ions in intact cells and tissues. *Ann. Rev. Biophys. Bioeng.* **13**: 221-46).
117. Rude R.K, Stephen A and Nadler J. (1991). Determination of red blood cell intracellular free magnesium by nuclear magnetic resonance as an assessment of magnesium depletion. *Magnes. Trace Elem.* **10**: 117-121.
118. Sachs J.R. (1988b). Interaction of magnesium with the sodium pump of the human red cell. *Journal of Physiology* **400**: 575-591.
119. Scarpa A. (1979). Measurements of cation transport with metallochromic dyes. *Methods Enzymol.* **56**, 301-338.
120. Scarpa A., Baldasserre J and Inesi G. (1972). *J. Gen. Physiol.* **60**: 735. (quoted from Pressman B.C. (1976). Biological applications of ionophores. *Ann. Rev. Biochem.* **45**: 501-30).
121. Shah G.M, Alvarardo P and Kirschenbaum M.A. (1990). Symptomatic hypocalcemia and hypomagnesemia with renal magnesium wasting associated with pentamidine therapy in a patient with A.I.D.S. *Am. J. Med.* **89**, 380-382.
122. Shechter M, Hod H, Chouraqui P, Kaplinsky E and Rabinowitz B. (1995). Magnesium therapy in acute myocardial infarction when patients are not candidates for thrombolytic therapy. *Am. J. Cardiol.* **75**: 321-3.
123. Singh J and Wisdom D.M. (1995). Second messenger role of magnesium in pancreatic acinar cells of the rat. *Molec. Cell Biochem* **149/50**, 175-182.

124. Skou J.C. (1957). The influence of some cations on an adenosine triphosphatase from peripheral nerves. *Biochim. Biophys. Acta* **23**, 394-401.
125. Smith P.R. and Benos D.J. (1991). Epithelial Na⁺ channels. *Annu. Rev. Physiol.* **53**, 509-530.
126. Speich M, Bouquet B. and Nicholas G. (1981). Reference values for ionised, complexed and protein bound magnesium in men and women. *Clin. Chem* **27** (2), 246-248.
127. Squire L.G. and Petersen O.H. (1987). Modulation of Ca²⁺- and voltage-activated K⁺ channels by intral Mg²⁺ in salivary acinar cells. *Biochimica. Biophysica. Acta* **899**, 171-175.
128. Taylor S. and Singh J. (1997). Characterisation of magnesium transport from rat, pig, cow and human erythrocytes. In: *Magnesium: current status and new developments* (Eds T. Theophanides and J. Anastassopoulou), pp 33-35. Kluwer academic publishers. Printed in Netherlands.
129. Teo K.K, Yusuf S., Collins R., Held R.H. and Peto R. (1991). Effects of intravenous magnesium in suspected acute myocardial infarction: overview of randomized trials. *Br. Med. J.* **303**: 1499-503.
130. Tosteson D.C. (1955). The effects of sickling on ion transport. *J. Gen. Physiol.* **39**: 55-65.
131. Tsien R.Y. (1983). Intracellular measurements of ion activities. *Annu. Rev. Biophys, Res. commun* **165**, 913-918.
132. Unicam (1995). AAS methods manual. Issue 2.

133. Vormann J. and Gunther T. (1993). Magnesium transport mechanisms: In: Magnesium and the cell. (Ed; N.J.Birch) Academic press, London pp 137-155.
134. Vormann J., Gunther T., Magdorf K. and Rob P. (1996). Changed erythrocyte magnesium transport in patients with cystic fibrosis and renal failure. *J. Physiol.*, **493P**: 66P.
135. Wacker W.E.C. (1968). The biochemistry and physiology of magnesium. *Annu. NY. Acad. Sci* **161**, 717-726.
136. Wacker W.E.C. (1980). In: Magnesium and man. Pub: Harvard University Press, Cambridge, MA (USA).
137. Watson K.V., Moldow C.F., Ogburn P.L. and Jacobs H.S. (1986). Magnesium sulphate: rationale for its use in preeclampsia. *Proc. Natl. Acad. Sci. USA* **83**: 1075-1078.
138. Whang R. (1993). Clinical perturbations in magnesium metabolism-hypomagnesaemia and hypermagnesaemia. In: Magnesium and the cell (Ed N.J.Birch). Academic Press, London, pp 5-14.
139. Whang R., Oei T. and Aikawa J.k *et al* (1984). Predictors of clinical hypomagnesaemia and hypokalemia, hypophosphatemia, hyponatremia and hypocalcemia. *Arch. Intern. Med.* **144**, 1794-1796.
140. Wisdom D.M., Geada M.M. and Singh J. (1996). Characterisation of sodium-dependent magnesium efflux from magnesium loaded rat pancreatic acinar cells. *Exp. Physiology* **81**, (3), 367-374.
141. Woods K.L., Fletcher S., Roffe C. and Haider Y. (1992). Intravenous magnesium sulphate in suspected acute myocardial infarction: results of the second Leicester Intravenous Magnesium Intervention Trial (LIMIT- 2). *Lancet* **339**: 1553-1558.

142. Woods K.L., Roffe C. and Fletcher S. (1994). Investigation of the effects of intravenous magnesium sulphate on cardiac rhythm in acute myocardial infarction. *Br. Heart J.* **71**: 141-145.
143. Wyrwicz A.M., Schofield J.C. and Burt C.T. (1982). In: *Noninvasive probes of tissue metabolism*. Ed J.S Cohen, pp 149-71. NY. Wiley Intersci.

Chapter Six

APPENDIX

Appendix I

Reagent preparation.

The standard PAR/pak[®] was not used. As a replacement ADP was prepared by appropriate dilutions to the stock. Thrombin was purchased from Sigma and an appropriate dilution series was performed. Another change to the protocol was to use varying concentrations of magnesium and calcium. Both the ADP and Thrombin solutions were kept in the freezer.

Equipment Operation.

1. When the PAP-3 reaches proper operating temperature (37°C), the first programmed instruction will come on. This instruction states “INSERT PPP” and “INSERT PRP WITH STIR BAR.” Place 0.45 ml of PRP and 0.5 ml of PPP into two different flat bottomed test tubes (BIO data vials 8.75 × 50 mm siliconised, Alpha lab. catalog No: 100336).
2. Incubate the PRP and PPP samples in the incubation block for approximately 3 minutes in order to bring them to 37°C.
3. Following the programmed instructions, insert the PPP sample completely into the test well labelled PPP. Place a stir bar (Alpha Lab. catalog No: 100337) into the PRP tube and insert the tube completely into the well marked PRP. This will deactivate the red flashing message “ADD STIR BAR TO PRP”. The next steps in the procedure

will appear **“PLATELET COUNT NORMAL - PUSH START BUTTON**. Pushing the start button will automatically calibrate and standardise the PAP-3.

However, if the PRP sample in the well has not been prepared correctly resulting in either a low or high platelet count corresponding warning indicators illuminate. The PAP-3 allows the platelet count in the range 50,000-75,000 per mm^3 to be measured. The optimum range for measurement is between 200,000-400,000 per mm^3 . A high platelet count is one, which exceeds this domain; hence it is necessary to dilute the PRP sample with the corresponding PPP until the required range is achieved. This is usually obtained by performing a simple 1:1 or 1:2 PRP: PPP dilution. Verification of the correct dilution is attained when the PRP is reinserted into the well and the message **“ PLATELET COUNT NORMAL”** appears.

The experiment proceeds until either it automatically stops this can be from 1-9 minutes, or it can be stopped manually at any time during the test. For this study the time varied from 2-3 minutes up to 5 minutes. Pressing the **“STOP TEST BUTTON”** stops the experiment. The aggregation on the display remains fixed at the final % until another test is started. The experiment was modified further by the addition of a third variable (varying concentrations of magnesium) in the presence of ADP and Thrombin. The Mg^{2+} levels varied from 1-10 mM.

Erroneous results at this stage may occur if the following conditions exist:

1. Light shields were left open during the test.
2. Test tubes were not completely seated in the test wells.
3. Incorrect volumes of plasma and reagents were used.

Compounds which may affect platelet aggregation reactions.

A wide range of chemical compounds including many commonly ingested drugs can inhibit platelet aggregation. Plasma samples taken from people who have ingested any of the following compounds may exhibit abnormal aggregation patterns.

Aggregation inhibitors include: -

Cocaine, Aspirin (acetylsalicylic acid), Dipyridamole, Non-steroidal Anti-inflammatory agents, Tricyclic antidepressants, Antihistamines and alcohol.

Many common patent and over the counter drugs contain aspirin and thus should be avoided. These include Alka-Seltzer, Bromo-Seltzer, cough medicines and a variety of cold remedies. **See attached appendix II for a more detailed list.**

Caution notes – Test Procedure.

Erroneous test results can occur if any of the following conditions exist either singularly or in a combination:

1. Blood is drawn in a glass syringe.
2. Blood specimens are improperly centrifuged resulting in packing or damage to the platelets.
3. Platelet-rich specimens are refrigerated or frozen.
4. Platelet-rich specimens have not been at room temperature for at least 60 minutes before testing.
5. Platelet-rich specimens have not been capped while standing to prevent changes in pH due to CO₂ loss.
6. Outdated reagents are used for testing.

7. Incorrectly formulated reagents are used for testing.
8. Platelet-rich specimens are tested which have been at room temperature for more than two hours.
9. Platelet-rich specimens containing less than 50,000-75,000 per mm³ platelets are used for testing.
10. The plasmas used were not adequately incubated for at least 2 – 3 minutes at 37°C before testing.
11. The plasmas used were incubated at 37°C for longer than 8 –10 minutes before testing.

Appendix II

Product	Manufacturer	Product	Manufacturer	Product	Manufacturer
Caps & No. 2	Scrip	Aspirin aluminum	Abbott	Cope	Glenbrook
bar*	Philips Roxane	Aspirin children's	Abbott	Coralsone modified*	Zemmer
sem*	Philips Roxane	Aspirin compound		Cordex*	Upjohn
nyl	Upjohn	c̄ Dover's powder*	Fellows	Cordex forte*	Upjohn
t	Noyes	Aspirin-Pb tab*	American Drug	Cordex buffered*	Upjohn
t c̄ Dovers powder*	Noyes	Aspirin-secobarbital		Cordex forte buffered*	Upjohn
t c̄ gelsemium	Noyes	Suppettes		Coricidin	Schering
Seltzer	Miles	No. 1 & 2 & 3 & 4*	Webster	Coricidin "D"	Schering
esic*	Elder	Aspirin Suppettes	Webster	Coricidin Demilets	Schering
esic c̄ ergotamine*	Elder	Aspirjen Jr Tabs	Jenkins	Coricidin Medilets	Schering
ne*	Ulmer	Aspirocalt	McNeil	Co-ryd	Daniels
in	Lemmon	Aspir-phen	Spencer-Mead & Robinson	Counter-Pain	Squibb
dyne*	Elder	Aspodyne	Blue Line	Covangesic	Mallinckro
al c̄ ASA*	Lilly	Aspodyne c̄ codeine*	Blue Line	D	
n	Whitehall	Axotal*	Warren-Teed	Darvon c̄ ASA*	Lilly
ia c̄ codeine	Massengill	B		Darvon-N c̄ ASA*	Lilly
ia-D*	Massengill	Babylove	Amer Pharm	Darvon compound	
ynos	Buffington	Ban-O-Pain	Daniels	32 & 65	Lilly
co No. 1 & 2	Massengill	Bayer	Glenbrook	Darvo-Tran*	Lilly
*	N Amer Pharm	Bayer children's	Glenbrook	Dasikon	Beecham- Massengi
ead*	Spencer-Mead	Bayer timed-release	Glenbrook	Dasin caps*	Beecham- Massengi
E codeine*	Various manu- facturers	Brogestic*	Brothers	Dasin-CS*	Beecham- Massengi
E Demerol	Various manu- facturers	Bufabar*	Philips Roxane	Dasin 1/4 strength*	Beecham- Massengi
E gelsemium*	Winthrop	Buff-A	Mayrand	Decagesic*	Merck, Sha & Dohm
dyne	Sutliff & Case	Buffacetin	Kay & Bowman	Delenar*	Schering
phen*	Gold Leaf	Buff-a-Comp*	Mayrand	Derfort*	Cole
a-Zene caps	Gold Leaf	Buffadyne	Lemmon	Derfule*	Cole
compound	Xttrium	Buffadyne 25	Lemmon	Dolcin	Dolcin
compound	Lilly	Bufferin	Bristol-Myers	Dolene compound 65*	Lederle
codeine*	Lilly	Bufferin arthritis strength	Bristol-Myers	Dolor	Geriatric Pharm
co No. 1 & 2	Jenkins	Buffinol	Otis Clapp	Doloral*	Wolly
phen	Schlicksup	C		Dorodol*	Durst
phen compound	Schlicksup	Calurin	Dorsey	Drinacet*	Philips Ro
a-phen	Ulmer	Camalnlay	Dorsey	Dristan Tab	Whitehall
deen-30*	Burroughs	Capron	Bryant- Vitarine	Drocogesic No. 3*	Century L
riptin	Wellcome	Causslin*	Amfre-Grant	Duopac*	Spencer-M
riptin c̄ codeine*	Rorer	Cephalgesic*	Smith, Miller & Patch	Duradyne	Durst
dine tab*	Rorer	Cheracol caps	Upjohn	Duragesic	Meyer
ergum	N Amer Pharm	Cirin	Zemmer	E	
ac-G*	Pharmaco	Clistanal*	McNeil	Ecotrin	Smith, Kli & Frenc
ac-G c̄ codeine	Central	Codasa tab*	Stayner	Empiral*	Burroughs Wellcom
encal	Central	Codempiral No. 2 & 3*	Burroughs Wellcome	Empirin	Burroughs Wellcom
ayte	Cole	Codessal No. 1 & 2*	Durst		
arbar	Cowley	Coldate	Elder		
r-C	Lannett	Colrex	Rowell		
reze	Jenkins	Colrex compound*	Rowell		
irin (USP)	Staniabs				
	Various manu-				

Appendix III

Recipes for solutions.

Mg²⁺ -Loading solution.

140 mM KCl.

50 mM sucrose.

5 mM glucose.

30 mM Hepes / Tris PH 7.4.

12 mM MgCl₂.

6 μM A23187 (ionophore).

Mg²⁺ -free solution (for efflux).

140 mM NaCl.

50 mM sucrose.

5 mM glucose.

30 mm Hepes / Tris pH 7.4.

Washing solution.

1% BSA (seals holes) in loading media.

Mg²⁺ Assay.

100 µl supernatant diluted with 1 ml 10% TCA / 0.175% LaCl₃. Measured by Atomic absorbance spectrophotometry.

Protein assay. - Bio rad protein assay.

(Standard assay protocol).

1). Preparation of working reagent.

Add 20 µl of reagent S to each ml of reagent A that will be needed for the run. (this working A' is stable for one week even though a precipitate will form after one day).

If a precipitate forms, warm the solution and vortex. If the samples do not contain detergent, you may omit step 1) and simply use reagent as supplied.

2). Prepare 3-5 dilutions of each protein standard containing from 0.2 mg / ml to about 1.5 mg / ml protein. A standard curve should be prepared each time the assay is performed. For the best results always prepare standards in the same buffer as the sample.

3). Pipette 100 µl of standards and samples into clean dry test tubes.

4). Add 500 µl of reagent A' or A into each test tube.

Vortex.

5). Add 4.0 ml reagent B into each test tube and vortex immediately.

6). After 15 minutes, the absorbance can be read at 750 nm. the absorbance will remain stable for at least 1 hour.

Method.

Control :- (repeat 5 times for statistical analysis).

1). Centrifuge 1 ml blood sample (not Mg^{2+} loaded).

2). Supernatant → Assay Mg^{2+} .

3). Sediment → haemolyse cells in 750 μ l H_2O .

Centrifuge + assay supernatant for Mg^{2+} (i.e. Mg^{2+} released from cells).

Protein assay also (to express per cell protein).

Experiment.

Centrifuge blood at 1000g for 10 minutes → remove plasma + buffy coat.

1). Incubate 10% cell suspension in Mg^{2+} loading solution for 30 minutes at 37 °C.

(30-50 μ l in total) shaking water bath.

2). Wash 3-4 times (i.e. centrifuge, decant etc), to remove A23187 → sample to check for [Mg^{2+}] loaded i.e. haemolyse cell + protein assay.

3). Suspend cells in 50 ml of Mg^{2+} free solution.

4). Time course → take 5 × 1 ml sample at 5, 10, 20, 30, 40, 50 minutes.

5). Centrifuge each sample at 10,000g for 1 minute.

Supernatant → Mg^{2+} assay.

Sediment → protein assay.

6). At 50 minutes also assay cells for Mg^{2+} i.e. haemolysis → supernatant.

Mg^{2+} contents to determine Mg^{2+} still remains in red blood cells.

A23187 : 10^{-3} M of stock.

0.1 ml made up to 1 ml = 10^{-4} M.

0.1 ml made up to 10 ml = 10^{-5} M.

0.1 ml made up to 100 ml = 10^{-6} M.

50 μ l made up to 50 ml = 10^{-6} M.

30 μ l made up to 30 ml = 10^{-6} M.

180 μ l made up to 30 ml = 6×10^{-6} M = 6 μ M.

Atomic absorbance spectrometry.

MgCl₂ standards 0.01 mm \rightarrow 0.00625 mm. (10 mM 1: 10 3 times).

10 mM stock.

0.1 ml made up to 100 ml (99.9 ml dist H₂O). + 0.01 mM.

Dilute 1/2 and 1/2 dist. H₂O. = 0.0025 mM.

↓

0.00125 mm.

↓

0.000625 mm.

5 standards entered in μ M.

0.625 (first).

1.25

2.5

5

10 (last).

Need 10% TCA / 0.175% LaCl₃ (mw 371.4) in each sample.

i.e. 1 sample : 10 TCA / LaCl₃.

Mg²⁺ loading solutions.

For 500 µl solutions :-

70 mmoles KCl (mw 74.56) = 5.2192g.

25 mmoles sucrose = 8.5575g.

2.5 mmoles glucose = 0.4504g.

15 mmoles Hepes = 3.5745g.

(KOH).

MgCl₂ :- make up 1 M solution (mw = 203.3).

i.e. 203.3g in litre = 1 M or 20.33g in 100 ml.

1 ml (0.1 M) in 100 ml H₂O = 1 mM.

or 12 ml in 100 ml H₂O = 12 mM.

∴ In 500 µl need 12 × 5 = 60 ml.

i.e. 60 ml MgCl₂ solution (0.1 M) in 500 ml total solution.

gassed for 15 minutes (95% O₂, 5% CO₂).

Add KOH until pH 7.4.

Mg²⁺ free solution.

For 500 ml solution.

70 mmoles NaCl (mw 58.44) + 4.0908g,

25 mmoles sucrose = 8.5575g.

2.5 mmoles glucose = 0.45504g.

15 mmoles Hepes (mw 238.3) = 3.5745g.

Gas for 15 minutes (95% O₂, 5% CO₂).

KOH for pH 7.4.

***** DO NOT ADD IONOPHORE A 23187 UNTIL REQUIRED *****

CAN STORE BOTH Mg²⁺ LOAD. SOL. & Mg²⁺ FREE SOL. IN
FRIDGE.

Mg²⁺ assay.

Mg²⁺ efflux was determined by diluting the supernatant 1 : 1000 with TCA / LaCl₃ and Mg²⁺ measured by AAS.

The Mg²⁺ content for the unloaded cells, loaded cells following 50 minutes efflux , was determined by haemolysing the cells in a 1 : 100 dilution with Triton X 100 overnight. The solution was then diluted with 1 : 10 with 10% TCA / 0.175% LaCl₃ to give a final dilution of 1 : 1000.

Mg²⁺ was measured with AAS.

Protein assay.

Cells haemolysed by 1:100 dilution with 10% TCA / 0.175% LaCl₃. The protein content of each sample was measured using the Bio-rad detergent -compatible protein assay kit.

- 1). 250 µl of reagent A was added to 50 µl of each sample and vortexed for 5 seconds.
- 2). 2 ml of reagent B was added and each sample vortexed for a further 5 seconds.
- 3). Following incubation at 37 °C in a shaking water bath for a minimum of 15 seconds, the absorption of each sample was measured at 750 nM.
- 4). Using BSA standards a calibration curve was then used to convert the absorbance readings to protein concentration.

Protein assay BSA standards.

(0.050g) 50 mg BSA made up to 5 ml volume with 1% Triton X-100. = 10 mg/ml

-1

(0.045g) 45 mg BSA made up to 5 ml volume with 1% Triton X-100. = 9 mg/ml⁻¹

(0.040g) 40 mg BSA made up to 5 ml volume with 1% Triton X-100. = 8 mg/ml⁻¹

(0.035g) 35 mg BSA made up to 5 ml volume with 1% Triton X-100. = 7 mg/ml⁻¹

(0.030g) 30 mg BSA made up to 5 ml volume with 1% Triton X-100. = 6 mg/ml⁻¹

(0.025g) 25 mg BSA made up to 5 ml volume with 1% Triton X-100. = 5mg/ml⁻¹

(0.024g) 24 mg BSA made up to 6 ml volume with 1% Triton X-100. = 4 mg/ml⁻¹

(0.021g) 21 mg BSA made up to 7 ml volume with 1% Triton X-100. = 3 mg/ml⁻¹

(0.016g) 16 mg BSA made up to 8 ml volume with 1% Triton X-100. = 2 mg/ml⁻¹

(0.009g) 9 mg BSA made up to 9 ml volume with 1% Triton X-100. = 1 mg/ml⁻¹

(0.00675g) 6.75 mg BSA made → 9ml volume with 1% Triton X-100. = 750 µg/ml⁻¹

(0.0045g) 4.5 mg BSA made → 9 ml volume with 1% Triton X-100. = 500 µg/ml⁻¹

(0.00225g) 2.25 mg BSA made → 9 ml volume with 1% Triton X-100. = 250 µg/ml⁻¹

For the blank use 1% Triton X-100 in 10 ml volume = 0 mg/ml⁻¹

For standard assay :-

13 × 100 mm test tubes.

Reservoir for working reagent (size is dependant on amount of reagent that will be prepared).

Pipettes accurately delivering 100 µl, 500 µl, and 4.0 ml.

Graduated cylinders or pipettes for reagent preparation.

Spectrophotometer set to 750 nm.

vortex mixer.

Plastic or glass cuvettes with 1 cm path length matched to the laboratory spectrophotometer.

Test tube rack to hold 13 × 100 mm test tubes.

Atomic Absorption Spectrometer (A.A.S).

1. Switch on the compressor, the A.A.S., the fume cabinet.
2. Switch on the A.A.S.
3. Clean the burner – take the cover off the front, unplug the burner. Clean with green mesh, run a piece of card through the aperture. Replace the burner.
4. Press the home key on the board to access main menu.
5. Enter system set-up.
6. Press next for next page.
7. MODE- flame absorption. LAMP 4 for Ca / Mg.
Take off the covers for the lamps, and manually rotate lamps round to required lamp. Once lamp is on (press on button on programme), leave for fifteen minutes to warm up.
8. FLAME SET UP (usually already set up on air / acetylene). Turn on gas cylinder at pressure .7 BAR (10 lb). Ignite flame. The flame should be a blue colour.
9. Press next until the standards page is seen. Enter the standards.
10. Analyse. Wait until “ASPIRATE BLANK AND PRESS RUN” appears on screen.
Run all standards beginning with the most dilute.
11. Run all samples.
12. On completion of analysis press STOP.
13. Clean nebuliser with deionised water.
14. Press off button to extinguish flame. Turn off the acetylene cylinder. Press off button to release any acetylene left in the pipe.
15. Press “home” key on the consul and the lamp set up page. Switch off the lamp.

16. Switch off the A.A.S., fume cupboard and compressor at the plugs.

OPERATING THE CHLORIDE TITRATOR

1. Add 15ml acid buffer & 10 drops gelatin to pot & stir.
2. Add 20 μ l 100mmol/l Cl⁻ then press cond. for 2 sec.
3. Display should increase then stop at above 100.
4. Repeat 2. Display should stop at ~ 100.
5. Titrator is now calibrated in units of mmol/l [Cl⁻].
6. Add 20 μ l of sample, press titrate for 2 sec.
7. Display should zero, then increase to give [sample].

OPERATING THE FLAME PHOTOMETER

1. Turn on natural gas supply at main stop-cock and on the bench.
2. Switch "*Power on*", if "*flame on*" LED does not illuminate switch off for 2 sec and repeat.
3. Select correct filter using lever.
4. Place tube in d.H₂O for 15 min then adjust "*blank*" till display reads 0.00
5. Aspirate top standard, wait 20sec then adjust reading using "*coarse*" & "*fine*"
6. Aspirate d.H₂O for 20 sec, adjust to 0.00 using "*blank*" then remove tube.
7. Repeat 5. & 6. until readings stabilise then the aspirate remaining standards to produce a standard curve. Aspirate samples.

Appendix IV.

NMR Protocol.

v 7

ING SAMPLES ON THE XWIN-NMR1.3 SYSTEM (VT WORK) Updated 11/2/97 JB

- (a) Insert your sample as normal.
- (b) Start the sample spinning. It should spin at 10 Hz.
use the spin meas button to check.
- (c) Once ok turn off the display

Type

edc<rtm>

Enter your sample details

File -

i.e. jb02h34

Experiment number- 10

Type :-

rpar PROTON all <rtm>

(NB Unix is case sensitive so this must be typed exactly!)

Type :-

eda

In the pink parameter box at the bottom of the eda box type :-

prosol

Click the button next to Prosol it should then read TRUE

Click on save

- a) In the XWIN-NMR window TYPE:-
lock CDC13 *5.0*
Wait until finished.

- a) Type:-

edte

A new box will appear.

- b) Click on the load parameters box and select the appropriate parameters. Usually qnp.norm should be selected.

N.B. Make sure that there is gas flowing through

the probe (Should be ~~670~~ 1/hr), the probe glassware may be damaged if this is not so!!!!!! *535 l/hr*

- c) Quit the display, the error message is bug!

- a) Type:-

te (Desired temperature)

N.B. specify the temperature to .2K

i.e. te 303.2 = 30oC

te 303.0 = 29oC !

N.B. CDC13 Boils at 330.2K
DO NOT EXCEED THIS TEMPERATURE

- b) Type:-
teset (This transfers the temperature defined by 'te' to the heater system)
- c) Type:-
temon (temperature monitor)
- d) Type:-
xau heater_on

- a) Once the desired temperature is reached type:-
tune manual_shim (Complete the Tune sequence) - 0.1
Wait until finished.
- b) Type:-
xaua (This will automatically acquire the data)
- c) Type:-
xaup (This will automatically process the data)

- (a) If another temperature is required
Type:-
edc

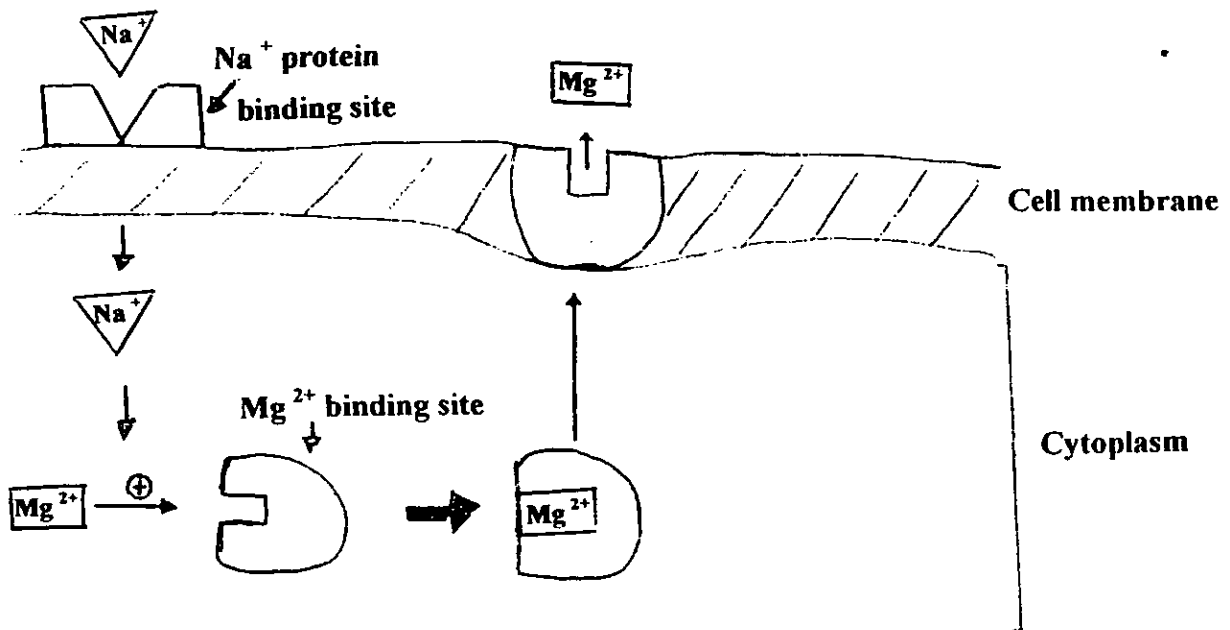
- (b) Increase the experiment number by 1 i.e. 11
Type:-
rpar PROTON all - P3: 610
- (c) go back to step 6 and repeat sequence.

VT

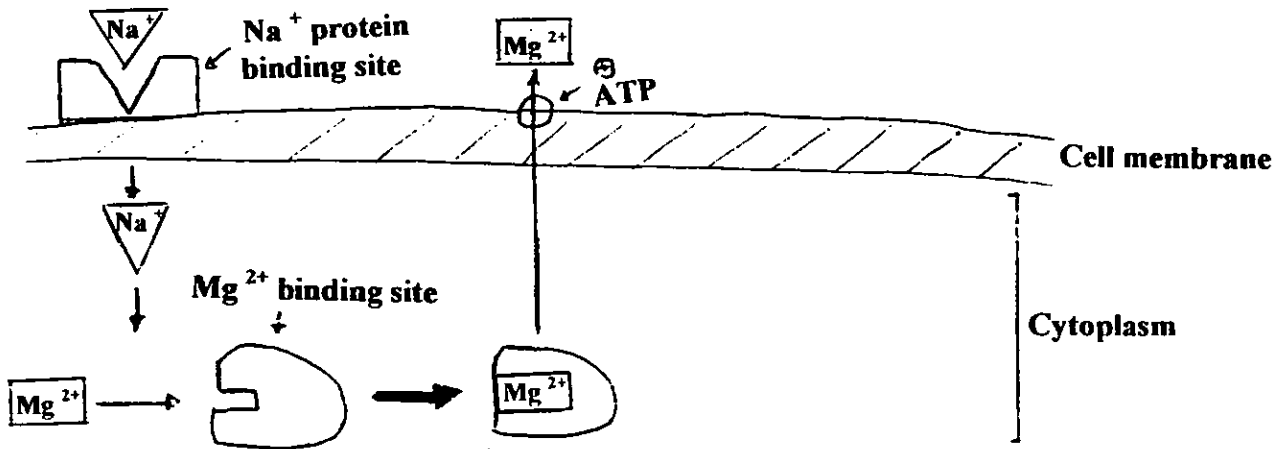
- WHEN FINISHED
- (a) Type:-
xmac hnoff
- (b) Type:-
te 293.2
teset
- (c) Wait until the temperature has dropped below 30oC / 303.2K
- d) Insert standard sample.
- e) Make sure that spinning is off.
- f) Type:-
bye
wait until xmac finished is displayed at bottom of screen.
- f) Select File in the xwin-nmr window and exit.
If all samples have been run ignore the messages and click :-
ok
- g) From Toolchest
click Desktop
click Logout..

Appendix V

(model a)



(model b)



Proposed schematic models of Mg^{2+} transport in red blood cells (Ludi and Schatzmann, 1987) (a / b) Na^+ binds to sodium binding site on the cell membrane. It causes a conformational change in the protein which allows sodium to enter into the cytoplasm. The presence of Na^+ allows the internal Mg^{2+} to gain access to its binding site. Mg^{2+} which is bound to the binding site is then transported out of the cell by either a passive process (Model a) or an active process (model b) in the presence of ATP.